ABSTRACT

Title of Document:	SPATIAL PATTERNS AND POTENTIAL MECHANISMS OF LAND DEGRADATION IN THE SAHEL
	Khaldoun Rishmawi, Doctor of Philosophy, 2013
Directed By:	Professor Stephen D. Prince Department of Geography

There is a great deal of debate on the extent, causes and even the reality of land degradation in the Sahel. On one hand, extrapolations from field-scale studies suggest widespread and serious reductions in biological productivity threatning the livelihoods of many communities. On the other hand, coarse resolution remote sensing studies consistently reveal a net increase in vegetation production exceeding that expected from the recovery of rainfall following the extreme droughts of the 1970s and 1980s, thus challenging the notion of widespread, subcontinental-scale degradation. Yet, the spatial variations in the rates of vegetation recovery are not fully explained by rainfall trends which suggest additional causative factors. In this dissertation, it is hypothesized that in addition to rainfall other climatic variables and anthropogenic uses of the land have had measurable impacts on vegetation production. It was found that over most of the Sahel, the interannual variability in

growing season ΣNDVI (used as a proxy of vegetation productivity) was strongly related to rainfall, humidity and temperature while the relationship with rainfall alone was generally weaker. The climate- ΣNDVI relationships were used to predict potential ΣNDVI; that is the ΣNDVI expected in response to climate variability alone excluding any human-induced changes in productivity. The differences between predicted and observed ΣNDVI were regressed against time to detect any long term (positive or negative) trends in vegetation productivity.

It was found that over most of the Sahel the trends either exceeded or did not significantly depart from what is expected from the trends in climate. However, substantial and spatially contiguous areas (~8% of the total area of the Sahel) were characterized by significant negative trends. To test whether the negative trends were in fact human-induced, they were compared with the available data on population density, land use pressures and land biophysical properties that determine the susceptibility of land to degradation. It was found that the spatial variations in the trends of the residuals were not only well explained by the multiplicity of land use pressures but also by the geography of soil properties and percentage tree cover.

SPATIAL PATTERNS AND POTENTIAL MECHANISMS OF LAND
DEGRADATION IN THE SAHEL

By

Khaldoun Rishmawi

Dissertation submitted to the Faculty of the Graduate School of the
University of Maryland, College Park, in partial fulfillment
of the requirements for the degree of
Doctor of Philosophy
2013

Advisory Committee:
Professor Stephen Prince, Chair
Professor Eric Kasischke
Professor Ralph Dubayah
Professor James Kellner
Professor Rachel Pinker

To my wife,

Monica …

Acknowledgements

Table of Contents

List of Tables

List of Figures

Chapter 1: Introduction

1.1 Background

Drylands encompass all lands where the climate is classified as arid, semi-arid and dry sub-humid[1] (UNEP 1992; UNEP 1997; Adeel *et al.* 2005). Global drylands are home to some 2 billion people and cover about 40% of Earth's land surface (Safriel *et al.* 2005; Safriel 2007a) with a total carbon pool of approximately 1420 gigatons (Gt) that is almost twice the size of the atmospheric pool (Lal 2004). Land degradation is considered as one of the major environmental problems in drylands (UNCED 1992; UNCCD 1994; Reynolds *et al.* 2007a). The livelihoods of some 250 million people are believed to be directly affected, a figure that is likely to increase substantially in the face of population growth and climate change (Reynolds *et al.* 2007b). In addition to its threat to human well-being, land degradation reduces carbon sequestration and organic soil carbon deposition (Falkowski *et al.* 2000; Prince 2002), disrupts the surface water balance (Balling *et al.* 1998; Taylor *et al.* 2002), increases atmospheric dust concentration (Prospero & Lamb 2003), reduces biodiversity (Maestre *et al.* 2012), and may intensify and prolong drought episodes through vegetation-climate feedbacks (Charney 1975; Clark *et al.* 2001; Taylor *et al.* 2002; Giannini *et al.* 2003).

The term "land degradation" has many definitions and several authors have provided useful compendiums (Mainguet 1991; Thomas & Middleton 1994; Reynolds 2001). It is generally agreed that land degradation implies long-term

---

[1] Arid (0.05≥ Precipitation(P)/Potential evapotranspiration (PET)<0.20, ≤75 growing days/yr), semi-arid (0.20≤ P/PET<0.50, 75≤ growing days/yr<120), and dry sub-humid (0.50≤ P/PET<0.65, 120≤ growing days/yr<180).

reductions in the biological productivity of the land resulting from one or a combination of processes including reductions in vegetation productivity and cover, soil degradation and changes in species composition. The term "land" has been defined by the United Nations Convention to Combat Desertification (UNCCD) as "the terrestrial bio-productive system that comprises soil, vegetation, other biota, and the ecological and hydrological processes that operate within the system" (UNCCD 1994).

Despite its acknowledged importance, the nature and causes of land degradation have remained stubbornly intractable (Thomas & Middleton 1994; Reynolds *et al.* 2002; Nicholson 2011a). This has been more evident in the Sahel region of Africa than in any other part of the world where divergent assessments have led to more disagreement and controversy than consensus (Helldén 1991; Nicholson *et al.* 1998). Much of the controversy, it is generally agreed, have resulted from unwarranted extrapolations from limited data or subjective "expert" opinions, from the lack of a consensus definition, and from the confusion between climate-induced short-term ecosystem dynamics (e.g. short-term response to periodic droughts) and land degradation -(a long-term response resulting from chronic and severe disturbances) - (Prince *et al.* 1998; Reynolds 2001; Batterbury *et al.* 2002; Prince 2002).

Prince (2002) strongly makes the case for quantitative assessment of land degradation through remote sensing. He argues that vegetation production which can be reliably measured form space is particularly useful since low productivity is at the heart of many land degradation definitions. In this dissertation remotely sensed data

were used to develop indicators of land degradation that can detect long-term reductions in vegetation production that cannot be explained by climate variability. Areas identified as degraded were compared to data on land use pressures to identify the human factors that might have caused degradation.

The human population of the Sahel is rapidly increasing (UN 2011). Pressure on the land is likely to increase accordingly (Barbier 2000; Reardon *et al.* 2001) and perhaps the extent and severity of land degradation. There is a pressing need for an objective and spatially explicit measure of land degradation and for an assessment of its linkages, if any, to human uses of the land (Batterbury *et al.* 2002; Dregne 2002; Safriel 2007b). The tragic shortage of data on human-induced land degradation is believed to have contributed to the failure of most interventions to reverse degradation and has brought about a policy dilemma on how to minimize further deterioration (Batterbury *et al.* 2002; Mortimore & Harris 2005).

1.2 Study area

The term "Sahel" is often applied to the general region extending across the east-west extent of Africa and between the latitudes of roughly 10°N and 18°N (figure 1.1). The region includes the Sahelian, Sudano-Sahelian, Sudanian and parts of the Guinean eco-climatic zones (White 1983) and is characterized by a steep north-south gradient in mean annual rainfall (Le Houérou 1980b). Vegetation cover in the northern Sahel consists of shrubs interspersed between annual and perennial grasses, and further south by grasslands and deciduous, open savanna woodlands, with woody cover only locally exceeding 5%. The Sudanian zone is dominated by deciduous shrublands with sparse trees, and further south by deciduous woodlands with grass

3

understory. Finally, the Guinean zone is dominated by semi-deciduous closed woodlands and evergreen forests (Le Houérou 1980b; White 1983).
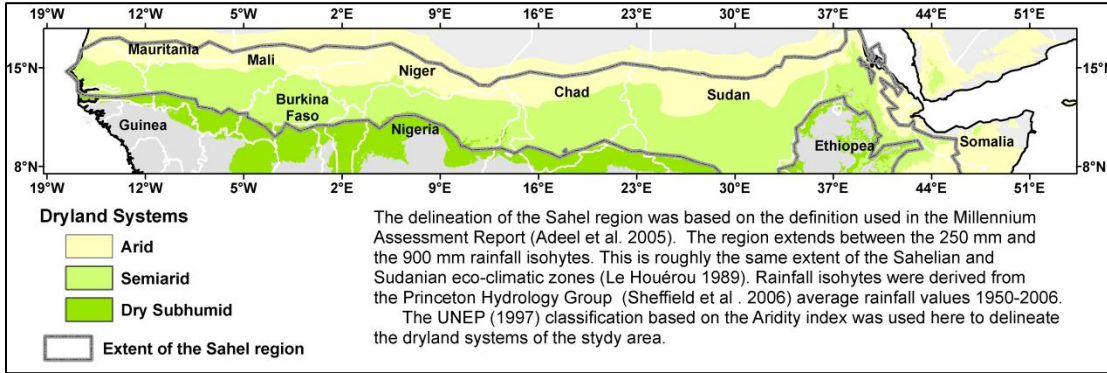
Figure 1.1 Dryland systems of the study area and the extent of the Sahel region.

Most of the Sahelian rainfall occurs during the northern hemisphere summer and is linked to periodic northwards excursions of the West African monsoon (Lebel *et al.* 2003; Dieng *et al.* 2008; Nicholson 2013). The onset of the monsoon proceeds slowly and is characterized by a succession of active and inactive phases (Lebel *et al.* 2003; Dieng *et al.* 2008). The initial wet spell in the northern Sahel does not usually produce significant rains. It is only when the Intertropical Convergence Zone (ITCZ) abruptly shifts from 5°N to 10°N that significant rain is rapidly observed over the Sahelian ecoclimatic zone (Sultan & Janicot 2000b; Lebel *et al.* 2003; Sultan & Janicot 2003). The mean onset date of the wet season in the Sahelian zone is the 24th of June with a standard deviation of 8 to 10 days (Sultan & Janicot 2000a; Sultan & Janicot 2003; Dalu *et al.* 2009) and most rains fall between mid-July and September (Lebel *et al.* 2003). On average, the length of the wet season increases from about 50 days in northern Sahel at 18°N to roughly 8 months in the coastal Guinean zone at 10°N (Zhang *et al.* 2005). Compared to the onset phase, the withdrawal phase is

relatively abrupt and rather uniformly distributed throughout the entire monsoon region (Nicholson 2013). The vegetation cycle closely responds to the seasonality in rainfall, with virtually all biomass production taking place in the wet summer months (Tucker *et al.* 1991; Tucker & Nicholson 1999; Herrmann *et al.* 2005a; Zhang *et al.* 2005).

During the last few decades, two sequences of extremely dry years in 1972-1973 and again in 1983-1984 struck the Sahel and were part of a longer drought that lasted from the end of the 1960s to the mid-1990s (Nicholson 2001; Le Barbé *et al.* 2002) (figure 1.2). This unusual dry spell was not limited to the Sahel but extended to regions more to the south as well (Le Barbé *et al.* 2002). The total number of rainfall events during the drought also decreased thus increasing the probability of dry spells during the rainy season (Le Barbé *et al.* 2002). Since 1994, annual rainfall totals somewhat recovered and varied around the mean of the standard climatological period of 1931-1960 (Nicholson 2001; Hiernaux *et al.* 2009b). These fluctuations in rainfall at intra-annual, interannual and decadal time scales made the Sahelian region of Africa the most dramatic example of climate variation that has been directly measured (Hulme 2001). The Sahel therefore provides (1) a valuable natural experiment on the effects of climatic variations on vegetation production and (2) a testing bed of indicators that attempt to differentiate climate-induced short-term ecosystem dynamics from land degradation.

Sahel precipitation anomalies (1930-2006)

June through October averages over 10-18N, 20W-45E, 1930-2006
climatology. NOAA NCDC.
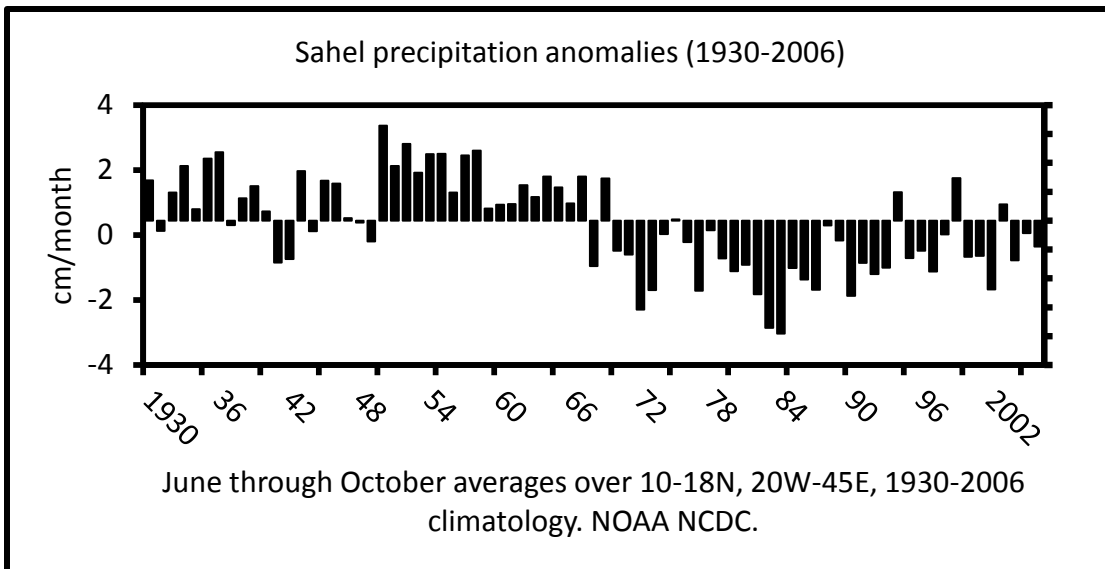
Figure 1.2 Wet season (June through October) Sahel precipitation anomalies (1930-2006). Data are from the National Oceanic and Atmospheric Administration (NOAA) National Climatic Data Center (NCDC).

1.3 The controversy surrounding land degradation in the Sahel

The Sahel region of Africa is supposed to be one of the world's most affected areas by degradation (Oldeman *et al.* 1990; Le Houérou 1992; UNEP 1992). During the last few decades, high population growth rates in the Sahelian and Sudanian ecoclimatic zones (collectively referred to here as the "Sahel", figure 1) have been accompanied with cropland expansion and with an increase in livestock numbers (Vierich & Stoop 1990; Ramaswamy & Sanders 1992; van de Koppel *et al.* 1997; Lambin *et al.* 2003; FAO 2011). These changes in the Sudano-Sahelian agricultural and pastoral regions coincided with the Sahelian drought (late-1960s to the mid-1990s) (Nicholson 2001; Le Barbé *et al.* 2002). Commensurate with these changes in land use and with the drought were catastrophic reductions in crop yields and rangeland carrying capacity (Nicholson 1978; Lamb 1983; Hiernaux *et al.* 2009b).

The resulting famines of the 1970s and 1980s plus anecdotal accounts of progressive southwards march of the Sahara desert (Norman 1987; Lamprey 1988) led to the widely accepted narrative that population growth drives cropland expansion, overgrazing and infrastructure extension and that these changes in land use have resulted in widespread land degradation (e.g. Le Houérou 1996; Le Houérou 2002). Furthermore, Charney (1975) controversially suggested that overgrazing and land degradation may have even been the cause of the extreme droughts of the 1970s through positive feedback between rainfall and surface albedo. Faced with what has seemed at the time as a new and sinister problem threatening human well-being, the United Nations agencies initiated programs to combat land degradation despite the lack of substantiated information on its location, severity and causes (Prince 2002).

Following the 1974 drought, various attempts have been made to inventory land degradation and to provide a baseline for monitoring (Dregne 1977; Dregne 1983; Oldeman *et al.* 1990; Dregne & Chou 1992; Lepers 2003). Yet, the paucity of data on land degradation and the lack of any readily measured, objective indicators have inhibited progress (Prince 2002). Estimates of the extent of land degradation have ranged between 4% and 60% of the total area of the Sahel. Nevertheless, the figure of 60% degradation drawn from the Global Assessment of Soil Degradation (GLASOD; Oldeman *et al.* 1990) has been cited more often than the others (Safriel 2007a). The GLASOD study drew its estimates from judgment by regional soil experts. While subjective in its approach, it was based on more rigorous and consistent set of guidelines than previous assessments (Prince 2002). In addition to mapping the extent and severity of soil degradation, the GLASOD study included an

assessment of the human activities responsible for degradation. Its findings reinforced the preconceived narrative that overgrazing, cropland expansion and excessive fuel wood collection have caused widespread degradation.

Agronomists, geographers and development economists have tried to explain the findings of widespread degradation. Vierich and Stoop (1990) argued that drought reduced agricultural yields while rapid population growth increased demand for food. The widening gap between food supply and demand drove the vast majority of farmers to shorten fallow periods and to expand cultivation onto marginal lands thus increasing the risks of soil fertility depletion, erosion and crusting (Vierich & Stoop 1990; Vlek 1990; Swift *et al.* 1994; Bationo *et al.* 1998; Drechsel *et al.* 2001). Reardon et al. (2001) contended that capital deficiencies, the elimination of fertilizer subsidies, and poor accessibility to markets hampered the adjustments of farming methods posited by Boserup's (1965, 2005) theory of agricultural intensification that are necessary to counteract the threat of degradation. Reardon et al. (2001) view paralleled that of other economists (e.g. Breman 1997; Barbier 2000) and geographers (e.g. Webber 1996; Drechsel *et al.* 2001) who further argued that once degraded, agricultural lands were often abandoned and new lands were brought into production resulting in a perpetuating cycle of agricultural extensification and land degradation. Agricultural extensification is also believed to have contributed, at least in part, to rangeland degradation (van Keulen & Breman 1990; van de Koppel *et al.* 1997; Barbier 2000). In the Sahel, it was hypothesized that arable lands expanded at the expense of pastures consequentially increasing livestock densities in areas remaining accessible to pastoralists. In these rangelands, over-stocking is thought to have

perturbed vegetation cover sufficiently to expose soils to wind and water erosion as well as to crusting and compaction by animal trampling (Le Houérou 1980a; Olsson & Rapp 1991; Le Houérou 1996).

The evidence supporting many of the aforementioned arguments is, however, surprisingly slim (Turner *et al.* 1993). On one hand, the thesis that Sahelian agriculture tends to be mainly extensive and degrading has been found to be in discordance with crop yield data recorded between the 1960s and late 1990s (Hellden 1991; Breman 1998; Harris 1998; Niemeijer & Mazzucato 2002; Mortimore & Harris 2005). On the other hand, claims of widespread rangeland degradation through overgrazing run counter to long term increases in livestock populations (Sullivan & Rohde 2002; Mortimore & Turner 2005). Extensive studies in the Sudan (Olsson 1985; Ahlcrona 1988; Helldén 1991) have also demonstrated that earlier reports of serious human-induced land degradation (e.g. Hammer-Digernes 1977; Baumer & Tahara 1979) were rather misinterpretations of natural ecological adjustments to climatic fluctuations. They demonstrated that while droughts have reduced vegetation cover and agricultural yields, the return of more favorable climatic conditions has been accompanied with full recovery of land productivity, suggesting that there has been no degradation. Similarly, analysis of satellite data from 1982-onwards has revealed a consistent trend of vegetation recovery from the extreme droughts of the 1970s and early 1980s (Tucker & Nicholson 1999; Eklundh & Olsson 2003; Herrmann *et al.* 2005a; Olsson *et al.* 2005; Heumann *et al.* 2007a; Fensholt & Rasmussen 2011), suggesting that the perceived widespread degradation in the Sahel can be largely attributed to climate variability and not to irreversible

changes in land productivity (Prince *et al.* 1998; Herrmann *et al.* 2005a; Fensholt & Rasmussen 2011). Furthermore, interannual variations in agricultural yields per unit cultivated area in Burkina Faso and Nigeria; two countries identified by the GLASOD study as the most degraded in the Sahel; have been found to be strongly related to rainfall variability (Niemeijer & Mazzucato 2002). In fact, in these countries agricultural yields per unit rainfall have increased since the mid-1960s (Niemeijer & Mazzucato 2002; Mortimore & Harris 2005) raising the possibility that the extent and magnitude of adverse changes in soil properties reported by regional studies (Oldeman *et al.* 1990; Stoorvogel & Smaling 1990; Some *et al.* 1992) have been grossly overestimated (Niemeijer & Mazzucato 2002).

Other accepted tenets of human-induced land degradation have also been challenged. Studies in the Western Sahel have shown that the capability or willingness of farmers to invest in sustainable farming methods have been underestimated (de Ridder *et al.* 2004) and that the expansion of agriculture onto marginal lands did not necessarily result in degradation mainly due to investments in soil and water conservation measures and to the emergence of mixed livestock-farming systems (e.g. Tiffen *et al.* 1994; Adams & Mortimore 1997; Mazzucato & Niemeijer 2000; Mortimore & Harris 2005; Mortimore & Turner 2005).

None of these studies however claim that land degradation has not occurred in the Sahel. There are several well documented cases of local degradation resulting from the excessive utilization of the land with respect to its resilience (Geist & Lambin 2004) but the premise that regional degradation can be characterized using extrapolations from limited local scale data (e.g. Somé *et al.* 1992; Stoorvogel &

Smaling 1990; Le Houérou 1996) or by upscaling of local "expert" opinions (e.g. Oldeman *et al.* 1990) are unwarranted and lack a certain objective rigor (Thomas & Middleton 1994; Prince *et al.* 1998; Stocking 2001; Batterbury *et al.* 2002; Koning & Smaling 2005; Mortimore & Turner 2005).

Several measurable indicators have been proposed to monitor land degradation such as: accelerated soil erosion rates (Stroosnijder 2007); deteriorating soil fertility (Batterbury *et al.* 2002); and long-term and irreversible reductions in vegetation cover or production efficiency (Nicholson *et al.* 1998; Prince *et al.* 1998; Batterbury *et al.* 2002; Prince 2002). However, soil measurements in the Sahel remain few and far between (Niemeijer & Mazzucato 2002; Fleitmann *et al.* 2007). Alternatively, long term and spatially contiguous changes in vegetation cover and its production, which are inherently linked to the major processes that lead to degradation (Prince 2002; Safriel 2007a; Nicholson 2011a), can be monitored using repeated satellite observations (e.g. Prince & Goward 1995; Myneni *et al.* 2002; Hansen *et al.* 2003; Running *et al.* 2004) and maybe able to answer some of the questions raised above.

1.4 Temporal scales for the detection of land degradation

It is generally agreed that human-induced land degradation is a long term process set in motion by inappropriate intensity or type of land use (Prince 2002; Wessels *et al.* 2007; Nicholson 2011a). Land uses which disturb vegetation cover and function may lead to the deterioration of the edaphic factors that contribute to plant growth (Schlesinger *et al.* 1990; Le Houérou 1992; Le Houérou 2002; Prince 2002). If so, the vegetation may transition to a new and less-productive vegetation

domain (Jeltsch *et al.* 1997; Prince 2002). As the degradation process proceeds, several transition domains may exist resulting in progressive and long term reductions in production efficiency (Jeltsch *et al.* 1997; Prince 2002; Nicholson 2011a); a concept that is embodied is state-and-transition models (Briske *et al.* 2005). The occurrence and severity of land degradation depend on the intensity of disturbances and the intrinsic characteristics of the soil, meteorological conditions, topography and post-disturbance land management (Lal *et al.* 1997; Eswaran *et al.* 2001). However, if land use intensity is reduced and vegetation recovers then there has been no degradation in the sense used here (Prince 2002). The time scale of post-disturbance vegetation recovery in the absence of soil degradation varies between biomes but field observations (Valone *et al.* 2002; Valone & Sauter 2005) and modeling studies (Wiegand & Milton 1996; Jeltsch *et al.* 1997; Weber *et al.* 2000) suggest time scales greater than 20 years. Therefore the time scales of observation necessary for monitoring land degradation should be greater than the normal sequence of vegetation recovery and the sequence of cultural practices such as periodic fallow and stocking rate cycles (Prince 2002).

1.5 Remote sensing of vegetation production

The Advanced Very High Resolution Radiometer (AVHRR/2 and /3) instruments carried on NOAA's Polar-orbiting Operational Environmental Satellites (POES) have been providing global daily measurements since 1981 (Robel *et al.* 2009). The Normalized Difference Vegetation Index (NDVI) calculated from the AVHRR red and NIR spectral bands have been found to have a strong linear relationship with the fraction of photosynthetic active radiation absorbed by

12

vegetation canopy (f_{PAR}) (Monteith 1972; Fuchs *et al.* 1984; Goward & Dye 1987; Sellers 1987; Goward & Huemmrich 1992; Myneni & Williams 1994; Sellers *et al.* 1997; Fensholt *et al.* 2006) and with maximum (i.e. unstressed) canopy photosynthetic uptake (Schloss *et al.* 1999; Merbold *et al.* 2009). This relationship has been exploited in light use efficiency (LUE) models to estimate Net Primary Production (NPP). The models require, in addition to f_{PAR}, incident PAR and measurements of the principal environmental stress factors, such as soil moisture, temperature and humidity. This approach (Prince & Goward 1995) has been adopted using the Moderate Resolution Imaging Spectroradiometer (MODIS) data as an operational, global productivity monitoring system (Running *et al.* 2004).

However, in arid and semi-arid areas, growing season sums of NDVI (ΣNDVI) alone, without the other components of a LUE model demanded by theory, have been found to be strongly related to NPP (Prince 1991; Rasmussen 1998; Seaquist *et al.* 2003) and above ground biomass measurements (Prince & Astle 1986; Prince & Tucker 1986; Fensholt *et al.* 2006). The reason for this is that the environmental stressors (e.g. acute water stress, intra-seasonal drought, land degradation) that limit photosynthetic canopy uptake generally induce changes in leaf display and hence in f_{PAR} and NDVI (Gamon *et al.* 1995; Wessels 2005). Similar to many earlier studies in drylands(e.g. Nicholson *et al.* 1990; Nicholson *et al.* 1998; Prince *et al.* 1998; Herrmann *et al.* 2005b; Olsson *et al.* 2005; Camberlin *et al.* 2007; Helldén & Tottrup 2008), growing season sums of NDVI will be used in this study as a proxy of vegetation productivity.

1.6 Monitoring land degradation with satellite remotely sensed data

A number of studies have demonstrated the utility of long term NDVI datasets to detect and monitor human-induced land degradation (e.g. Pickup & Chewings 1994; Geerken & Ilaiwi 2004; Li *et al.* 2004; Wessels *et al.* 2007). These studies have shown that in areas where vegetation production is tightly coupled to seasonal precipitation, human-induced land degradation results in negative temporal trends in vegetation production per unit rainfall. For example, Wessels *et al.* (2007) and Prince *et al.* (2009) found that in contrast to the non-degraded commercial areas, the excessively utilized and degraded communal areas in Zimbabwe and South Africa exhibited negative temporal trends in the ΣNDVI-rainfall relationship. Similar findings have been reported in the Syrian Steppe (Geerken & Ilaiwi 2004; Hirata *et al.* 2005), Australian drylands (Pickup & Chewings 1994) and in the Sahel (Herrmann *et al.* 2005). Nevertheless, precipitation is not the only factor that controls production and poor relations have been reported in the Sahel (Goward & Prince 1995a; Tracol *et al.* 2006; Williams *et al.* 2008; Hiernaux *et al.* 2009b; Hiernaux *et al.* 2009c; Fensholt & Rasmussen 2011) and elsewhere (Fuller & Prince 1996; Knapp & Smith 2001; Reynolds *et al.* 2004b). In areas where rainfall is not the only climatic factor limiting plant growth, negative temporal trends in vegetation production per unit rainfall do not necessarily indicate land degradation (Fensholt & Rasmussen 2011).

Several factors may influence the rainfall-production relationship in drylands. Nicholson *et al.* (1990), Fuller & Prince (1996) and Potts *et al.* (2006), for example, found positive feedbacks between vegetation production and antecedent rainfall at

monthly and interannual timescales. These feedbacks are sometimes likened to a "memory" in land surface processes (Goward & Prince 1995b; Prince & Goward 2000; Wiegand *et al.* 2004) and can arise from purely physical reasons, such as soil moisture carried over from antecedent rainfall (Goward & Prince 1995a; Fuller & Prince 1996) or can result from inter-annual carryover of soil nutrients and seed banks (Lauenroth & Sala 1992; Nouvellon *et al.* 2001; Oesterheld *et al.* 2001). Such relations, however, are complex and feedbacks are not found in all climatic vegetation types (Fuller & Prince 1996; Grist *et al.* 1997). For instance, Reynolds *et al.* (2004a) and Knapp *et al.* (2008) argue that, in most ecosystems, growing-season precipitation should have the most direct impact on vegetation production. On one hand, a large portion of Sahelian precipitation falling at the beginning of the wet season may be lost to evaporation before it can be used for photosynthesis (Huxman *et al.* 2004) and, while early season precipitation event(s) may trigger germination of annual plants, seedling development and culm elongation are aborted unless subsequent rain events allow seedlings to survive and grow (Elberse & Breman 1989; Elberse & Breman 1990; Huxman *et al.* 2004; Hiernaux *et al.* 2009c). On the other hand, precipitation falling after fructification is not used for production by most annuals (Hiernaux *et al.* 2009c) and, while leaves of trees and some shrubs developed early in the growing season are usually retained until late in the season, they typically have lower photosynthetic capacity than younger leaves (Chabot & Hicks 1982).

The frequency and intensity of precipitation events can also influence vegetation production (Noy-Meir 1973; Sala & Lauenroth 1982; Prince *et al.* 1998; Wainwright *et al.* 1999; Jobbagy & Sala 2000; Paruelo *et al.* 2000; Knapp & Smith

2001; Knapp *et al.* 2002; Reynolds *et al.* 2004b; Schwinning & Sala 2004; Knapp *et al.* 2008; Williams *et al.* 2008; Heisler-White *et al.* 2009; Robertson *et al.* 2009) either by altering soil moisture levels (Lebel *et al.* 2003; Knapp *et al.* 2008; Good & Caylor 2011) or nutrient availability (Belnap *et al.* 2005) or both. A number of field experiments in North American grasslands and shrublands have demonstrated the sensitivity of vegetation production to an intensified precipitation regime (Jobbagy & Sala 2000; Paruelo *et al.* 2000; Knapp & Smith 2001; Knapp *et al.* 2002; Heisler-White *et al.* 2009; Robertson *et al.* 2009). For the same amount of total rainfall, vegetation production in dry biomes have been found to respond positively to more intense and less frequent precipitation events, whereas in the wetter biomes vegetation production have been found to decrease in response to an intensified precipitation regime (Knapp & Smith 2001; Knapp *et al.* 2002; Heisler-White *et al.* 2009). Modeling studies suggest that this asymmetrical response to precipitation regimes is mainly due to differences between biomes in the proportional losses of precipitation to evaporation and runoff (Reynolds *et al.* 2004b; Knapp *et al.* 2008).

In addition to the timing, frequency and intensity of precipitation events, air humidity and temperature can also affect vegetation production either directly by influencing stomatal conductance and photosynthetic reaction rates (Collatz *et al.* 1991; Collatz *et al.* 1992; Reichstein *et al.* 2007; Williams *et al.* 2008) or indirectly by altering soil evaporative demands (Xue *et al.* 1991a; Reichstein *et al.* 2007). By analyzing eddy-covariance measurements across a range of vegetation types and climate zones in Africa, Merbold et al. (2009) found strong relations between net photosynthetic accumulation by C_3-plants and vapor pressure deficit but these

relations were poor to non-existent at the C_4-plant dominated sites. These and land surface modeling studies that have investigated the relative influence of climatic factors on vegetation production have indicated that in addition to precipitation, air humidity (Williams *et al.* 2008) and temperature (Beer *et al.* 2010) may play an important, yet secondary role in limiting vegetation production in drylands.

Similar to many earlier studies (e.g. Goward & Prince 1995a; Tracol *et al.* 2006; Williams *et al.* 2008; Hiernaux *et al.* 2009b; Hiernaux *et al.* 2009c), Fensholt & Rasmussen (2011) found that the inter-annual variations in vegetation production were poorly explained by annual rainfall totals. It is very likely that in addition to precipitation, other climate factors acted synergistically to influence vegetation production by altering soil moisture levels (Sala *et al.* 1988; Epstein *et al.* 1997; Lebel *et al.* 2003; Reichstein *et al.* 2007; Knapp *et al.* 2008; Good & Caylor 2011), nutrient levels (Belnap *et al.* 2005), and stomatal resistance and photosynthetic reaction rates (Collatz *et al.* 1991; Collatz *et al.* 1992; Williams *et al.* 2008; Merbold *et al.* 2009; Beer *et al.* 2010). This suggests that it might be necessary to account for climate factors other than precipitation alone in order to distinguish between climate-induced fluctuations in vegetation production and human-induced changes which are generally more subtle and gradual (Evans & Geerken 2004; Fensholt & Rasmussen 2011).

It is unlikely that any stand-alone remote sensing-based method will be able to unequivocally map human-induced land degradation. In addition, the evaluation of these methods has proven difficult owing to the paucity of field validation data (Batterbury *et al.* 2002; Wessels *et al.* 2008). Also, remotely sensed indicators

provide little if any information on the social processes that give rise to degraded landscapes. To complement the monitoring process, Batterbury *et al.* (2002) and Nicholson (2011a) argue that it is important to identify the human factors that act as drivers to degradation not only to alert officials to unsustainable land use practices but also to determine whether long term reductions in production efficiency are in fact human-induced. Recent studies have produced highly resolved spatial data on human demographics and anthropogenic uses of the land (Imhoff *et al.* 2004; CIESIN 2005; Robinson *et al.* 2007; Ramankutty *et al.* 2008). These data, together with remotely sensed indicators of land degradation, can be used to investigate the spatial component of demographic and anthropogenic land use pressures.

1.7 Research Objectives

The fundamental goal of this dissertation is to examine whether there is evidence of human-induced land degradation in the Sahel and, if so, its location and intensity. The general hypothesis was that long-term negative trends in production efficiency can be used to detect human-induced land degradation. To test whether the negative trends were in fact human-induced, they were compared with the available data on population density, land use and land biophysical properties that determine the susceptibility of land to degradation.

The following specific research objectives were addressed:

1. Characterize the correlations between remote sensing estimates of vegetation production and the meteorological variables, namely precipitation, seasonal precipitation distribution, air humidity and temperature. (Chapter 2)

18

2. Explore the biophysical mechanisms of vegetation response to climate variability at the process level using a Soil-Vegetation-Atmosphere Transfer (SVAT) model. (Chapter 2)

3. Identify any long term trends in vegetation production which are not caused by natural ecological adjustments to episodic droughts and changes in air humidity and temperature. (Chapter 3)

4. Explore the relationship between long-term trends in vegetation production, population density, human appropriation of NPP, livestock, and cropping. (Chapter 4)

1.8 Outline of Dissertation

This dissertation consists of five chapters. Chapter 1 introduces the topic of land degradation, reviews the ongoing debate on the extent, severity and causes of land degradation in the Sahel and sets the research objectives. In Chapter 2, the relationship between growing season sums of daily AVHRR NDVI data (ΣNDVI) and meteorological variables from 1982 to 2006 are characterized for the study area. This was done to identify the meteorological variables that influence vegetation production. The biophysical mechanisms that can explain the observed relationship are explored using a SVAT model.

In Chapter 3, the ΣNDVI-climate relationships were used to estimate potential ΣNDVI for each year in the satellite record; that is the ΣNDVI expected from the response of vegetation to climate variability alone excluding other factors that limit

vegetation production, including human land use. The residuals (observed – potential ΣNDVI) were used to normalize for the effects of climate variability on vegetation production (Prince 2002; Geerken & Ilaiwi 2004). Significant negative residual trends were then mapped to identify areas where there may be human-induced land degradation. This approach is similar to the method which was used to identify negative trends in the production-rainfall relationship in the degraded areas of South Africa and Syria (Prince 2002; Hirata *et al.* 2005; Wessels *et al.* 2007) but extends the climatic controls to include in addition to rainfall the other meteorological variables that were found to influence vegetation production. However, it should be stressed that even when NDVI or NPP falls below the potential set by the meteorological conditions, the cause is not necessarily human-induced.

Chapter 4 compares the residual trend maps with the available data on population density and land use to investigate whether the type and intensity of land use is associated with negative trends in vegetation production. Furthermore, chapter 4 investigates whether the influence of land use varies with the geography of land biogeophysical properties that determine the resilience of land to degradative processes. Chapter 5 summarizes the findings, discusses the limitations of remotely sensed estimates of land degradation, and how these limitations may be addressed in future research. Finally, the methods used for the reconstruction of daily AVHRR NDVI data are presented in Appendix I.

Chapter 2: Vegetation responses to climate variability

2.1 Introduction

The effect of climate variation on vegetation production is a major research focus in African drylands (Fuller & Prince 1996; Olsson *et al.* 2005; Hiernaux *et al.* 2009c) and elsewhere (Goward & Prince 1995a; Fang *et al.* 2001; Nemani *et al.* 2003). More recently, interest has intensified as global circulation models project an increase in inter-annual precipitation variation, higher temperatures, and an intensified precipitation regimes (through larger individual precipitation events) with longer intervening dry periods than at present (Easterling *et al.* 2000; IPCC 2007).

Vegetation production in drylands is often assumed to be closely related to inter-annual rainfall variability (Le Houérou *et al.* 1988; Herrmann *et al.* 2005a). Le Houérou (1984) suggested that the ratio of NPP to precipitation (Rain Use Efficiency, RUE) in drylands has a stable value (≈4 kg dry matter/ha/year/mm rainfall). Wessels *et al.* (2007) and Nicholson *et al.* (1990) found moderate to strong linear relationships between rainfall and vegetation production in parts of arid and semi-arid South Africa and the Sahel. Nevertheless, precipitation is not the only factor that controls production and poor relations have been reported in the Sahel (Goward & Prince 1995a; Tracol *et al.* 2006; Williams *et al.* 2008; Hiernaux *et al.* 2009b; Hiernaux *et al.* 2009c; Fensholt & Rasmussen 2011) and elsewhere (Fuller & Prince 1996; Knapp & Smith 2001; Reynolds *et al.* 2004b).

In drylands, soil properties, the frequency and intensity of rainfall events, air humidity and temperature combine to influence vegetation production (Noy-Meir

1973; Prince *et al.* 1998; Sankaran *et al.* 2005; Williams *et al.* 2008; Good & Caylor 2011) by altering infiltration rates, evaporative demands, nutrient availability and leakage losses from the soil column (Sala *et al.* 1988; Epstein *et al.* 1997; Lebel *et al.* 2003; Reichstein *et al.* 2007; Knapp *et al.* 2008; Good & Caylor 2011). Furthermore, air humidity and temperature may also directly influence vegetation production by altering stomatal resistance and photosynthetic reaction rates (Collatz *et al.* 1991; Collatz *et al.* 1992; Williams *et al.* 2008; Merbold *et al.* 2009; Beer *et al.* 2010).

While several remote sensing studies have investigated the nature of the relation between NDVI (used as a proxy of vegetation productivity) and rainfall in the Sahel (e.g. Nicholson *et al.* 1990; Nicholson *et al.* 1998; Prince *et al.* 1998; Herrmann *et al.* 2005b; Olsson *et al.* 2005; Camberlin *et al.* 2007; Helldén & Tottrup 2008), only few studies have expanded beyond that to include other meteorological variables that might influence vegetation production (Nemani *et al.* 2003; Beer *et al.* 2010).

The purpose of this study was twofold; (i) to characterize empirically the nature of the relationship between remotely sensed estimates of vegetation production and climate variability and (ii) to explore, using a land surface model, the underlying hydraulic and biophysical processes to which these relationships can be attributed.

Bias-corrected-hybrid meteorological datasets constructed by combining a suite of global observation-based datasets with numerical weather prediction and assimilation models are becoming available at higher temporal and spatial resolutions (Sheffield *et al.* 2006). These, along with recent developments in Advanced Very

High Resolution Radiometer (AVHRR) data processing (Pedelty *et al.* 2007), provided the opportunity to expand on previous studies of vegetation responses to climate variability (Nicholson *et al.* 1990; Helldén 1991; Olsson & Rapp 1991; Nicholson 2001; Nemani *et al.* 2003; Herrmann *et al.* 2005a; Olsson *et al.* 2005; Helldén & Tottrup 2008; Hiernaux *et al.* 2009c; Beer *et al.* 2010).

While the empirically derived relationships may reveal the direction and magnitude of vegetation responses to climate variation, they offer little understanding of the underlying biophysical processes to which these relations can be attributed. To address this problem, a land surface model was used to explore these processes. The model selected was the Simplified Simple Biosphere (SSiB2 ver.2) (Xue *et al.* 1991b; Zhan *et al.* 2003). SSiB2 is a process-oriented model that simulates explicitly the interactions between climate, soil, and plants. In SSiB2, the rates of carbon sequestration change with temperature, the proportion of incident photosynthetically active radiation absorbed by green vegetation (fPAR), and intracellular CO_2 concentration. The Farquhar and Collatz (Farquhar *et al.* 1980; Collatz *et al.* 1991; Collatz *et al.* 1992) formulations are used to model CO_2 uptake within the leaf. CO_2 uptake at the canopy scale is regulated by stomatal conductance which, in turn, is limited by stress multipliers of air-to-leaf vapor pressure deficit and soil moisture (Zhan *et al.* 2003). The focus of the modeling approach was to investigate, in different climates and for different vegetation types, the sensitivity of soil moisture, leaf temperature, and stomatal conductance to changes in precipitation, temperature, and humidity and whether climate-induced changes in soil moisture, stomatal conductance and leaf temperature, if any, influence vegetation production.

Establishing the relationship between remotely sensed estimates of vegetation production and meteorological variables is essential for developing a reliable land degradation monitoring approach that is capable of distinguishing human-induced land degradation from climate-induced vegetation dynamics (Reynolds 2001; Prince 2002; Geerken & Ilaiwi 2004).

2.2 Material and Methods

2.2.1 Remote sensing data

Version 2 of the Long-term Data Record (LTDR) daily time series of the National Oceanic and Atmospheric Administration (NOAA) AVHRR Global Area Coverage (GAC) reflectance data (Pedelty *et al.* 2007) for the years 1982 to 2006 were used in this study (http://ltdr.nascom.nasa.gov). While the spatial resolution of the AVHRR instrument is ~1.1 km at nadir, the NOAA satellites transmit the reduced resolution (~4.4 km) GAC data generated onboard by averaging the reflected radiances from a sample of four out of every five measurements along every third scan line (i.e. a sampling frequency of 4 out of every 15 measurements) (Kidwell 1998). The LTDR data processing stream ingests the GAC data from NOAA satellites 7,9,11 and 14 and creates a daily reflectance product using a geographic projection at a spatial resolution of 0.05°. LTDR data processing includes a vicarious sensor calibration of the red (0.58–0.68 μm) and near infrared (0.725–1.10 μm) channels using cloud/ocean techniques to remove variations caused by changes in sensors and sensor drift (Vermote & Kaufman 1995; Vermote & Saleous 2006a). LTDR processing also includes an improved atmospheric correction scheme to reduce

the effects of Rayleigh scattering, ozone, and water vapor but does not include corrections for the effects of aerosols (Pedelty *et al.* 2007).

For the present study, the LTDR reflectances in the red (0.58–0.68 μm) and near infrared (NIR) (0.725–1.10 μm) were: (1) spatially aggregated to 0.15° (3x3 pixels); (2) normalized to a standard sun-target-sensor geometry; and (3) filtered for cloud-contaminated observations which were then replaced with reconstructed values interpolated from preceding and succeeding clear-sky observations. An account of the Bidirectional Reflectance Distribution Function (BRDF) correction, cloud filtering, and interpolation procedures is given in Appendix 1. Daily NDVI values were subsequently calculated (NDVI = (NIR-red) / (NIR+red)).

Spatial aggregation to 0.15° reduces most of the errors introduced by the GAC sampling scheme (Rembold & Maselli 2010) and aggregation to 0.25° or 0.35° only results in marginal further improvements (Nagol 2011). Because of this, analyses of the AVHRR data were conducted at 0.15° spatial resolution.

BRDF and atmospheric corrections reduce noise in surface NDVI data (Nagol *et al.* 2009) that would otherwise result from the strong bidirectional properties of vegetation (Gutman 1991; Vermote *et al.* 2009a; Fensholt *et al.* 2010) and the considerable absorption in the AVHRR NIR channel by atmospheric water vapor (Cihlar & Howarth 1994). The resulting daily data were intended to enable more precise identification of vegetation dynamics (Viovy *et al.* 1992) than maximum value compositing (generally 10 days or monthly), particularly in the drier areas with short growing season.

2.2.2 Meteorological data

The Princeton Hydrology Group (PHG) 1.0° dataset of daily precipitation, surface air temperature, specific humidity, atmospheric pressure and incident solar radiation (Sheffield *et al.* 2006) were used in this study. The dataset is constructed from the NCEP–NCAR[2] reanalysis data and corrected for biases using observation based datasets of precipitation and air temperature. Daily data for the period 1982-2006 were downscaled from 1° to the 0.15° resolution of the AVHRR dataset using bilinear interpolation.

2.2.3 Estimating phenological transition dates and the length of the growing season

The rates of change of daily NDVI data were used to define key phenological transition dates of the growing season (Zhang *et al.* 2003). These were the "onset of greenness increase", the "onset of maturity", the "onset of greenness decrease", and the "onset of dormancy", hereafter referred to as green-up, maturity, senescence and dormancy; respectively. Green-up is the date when NDVI begins to increase rapidly indicating the onset of leaf development. Maturity is the date when the rate of increase in NDVI slows and NDVI approaches its maximum indicating peak green leaf area. Senescence is the date when NDVI begins to decrease rapidly indicating leaf senescence. Dormancy is the date when NDVI approaches its minimum annual value owing to death of annuals and suspension of growth and true dormancy in perennials.

---

[2] NCEP-NCAR: National Center for Environmental Prediction(NCEP)–National Center for Atmospheric Research(NCAR)

To estimate the phenological transition dates, piecewise sigmoid functions (equation 2.1) were fitted to periods of sustained NDVI increase (i.e. growth) and decrease (i.e. senescence). The rates of change in the curvature of the fitted sigmoid functions (i.e. the second derivative) were then calculated. During the period of sustained NDVI increase, the local maxima of the second derivative were used for the dates of green-up and maturity, and the local minima of the second derivative during the period of sustained NDVI decrease were used for senescence and dormancy (Zhang *et al.* 2003). The phenological transition dates were compared with MODIS Land Cover Dynamics Science Dataset Collection 4 (Zhang *et al.* 2006) during the overlapping period (2002-2006).

$$y(t) = \frac{c}{1 + e^{a+bt}} + d \dots eq(2.1)$$

where *t* is time in days, *y(t)* is the NDVI value at time *t*, *a* and *b* are fitting parameters, *d* is the initial minimum NDVI value and *c+d* is the maximum NDVI value.

The onset of leaf development and leaf senescence were then used to define the timing and duration of the growing season. Annual and growing season sums of daily NDVI, precipitation, temperature, and humidity were calculated for each year (1982-2006).

2.2.4 Relationship of annual ΣNDVI with annual total precipitation

The relationships of annual and growing season sums of precipitation and ΣNDVI were characterized using linear regressions for every three by three pixels. The coefficients of determination (r^2) were mapped to show the geographical patterns

of the ΣNDVI -total precipitation relationships for the entire year and for the growing season alone.

2.2.5 Relationship of growing season ΣNDVI with intraseasonal precipitation distribution

A series of small precipitation events may have a different effect on vegetation production than an equivalent amount of rainfall occurring in a few intense events (Reynolds *et al.* 2004b; Good & Caylor 2011). To describe the statistical manner by which precipitation arrived on the landscape, two higher order moments of intraseasonal precipitation distribution were calculated from daily precipitation data. These were the growing season precipitation variance and its skewness. Summary statistics were used since it is impractical to specify explicitly the enormous number of seasonal patterns of rainfall frequency and amount that can occur for more than a few pixels. High precipitation distribution variance indicates higher than normal deviation from mean seasonal precipitation and can result from extended periods of drought or from intense precipitation events or a combination of both, while the skewness is a measure of the dominant frequency of either high intensity precipitation events (negative skewness) or low intensity precipitation events (positive skewness).

The relation of growing season ΣNDVI to seasonal precipitation totals, precipitation variance and skewness were characterized using multivariate linear regression analysis. To reduce the effects of multicollinearity between input variables and consequent overfitting (Dielman 2005), a subset of independent variables that 'best' explained ΣNDVI variation were selected for each 3 by 3 pixels using the computational approach of (Furnival & Wilson 1974).

The computational approach of (Furnival & Wilson 1974) searches for the variable subsets with the highest r^2 value adjusted for degrees of freedom (adjusted r^2). The variables of the regression model with the highest adjusted r^2 were tested for multicollinearity and the model regression coefficients were tested to determine whether they were significantly different from zero. To test for multicollinearity, the variance inflation factors (VIFs) of the model independent variables were evaluated relative to the r^2 value of the model (Dielman 2005a).   Multicollinearity was considered strong enough to affect the model coefficient estimates whenever any of the VIFs was larger than $1/(1- r^2)$ (Freund & Wilson 1998).   A t-test was used to test the null hypothesis that the model regression coefficients $B_{kl...n}$ were equal to zero. If there was insufficient evidence to reject the null hypothesis ($H0_{kl...n}$: $B_{kl...n} = 0$, $p >$ 0.05) or if multicollinearity was strong enough to affect model estimates then the regression model with the second to highest adjusted r^2 was subjected to the same tests. The procedure was repeated until the test conditions were met.

2.2.6 Relationship of growing season ΣNDVI with intraseasonal precipitation distribution

The relationships of growing season ΣNDVI and seasonal precipitation totals, specific humidity and air temperature were characterized by regression analysis using the same computational approach described in the previous section. Furthermore, the three meteorological variables and the ΣNDVI data were standardized to zero mean and a standard deviation of one. The standardized regression coefficients were then estimated to measure the relative contribution of each meteorological variable to the observed ΣNDVI variation.   The standardized regression coefficients were summarized by the landcover types in the study area (Friedl *et al.* 2002) in order to

29

characterize the relative contribution of each of the meteorological variables to the observed NDVI variation in grasslands, shrublands, and savannas.

2.2.6 Soil-vegetation-atmosphere transfer modeling
2.2.6.1 Model description

The Simplified Simple Biosphere (SSiB2 ver.2) land surface model (Xue *et al.* 1991b; Zhan *et al.* 2003) was used in its "offline" mode to represent ecosystem physiology as driven by prescribed meteorology and vegetation phenology. SSiB2 is a simplified version of the Simple Biosphere model (SiB) originally designed by (Sellers *et al.* 1986). SSiB2 models vegetation as a single layer instead of the two in SiB, and implements a less computationally expensive scheme to calculate aerodynamic resistance. In addition, the prognostic equations in SiB that relate stomatal conductance to soil moisture and calculate the diurnal variation in radiation absorption and albedo are replaced with empirical relations that require fewer parameters. SSiB2 replaces Jarvis' empirical approach for the estimation of stomatal conductance (Jarvis 1976) with a modified version of Farquhar et al. (1980) biochemical photosynthesis model (Collatz *et al.* 1991; Collatz *et al.* 1992), scaled by the canopy integration scheme of (Zhan *et al.* 2003) and coupled to the Ball-Berry semi-empirical stomatal conductance model so that stomatal conductance and canopy net photosynthesis are estimated simultaneously. In the model, the rate of photosynthesis changes with temperature, f_{PAR}, and intercellular CO_2 concentration. The latter is regulated by stomatal conductance. Stomatal conductance is limited by stress multipliers of air-to-leaf vapor pressure deficit and soil moisture (Zhan *et al.* 2003). The SSiB2 standard model parameters have been refined for several soils and vegetation functional types (Chen *et al.* 1996; Xue *et al.* 1996a; Xue *et al.* 1996b;

Schlosser *et al.* 1997; Zhan *et al.* 2003; Sun & Xue 2004), including some of those found in the Sahel region (Kahan *et al.* 2006).

Parameterization and validation studies and land surface model inter-comparison experiments (Robock *et al.* 1995; Wetzel *et al.* 1996; Liang *et al.* 1998; Lohmann *et al.* 1998; Wood *et al.* 1998) have demonstrated that SSiB2 can reasonably reproduce measured energy and water fluxes at diurnal, seasonal, and multi-annual scales across diverse climates and vegetation functional types.

2.2.6.2 Sensitivity experiments

SSiB2 was used to explore the underlying hydrological and physiological processes to which the empirical relationships, revealed in the statistical analysis of co-variation between meteorology and vegetation productivity, can be attributed. The model was run for the period 1999–2007 with a 3-hourly time step for a number of sites representative of different vegetation types and climatologies throughout the Sahel (table 2.1). Model inputs for the base run were Princeton Hydrology Group meteorology, LAI and fraction vegetation cover (Baret *et al.* 2007).

To investigate the sensitivity of vegetation to precipitation variation during the early stages of phenological development (i.e. greenup to maturity), SSIB2 was run eight times with the precipitation data modified for the corresponding period (±0.5, ±1, ±1.75 and ±2.5 standard deviations from the values used in the base run; changed values that exceeded the range of long term (1982-2007) natural meteorological variation were reset to the minimum and maximum of observed meteorological variation, as appropriate) while keeping the remaining meteorological variables

unchanged. The sensitivity experiments were repeated for the maturity stage (i.e. from maturity to senescence). The same approach was used to investigate the sensitivity of vegetation to changes in humidity and temperature. The resulting changes in soil moisture and stomatal conductance and their relation to canopy scale net photosynthesis were summarized at a daily time step and averaged over each of the two stages of phenological development.

Location name	Land cover	Latitude	Longitude	Elevation (m)	Growing season mean and standard deviation of cumulative precipitation (mm)	Growing season mean and standard deviation of daily temperature (°K)	Growing season mean and standard deviation of daily specific humidity values (g H2O/kg dry air)	Maximum LAI and its interannual variation	Mean length of GUMA (Days)	Mean length of MASE (Days)
Koumbi Saleh	Grasslands	15.775°N	10.175°W	187	300±60	303.6±0.71°K	18±1.0	1.39±0.37	75±23	21±3
Fadjé	Shrublands with grass ground cover	11.625°N	15.925°E	325	410±99mm	301.2±0.64°K	16±0.8	2.79±0.35	66±21	38±10
Kem Kem	Cropland	12.075°N	37.825°E	1870	678±103	292.7±0.52°K	13±0.5	2.51±0.13	65±18	72±11
Abyie	Woody savannas	09.525°N	28.425°E	400	792±110	301.3±0.70°K	21±1.0	2.40±0.20	95±15	70±12
Quarda Djallé	Savannas with grass ground cover	08.775°N	22.375°E	682	861±108	299.5±0.62°K	18±0.6	3.25±0.25	128±11	105±11

Table 2.1 Information on sites used for sensitivity studies. GUMA: the period of Greenup to maturity. MASE: the period of Maturity to senescence.

2.3 Results

2.3.1 Phenological transition dates

For the transition dates of greenup, maturity and senescence, the comparison between the AVHRR and MODIS (Zhang *et al.* 2006) measurements revealed a good agreement with root mean square errors only slightly higher than the reported accuracies of the MODIS products (Zhang *et al.* 2003; Zhang *et al.* 2006). However, the measurements of the dormancy transition dates did not agree and the root mean square error (RMSE = 29 days) of the dormancy comparison was one order of magnitude higher than the RMSE values for greenup, maturity and senescence (figure 2.1). This is perhaps due to the less pronounced transitions in the rates of change in NDVI curvature towards the end of the growing season which renders derivatives of the dormancy dates more sensitive to errors in NDVI measurements.

The greenup transition dates were characterized by a pronounced north-south gradient with greenup detected as early as February at lower latitudes (7.5^{o}N) and as late as August at higher latitudes (17.5^{o}N). The senescence transition dates also had a pronounced north-south gradient but with the dates detected earlier at higher latitudes (late August) than at lower latitudes (late October). Both dates were found to vary between years with grasslands in the arid region showing the highest temporal variability in greenup dates. On average, the length of the growing season (the difference between the two dates) varied from approximately 20 days at the southern edge of the Sahara desert to approximately 250 days in the wetter parts of the study area (figure 2.2).
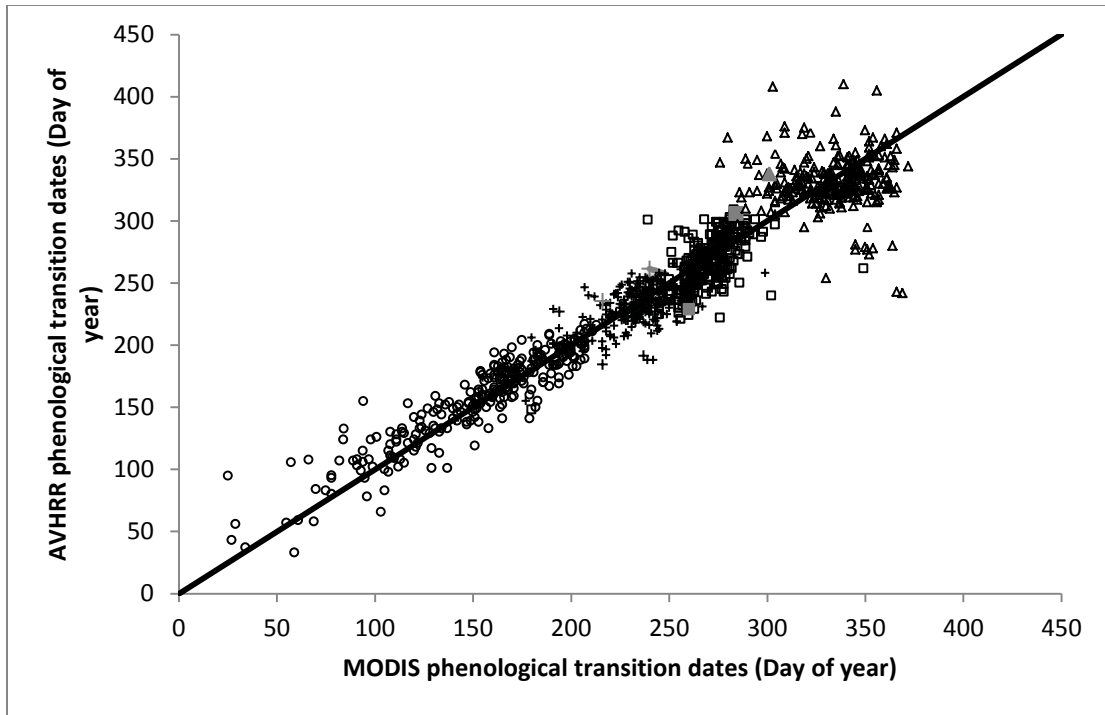
Figure 2.1 Scatter plot of MODIS and AVHRR phenological transition dates of 250 randomly selected points from the study area. Open circles (○) represent the dates of onset of greenness increase (RMSE = 15.5 days, r=0.89). Crosses (+) represent the dates of onset of maturity (RMSE = 14.9 days, r = 0.71). Open squares (□) represent the dates of onset of greenness decrease (RMSE = 17 days, r = 0.63). Open triangles (Δ) represent the dates of onset of dormancy (RMSE = 29 days, r = 0.2).
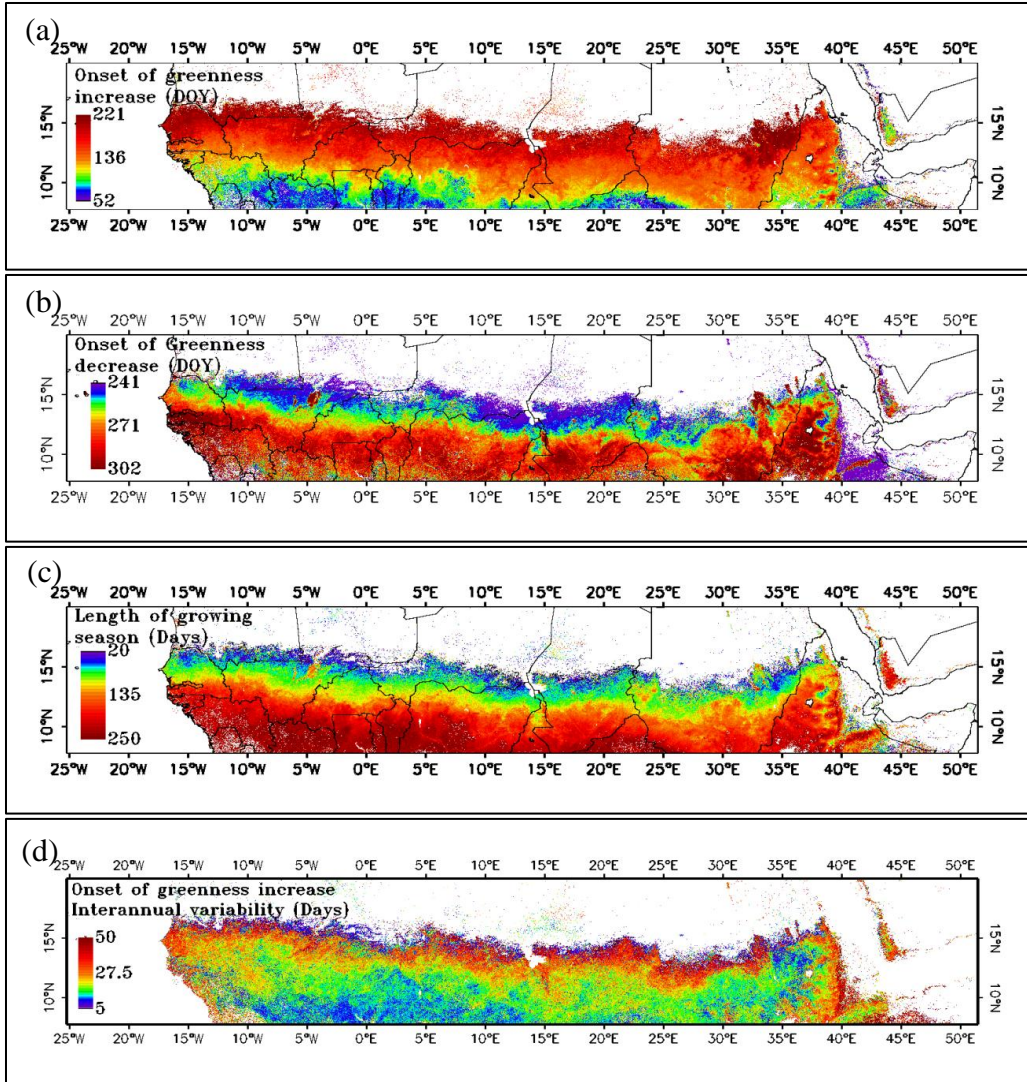
Figure 2.2 Spatial variation in averaged values (1982-2006), of (a) greenup "onset of greenness increase", (b) senescence "onset of greenness decrease", and (c) length of growing season (days). The map in (d) is the between years variation (±2 standard deviations) in the onset date of greenness increase. The abbreviation DOY is the Julian day of the year.

2.3.2 Relationship of NDVI with rainfall

The relationships of annual and growing season sums of rainfall and NDVI differed in strength and to some extent in their spatial patterns. The growing season rainfall-ΣNDVI relationships were generally the stronger one (figure 2.3). The

growing season rainfall-ΣNDVI relationships were significant[3] in approximately 58%

of the study area whereas the annual rainfall-ΣNDVI relationships were significant in

37% of the study area.

A belt of significant annual ΣNDVI-rainfall relationships was evident around

the 700mm rainfall isohyet (figure 2.3a). However, areas receiving less than 400mm

rainfall/year and areas receiving more than 1000mm rainfall/year were generally

characterized by insignificant relationships (figure 2.4).   On average, stronger

growing season ΣNDVI-rainfall relationships were found in the arid and semi-arid

areas with shrubland and grassland landcover ($r^2 = 0.43\pm0.17^4$) than in sub-humid

areas with woody savanna land cover ($r^2 = 0.3\pm16^4$).
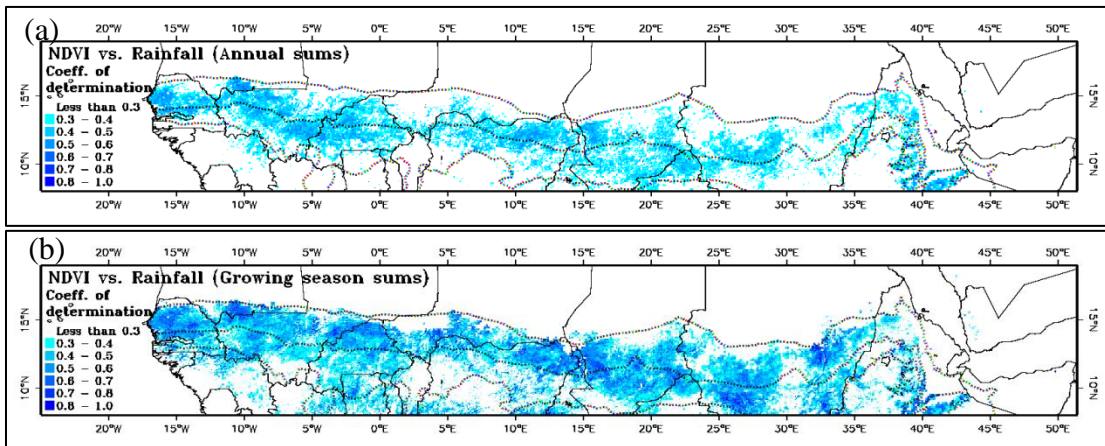
Figure 2.3 Coefficients of determination (r^2) for (a) annual rainfall-ΣNDVI and (b)
growing season rainfall-ΣNDVI regressions. The dashed lines from north to south are
the 300mm, 700mm and 1100mm rainfall isohyet.

---

[3] Critical t-values calculated for each pixel indicated that, in general, regressions with r^2 values greater
than 0.3 were significant ($p<0.05$).
[4] Mean ± one standard deviation
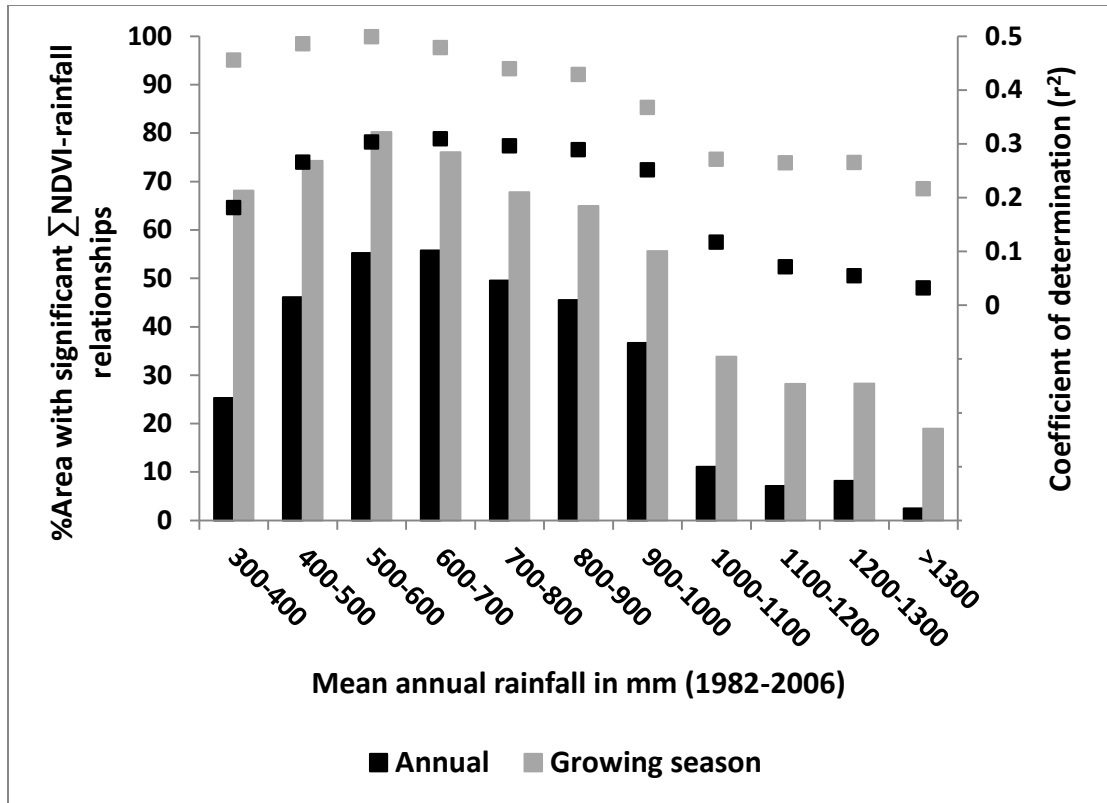
Figure 2.4 Percentage area with significant ΣNDVI-rainfall relationships (bars) in each rainfall range and the spatial average of the coefficient of determination (r^2) values (points) of all pixels within each rainfall range.

2.3.3 Relationship of growing season ΣNDVI with intraseasonal precipitation distribution

The multivariate regressions between ΣNDVI, total growing season rainfall and the two moments of rainfall distribution (variance and skewness) provided robust yet simple statistical models of NDVI variation (figure 2.5a). Compared to the growing season ΣNDVI-rainfall relationships, adding the two moments increased the ability of the models to explain NDVI variation (figure 2.5b). The changes in percentage variance explained varied spatially but these were not significantly related to either the aridity gradient or to the spatial distribution of land cover types.
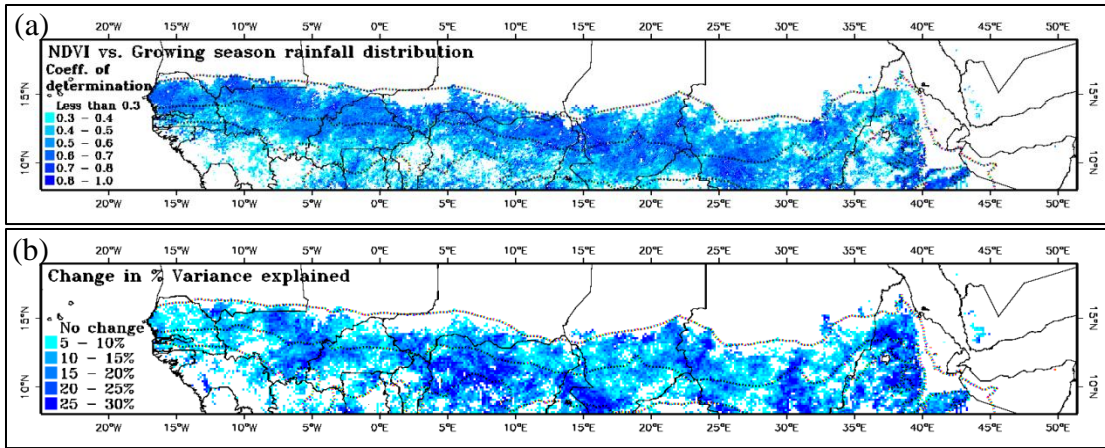
Figure 2.5 Spatial distributions of (a) the coefficients of determination (adjusted r^2) for the multiple regression of ΣNDVI on total growing season rainfall, its variance and its skewness. (b) The change in the percentage of variance explained by including the additional variables over the percentage variance of ΣNDVI and rainfall alone. The dashed lines from north to south are the 300mm, 700mm and 1100mm rainfall isohyet.

The coefficients of the multivariate linear regressions quantified the direction and magnitude of the relationship between precipitation distribution and growing season NDVI.   In general, growing season NDVI was positively related to precipitation totals and to the skewness of precipitation distribution but negatively related to its variance which suggest that, for a given precipitation total, the seasonally summed NDVI values were higher when precipitation arrived in more frequent and less intense precipitation events (figure 2.6).
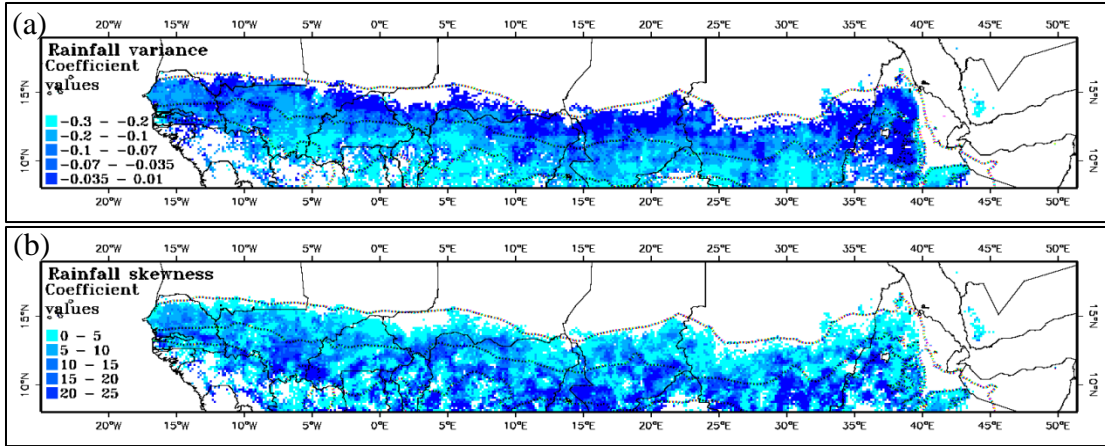
Figure 2.6 Coefficients of (a) seasonal rainfall variance, and (b) seasonal rainfall skewness obtained from the multivariate regressions of growing season ΣNDVI on total seasonal precipitation, precipitation variance and skewness. Missing values (white pixels) are areas with high multicollinearity between explanatory variables, or where the coefficients were insignificantly different from zero ($p>0.05$). The dashed lines from north to south are the 300mm, 700mm and 1100mm rainfall isohyet.

2.3.4 Relationship of growing season ΣNDVI with humidity and temperature

The adjusted r^2 of the multivariate regressions of growing season ΣNDVI on total growing season precipitation, specific humidity and temperature are shown in figure 2.7a. Compared to the growing season ΣNDVI-rainfall relationships, adding specific humidity and temperature increased the ability of the models to account for NDVI variation (figure 2.7b). On average, the largest gains in the percentage NDVI variance explained were to the south of the 700 mm rainfall isohyet (figure 2.7b). However, the relationships remained insignificant in the humid coastal Guinean zone. This might be due to the saturation of NDVI at high values of LAI (Sellers 1987; Malo & Nicholson 1990), to the persistence of cloud cover which adversely affects the quality of ΣNDVI values (Nagol 2011a), or to the influence of other climatic and

non-climatic factors on NPP, such as low plant nutrient availability or low incident photosynthetic radiation (Davenport & Nicholson 1993; Beer *et al.* 2010).
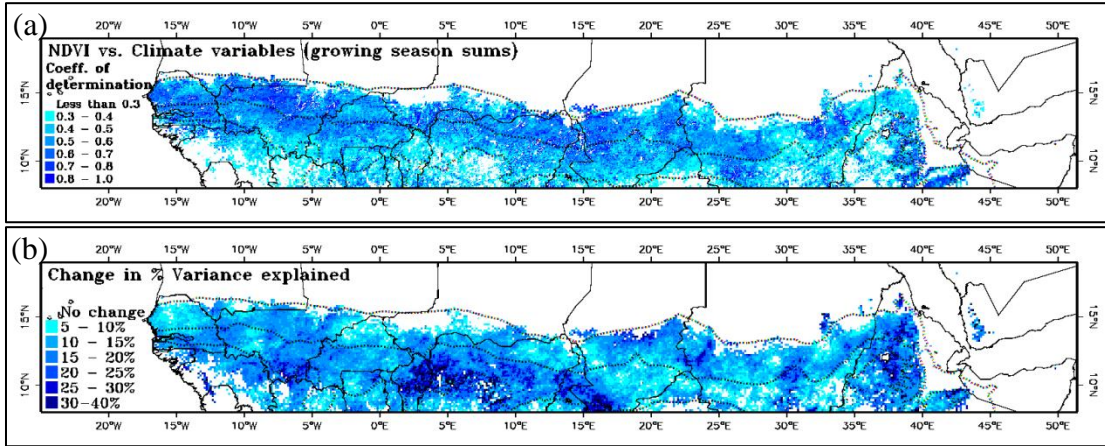
Figure 2.7 Adjusted r^2 for (a), the relation of ΣNDVI with total growing season rainfall, air humidity and temperature. (b) The change in the percentage of variance explained by including the additional variables over the percentage variance of ΣNDVI and rainfall alone. The dashed lines from north to south are the 300mm, 700mm and 1100mm rainfall isohyet.

The regression coefficients calculated for every grid cell provided a statistical estimate of the mean rate of change in ΣNDVI in relation to variations in rainfall, humidity, and temperature. The highest precipitation coefficient values ($0.08 - 0.1$ $ΣNDVI.mm^{-1}$) were evident in the arid margins whereas the lowest (0.01-0.02) were in the wetter parts of the study area (figure 2.8a). Conversely, the humidity coefficient values were generally the lowest in the northern arid zone (figure 2.8b). The temperature coefficient values, on the other hand, differed in sign with spatially coherent positive ΣNDVI relations to temperature evident in the Bongos mountain range (in western Southern Sudan and northern Central African Republic) and in northern Ethiopian highlands (figure 2.8c), while negative ΣNDVI relations to temperature were more common in the arid zone (300-700mm).
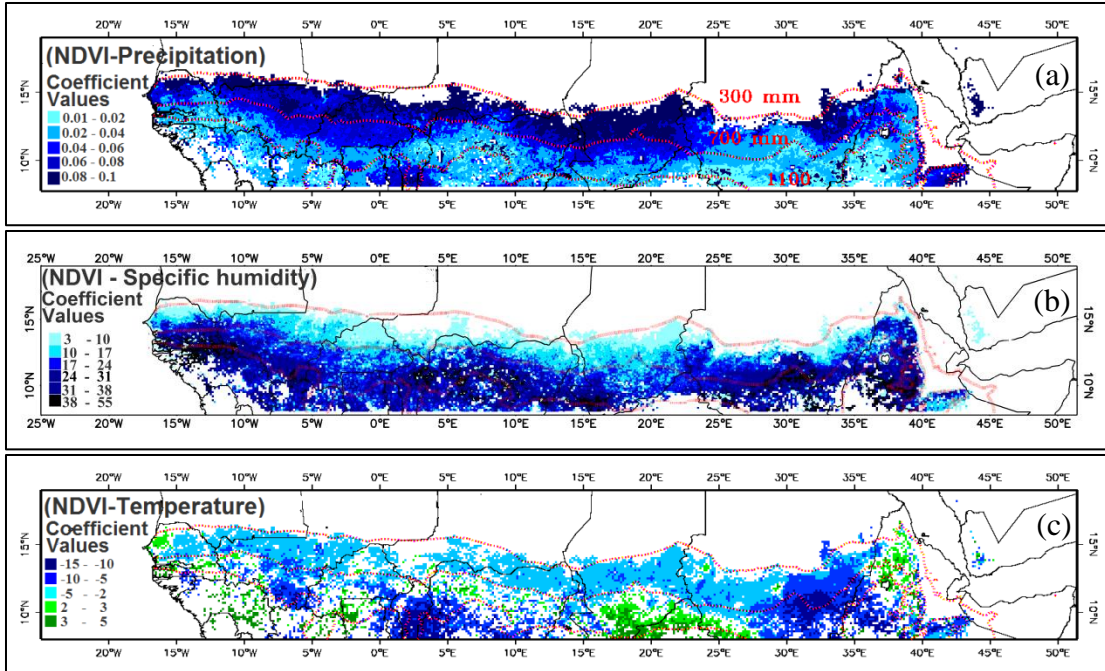
Figure 2.8 Regression coefficients of (a) specific humidity, and (b) air temperature obtained from the multivariate regressions of growing season ΣNDVI on precipitation, specific humidity and temperature. Missing values (white pixels) are areas with high multicollinearity between explanatory variables, or where the coefficients were insignificantly different from zero ($p>0.05$). The dashed lines from north to south are the 300mm, 700mm and 1100mm rainfall isohyet.

A negative exponential pattern emerged when the precipitation coefficients were plotted against rainfall climatology (figure 2.9a). However, there were some wet sites with comparatively high precipitation coefficients (green circle; figure 2.9a). These were generally associated with the agricultural landscapes in eastern Ghana, southern Benin and Togo. In these landscapes, the percentage of land used for farming was estimated to range between 45-90% of the total area (Ramankutty *et al.* 2008). Here the high ΣNDVI was probably dependent on irrigation rather than on local rainfall where several small scale periurban irrigation systems (Gruber *et al.* 2009) and large irrigation projects expanded the irrigation network in the Ouémé

42

Catchment in Benin (ADBG 1998) and the Volta river basin in Benin, Togo and

Ghana (Hanjra & Gichuki 2008). In contrast, a positive linear pattern emerged when

the humidity coefficients were plotted against rainfall climatology (figure 2.9b) and

there was no distinctive relationship between temperature coefficients and rainfall

climatology (not shown).
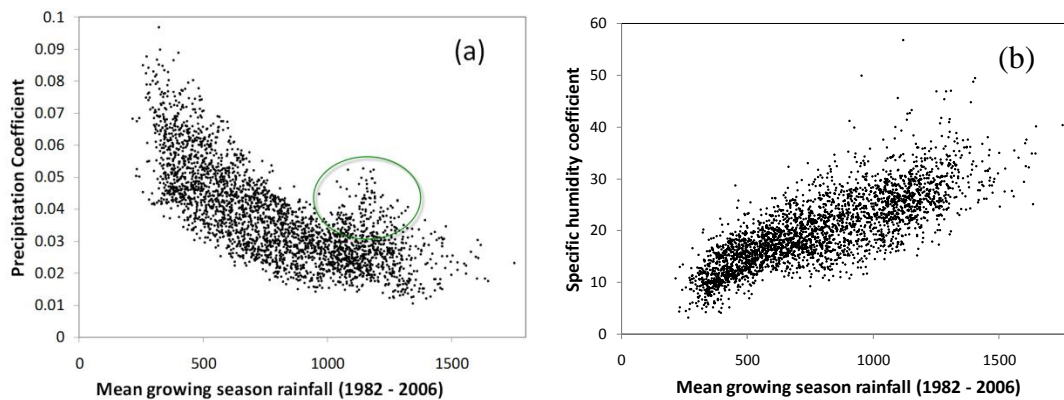
Figure 2.9 A randomly drawn sample (10%) representing the relationship of rainfall climatology to (a) precipitation coefficient (ΣNDVI.mm^{-1}) and (b) specific humidity coefficient (ΣNDVI.$(kg_{H2O}/kg_{Air})^{-1}$)

The standardized coefficients of the multivariate regression models were

calculated to estimate the relative contributions of growing season precipitation,

specific humidity and temperature on ΣNDVI variations. When summarized for the

land cover types in the study area, precipitation emerged, on average, as the primary

factor influencing NDVI, followed by specific humidity and then temperature (figure

2.10). Except in woody savanna and forests, the precipitation standardized

coefficients were significantly higher ($p < 0.01$) than the standardized specific

humidity coefficients and approximately three to four orders of magnitude higher

than the standardized temperature coefficients (figure 2.10). The standardized

specific humidity coefficients, on the other hand, were significantly higher ($p < 0.01$) than the standardized temperature coefficient in woody savannas and forests but not for the other land cover types (figure 2.10).
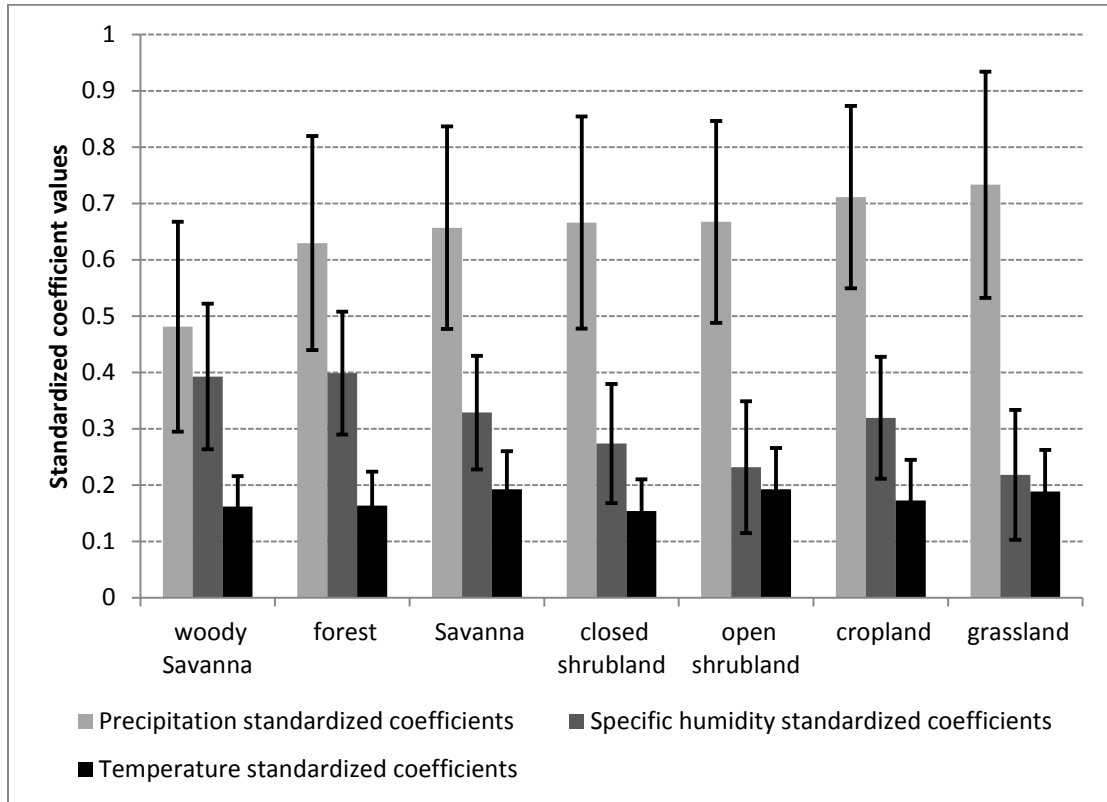
Figure 2.10 Mean absolute values of the standardized coefficients of the multivariate regression between NDVI and explanatory variables (precipitation, specific humidity and temperature) summarized for the land cover types. Error bars are ±1 standard deviation around the mean.

2.3.5 Soil-vegetation-atmosphere transfer modeling

The SSiB2 model was used to explore the hydrological and physiological mechanism that can explain the empirical relations found by correlation between meteorological variables and vegetation ΣNDVI. Five sites are provided to illustrate the overall results (table 2.1). Koumbi Saleh (southern Mauritania) is the driest and

the warmest with a cumulative growing season precipitation of 300 mm, a mean growing season daily temperature of 30.45°C, and growing season length of 3 months. Fadjė, located to the southeast of Lake Chad, is considerably wetter and 2.5°C cooler than Koumbi Saleh. Growing season precipitation for the remaining three sites is greater than 650mm (Kem Kem, Abyie, and Quadra Djallė) but the sites differ greatly in mean growing season temperature and mean growing season specific humidity (table 2.1).

The daily modeled responses of soil moisture, stomatal resistance, and net primary productivity (NPP) to changes in precipitation, air temperature, and specific humidity were summarized for the two periods of the growing season (green-up to maturity, and maturity to senescence) and are shown in figures 2.11 to 2.13. Higher specific humidity reduced evapotranspiration demand (not shown) resulting in higher volumetric soil moisture content in the root zone (figure 2.11). Particularly at drier sites or during dry periods, higher volumetric soil moisture content and higher atmospheric vapor pressure combined to increase modeled stomatal conductance (figure 2.12) and therefore canopy-scale NPP (figure 2.13). In the wetter sites such as, Kem Kem, Abyie and Quadra Djallė, higher specific humidity also increased leaf temperature at a rate of approximately 0.25°C per unit increase in specific humidity (g H_2O/kg dry air). Higher leaf temperatures below the temperature inhibition point can also increase NPP by increasing the photosynthetic reaction rates (Collatz *et al.* 1991).

Dry sites such as Koumbi Saleh and Fadjė showed a strong increase in NPP in response to precipitation during the greenup period, and somewhat less in the

maturity period (figure 2.13). In the wetter sites Quadra Djallė and Kem Kem, there were not any noticeable changes in modeled NPP in response to precipitation during either the greenup or maturity periods (figure 2.13). At these sites changes in soil moisture content in response to precipitation (figure 2.11) did not induce noticeable changes in stomatal resistance (figure 2.12) and hence NPP. The productivity in these sites, however, was sensitive to changes in temperature where increases in temperature increased modeled NPP (figure 2.13). The woody savanna site (Abyie) which is wetter than Kem Kem but drier than Quadra Djallė showed a strong increase in stomatal conductance and NPP in response to precipitation during the greenup period but no responses during the maturity period (figure 2.13). At Abyie and Fadjė, changes in temperature produced contrasting responses in modeled NPP (figure 2.13). During the maturity period, when productivity was not limited by available soil moisture, productivity responded positively to higher temperatures. However, during the green-up period when soil moisture levels were comparatively lower (figure 2.11), higher temperature lowered productivity.

Soil moisture (%Vol) averaged for the period between onset of
greenness increase and onset of maturity (grey symbols).
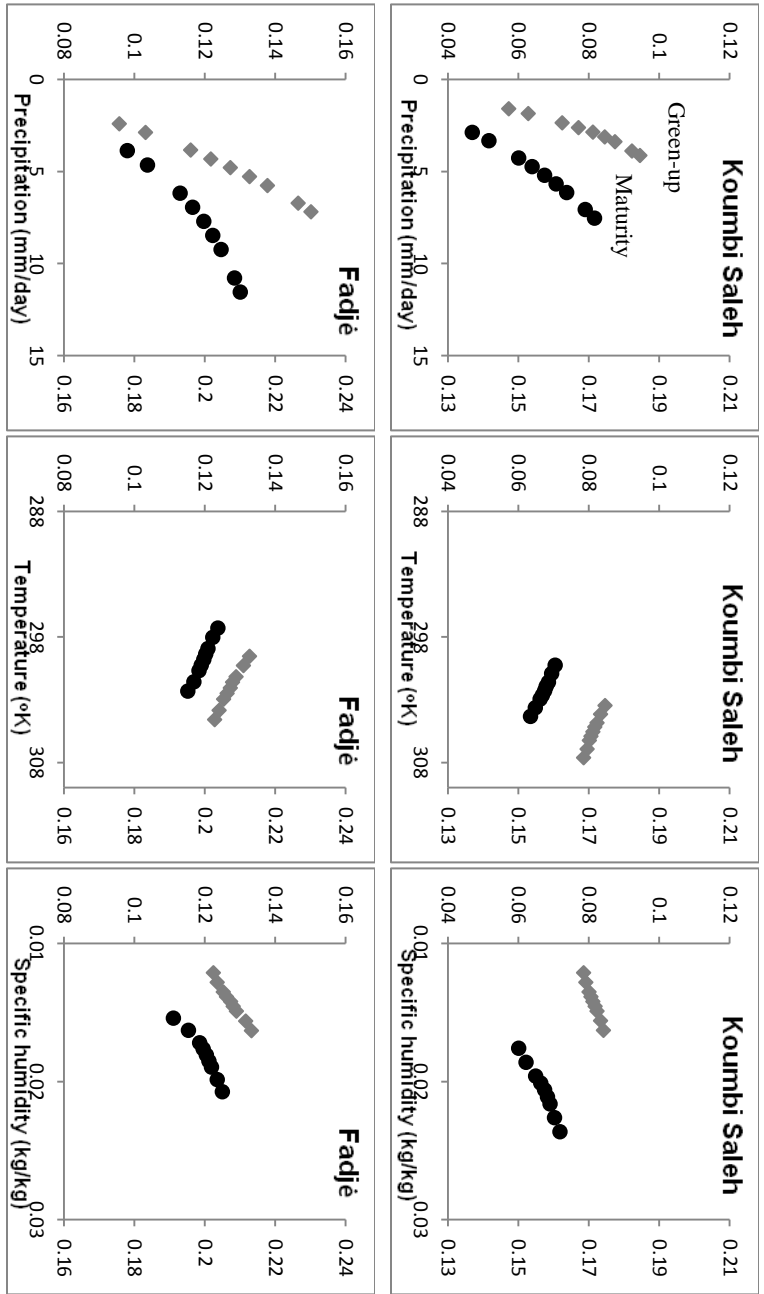
Figure 2.11 The response of daily soil moisture at root depth to changes in precipitation, temperature, and specific humidity averaged for the period from green-up to maturity (green-up period, grey diamonds; left hand axis) and from maturity to senescence (maturity period, black circles; right hand axis). Note the different ranges on the y axis between sites. Figure continued on next page.

Soil moisture (%Vol) averaged for the period between onset of
maturity and onset of greenness decrease (black symbols).

47

Soil moisture (%Vol) averaged for the period between onset of greenness increase and onset of maturity (grey symbols).
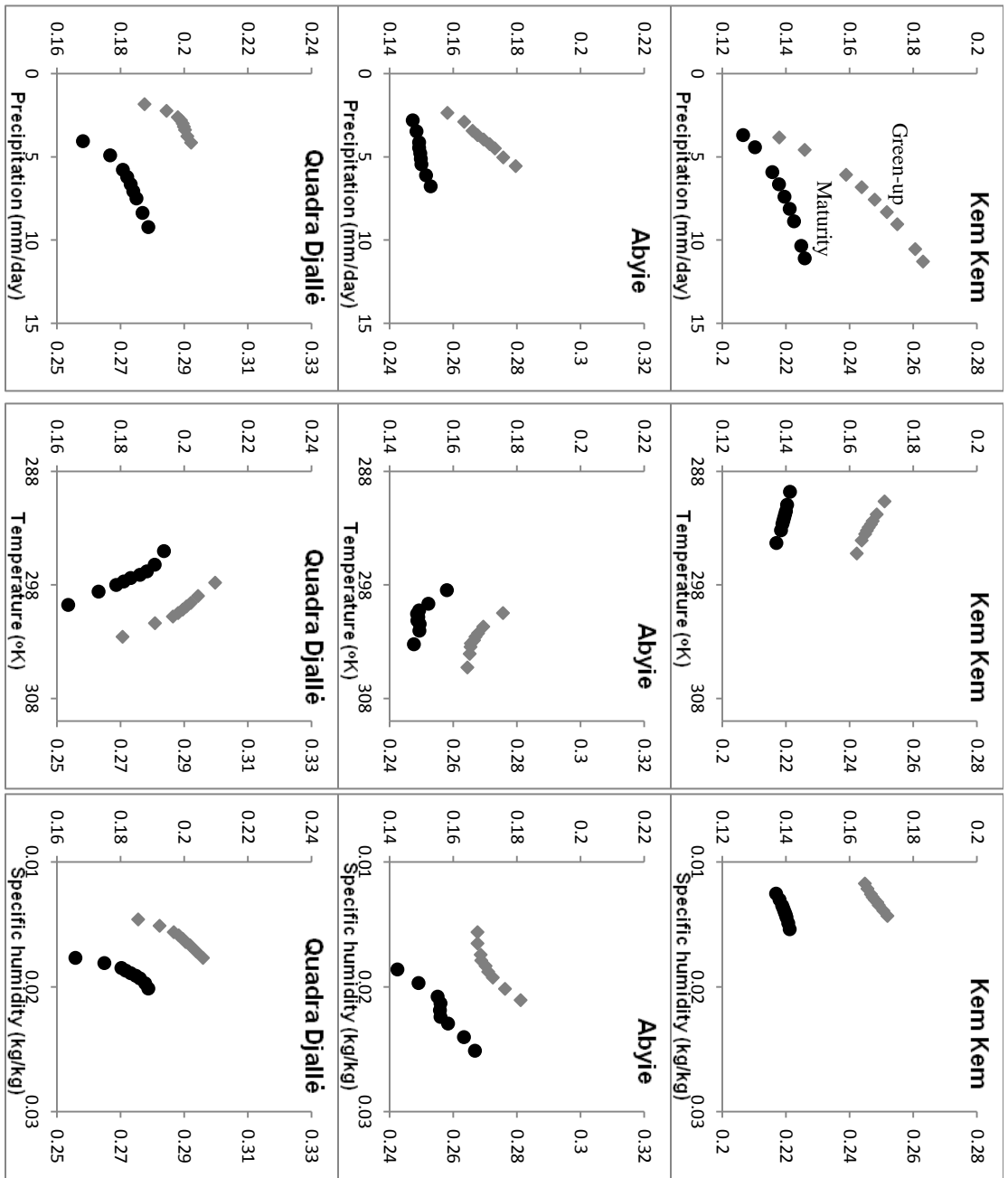
Figure 2.11 Continued.

Soil moisture (%Vol) averaged for the period between onset of maturity and onset of greenness decrease (black symbols).

Stomatal resistance (s.m^{-1}) averaged for the period between onset
of greenness increase and onset of maturity (grey symbols).
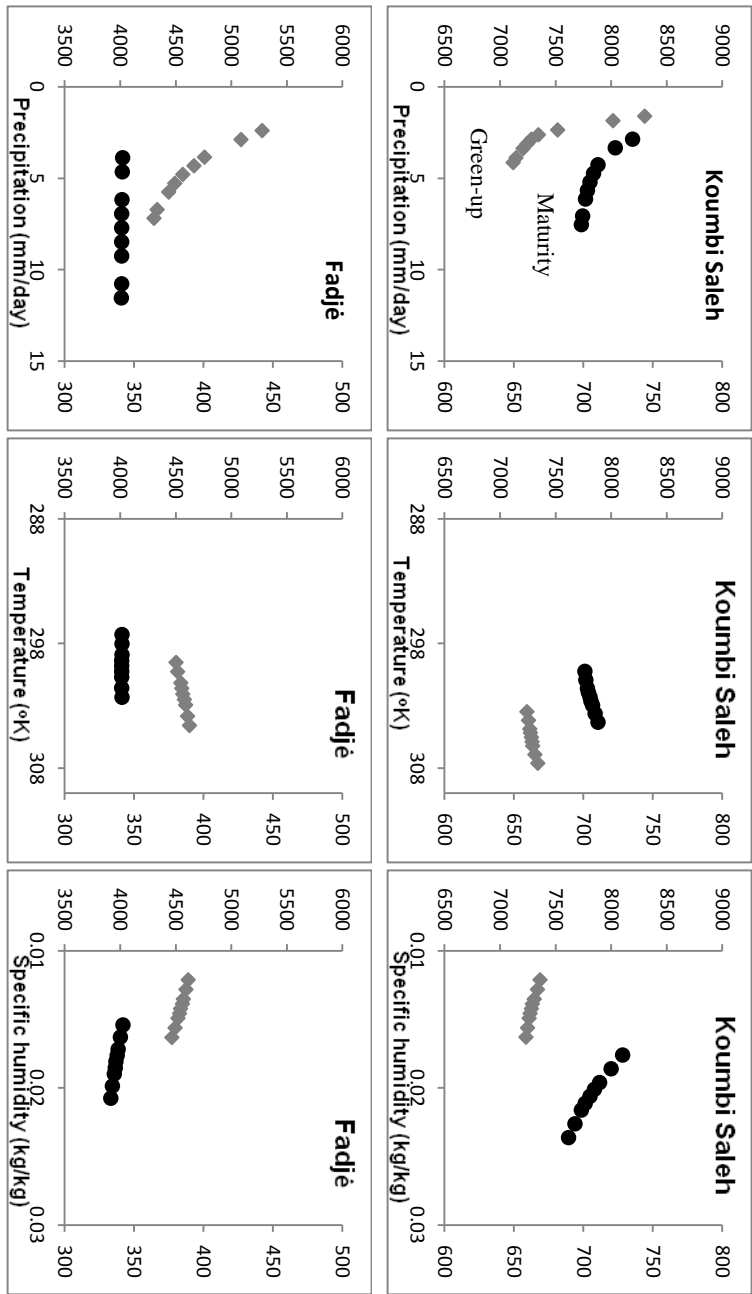
Figure 2.12 The response of stomatal resistance (s.m^{-1}) to changes in precipitation, temperature, and specific humidity averaged for the period from green-up to maturity (green-up period, grey diamonds; left hand axis) and from maturity to senescence (maturity period, black circles; right hand axis). Note the different ranges on the y axis between sites. Figure continues on next page.

Stomatal resistance (s.m^{-1}) averaged for the period between onset
of maturity and onset of greenness decrease (black symbols)

49
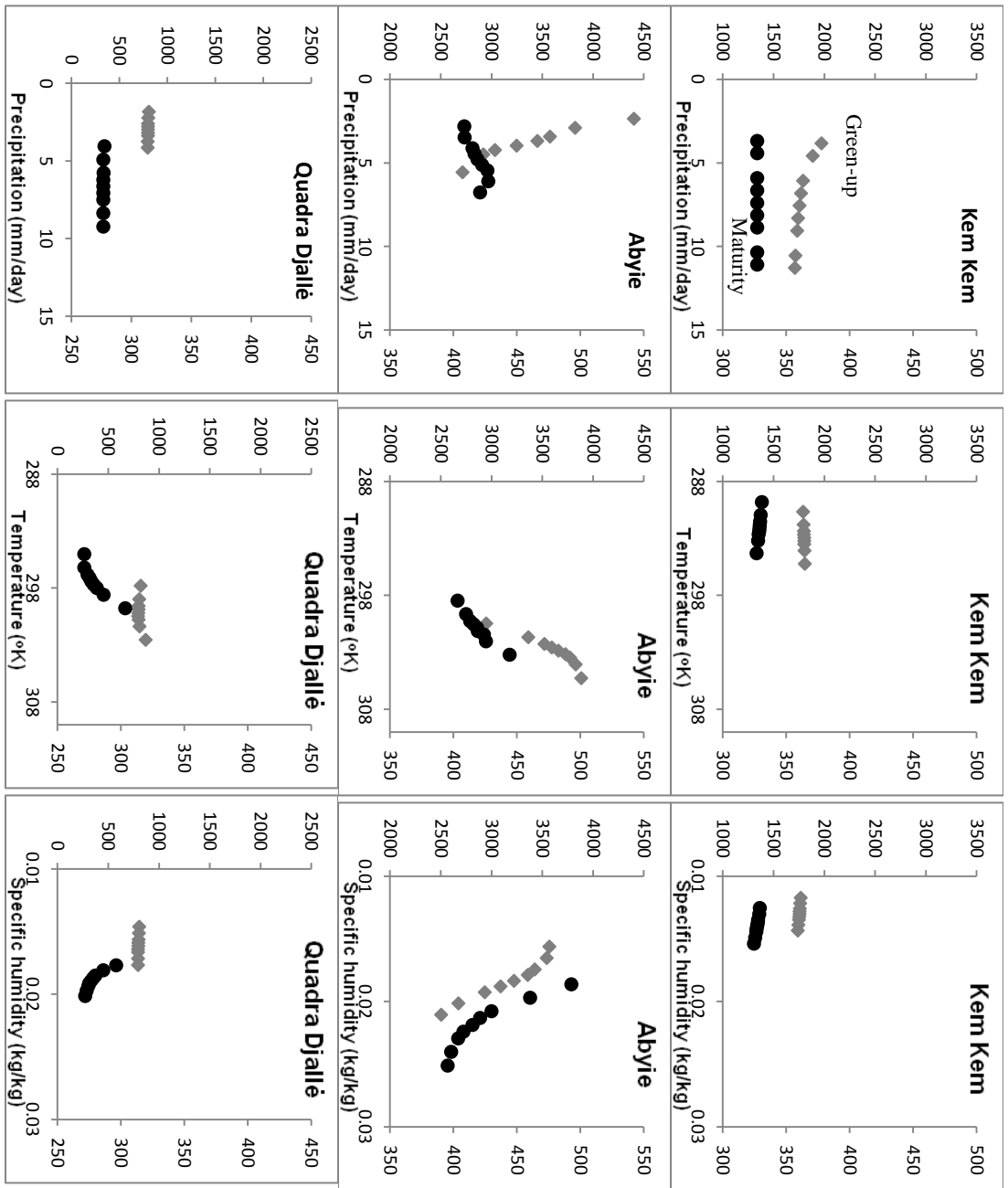
Stomatal resistance (s.m^{-1}) averaged for the period between onset of greenness
increase and onset of maturity (grey symbols).

Figure 2.12 Continued

Stomatal resistance (s.m^{-1}) averaged for the period between onset of maturity and
onset of greenness decrease (black symbols)

Net primary productivity (μmol.m^{-2}.s^{-1}) averaged for the period between onset of greenness increase and onset of maturity (grey symbols).

Fig. 2.13 The response of Net primary productivity (μmol.m^{-2}.s^{-1}) to changes in precipitation, temperature, and specific humidity averaged for the period from green-up to maturity (green-up period, grey diamonds; left hand axis) and from maturity to senescence (maturity period, black circles; right hand axis). Note the different ranges on the y axis between sites. Figure continues on next page.

Net primary productivity (μmol.m^{-2}.s^{-1}) averaged for the period between onset of maturity and onset of greenness (black symbols) decrease.

Net primary productivity (μmol.m^{-2}.s^{-1}) averaged for the period between onset of greenness increase and onset of maturity (grey symbols).
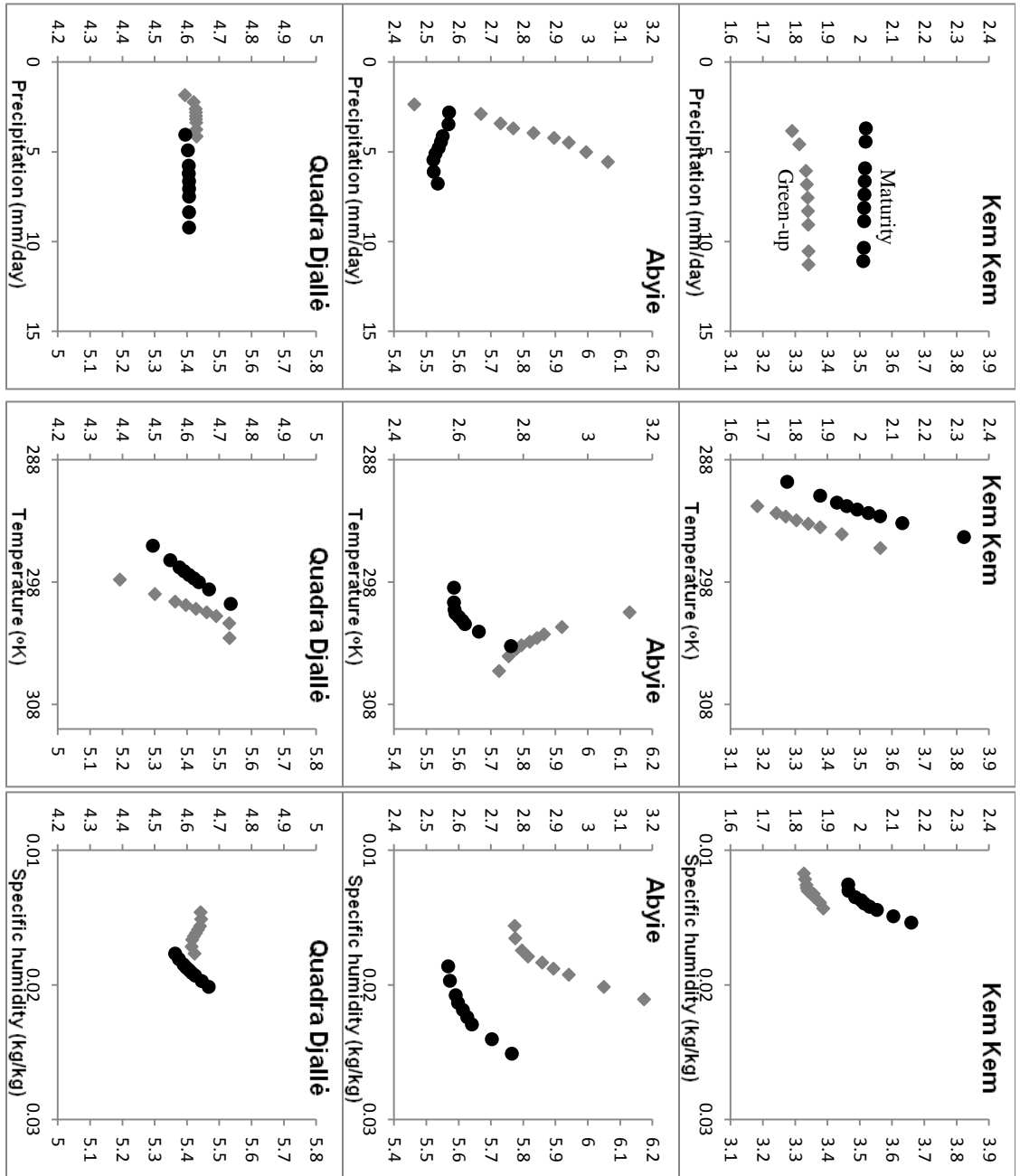
Figure 2.13 Continued.

Net primary productivity (μmol.m^{-2}.s^{-1}) averaged for the period between onset of maturity and onset of greenness (black symbols) decrease.

2.4 Discussion

2.4.1 Phenological transition dates

The interannual variation in the timing of greenup was highest in the arid regions dominated by grasslands, for which there are several possible causes. In the Sahelian eco-climatic zone, the onset of the summer monsoon in successive years can vary by more than 30 days (Sultan & Janicot 2003). After the start of the wet season, above ground biomass production starts when seedlings establish their root system (Hiernaux *et al.* 2009c). This is followed by rapid growth that produces a detectable increase in NDVI. However, the length of time between the start of the wet season and rapid growth has also been found to vary between years (Hiernaux *et al.* 2009c). In this study, in general, the interannual variation in the timing of green-up decreased from north to south probably because of the lower interannual variability in the onset of rainy season at lower latitudes (Le Barbé *et al.* 2002).

In addition to the interannual variability in the timing of the start of the growing season the results revealed a pronounced north-south gradient in the length of the growing season (the period between greenup and senescence) (Figure 2.2). The spatiotemporal variability in the timing and duration of the growing season throughout the Sahel clearly indicates that daily data, as were used here, are needed to monitor the shorter growing seasons particularly in the northern Sahel. It also indicates that using a standard integration period such as the June-August period that is often used to cover the growing season in the Sahel (e.g. Fensholt & Rasmussen 2011; Huber *et al.* 2011) can miss significant parts of the growing season.

2.4.2 Relationship of ΣNDVI with climate variability

In arid and semi-arid regions, NPP and ΣNDVI have been shown to have a strong relationship with precipitation (Le Houérou *et al.* 1988; Le Houérou 1989; Wessels *et al.* 2007). Indeed, average NPP has been shown to increase linearly or near-linearly with mean annual precipitation, to an upper limit (Lieth 1975; Breman & de Wit 1983; Le Houérou *et al.* 1988; Merbold *et al.* 2009). However, the interannual variability in NPP does not always exhibit such a strong relation, as evidenced by the weak correlations between annually summed NPP and rainfall (Knapp & Smith 2001; Tracol *et al.* 2006; Hiernaux *et al.* 2009a; Hiernaux *et al.* 2009c) and between ΣNDVI and rainfall (Goward & Prince 1995a; Helldén & Tottrup 2008; Fensholt & Rasmussen 2011). Also, RUE, which was assumed to be a conservative parameter (Le Houérou 1984), has been found to vary through time and space (Prince *et al.* 1988; Wessels 2005). Similarly, in this study, the correlations between annually summed NDVI and rainfall, in general, did not reveal strong relationships, yet there were some systematic, though weak, correlations in areas receiving intermediate precipitation (figures 2.3a, 2.4). Helldén & Tottrup (2008) and Fensholt & Rasmussen (2011) similarly found that the degree of ΣNDVI variance explained by rainfall was high in some areas and low in others with weak to insignificant relationships more common in the dry and wet margins of the Sahel.

Nicholson *et al.* (1990) suggested that the apparent lack of ΣNDVI response to additional precipitation in the dry sub-humid Sahel may be caused by the low sensitivity of f_{PAR}, and thus NDVI, to additional rain during wet years. Another plausible explanation is that precipitation in the wetter areas is not the primary factor

controlling vegetation growth (Knapp & Smith 2001). The simulations of net primary productivity in the dry sub-humid areas such as at Quadra Djallė and Kem Kem (figure 2.13) shown here revealed little or no sensitivity of NPP to variations in precipitation. At these sites, the modeled volumetric soil moisture in the root zone remained above approximately 14% by volume (figure 2.11) which is unlikely to induce acute water stress, stomatal closure and a drop in NPP (figure 2.12). Similarly, modeling results by Williams $et\ al.$ (2008) suggested that the woody plant associations in the wetter parts of the Sudanian and the Guinean ecoclimatic zones had sufficient soil moisture to meet evapotranspirational demands even during years with below-average precipitation.

The variance of ΣNDVI explained by rainfall in the northern boundary of the Sahel was generally low. This was expected since RUE has been found to vary over a wide range in dry areas and at low rainfall (Prince $et\ al.$ 1988; Wessels 2005). However, several studies have reported a strong coupling between NDVI and rainfall in northern Sahel (Malo & Nicholson 1990; Nicholson $et\ al.$ 1990; Davenport & Nicholson 1993; Herrmann $et\ al.$ 2005b). The analyses carried out in those studies used time-series of moving average monthly precipitation and ΣNDVI data. Successive monthly values of precipitation and ΣNDVI are usually highly autocorrelated (Herrmann $et\ al.$ 2005a). Regression of autocorrelated variables can cause overestimation of the strength and significance of the relationship (Granger & Newbold 1974). Whether the differences between the strength of the relationship found here and those reported in Nicholson $et\ al.$ (1990), Malo & Nicholson (1990),

Davenport & Nicholson (1993) and Herrmann *et al.* (2005) were the result of using different integration periods cannot be deduced from the current analysis.

In the arid and semi-arid Sahel, the correlations between growing season, compared with annual integrated ΣNDVI and precipitation totals, were generally higher (Figures 2.3 & 2.4), confirming that occasional rainfall outside the main growing season has little effect on vegetation production (Yang *et al.* 1998; Wang & Eltahir 2000; Wessels 2005; Wessels *et al.* 2007; Knapp *et al.* 2008). Long periods of drought following early rain, the probability of which increases as the climate gets drier northwards (Barron *et al.* 2003; Frappart *et al.* 2009; Yengoh *et al.* 2010), have been found to kill the seedlings of fast-germinating species favoring species with long-lived seed banks which have reserves of seeds that germinate when the rainy season resumes (Elberse & Breman 1989; Elberse & Breman 1990). On the other hand, rains falling later than senescence may not be used for production by most annuals irrespective of the amount of precipitation as vegetative growth ends with fructification which date is set by sensitivity to photoperiod (de Vries & Djitèye 1983; Hiernaux *et al.* 2009c).

Interestingly, the geographical distribution of the precipitation coefficients (figure 2.8a) was correlated with precipitation totals; higher precipitation coefficients in dry areas and lower in wet areas (figure 2.9a). This does not completely agree with the findings of Le Houérou (1984), who found that the ratio of NPP to precipitation (RUE) decreased with increasing aridity. Le Houérou (1984) attributed the low RUE values in dry area to the higher proportional losses of precipitation to evaporation in dry areas compared to wet areas. However, the results of this study are in agreement

56

with other studies in the Sahel (Prince *et al.* 1998) and South Africa (Wessels 2005). Higher precipitation coefficients could be the result of overestimation of very low $\sum$NDVI values by satellite observations (Prince, 1991), or an upward shift in the RUE in desert margin vegetation (Prince et al., 1998). Also, by analyzing eddy-covariance measurements across a range of vegetation types and climate zones in Africa, Merbold et al. (2009) similarly found that NPP at the wetter sites varied over a narrow range in relation to precipitation variability, whereas NPP at the drier sites responded more strongly. The maximum photosynthetic response to precipitation variation was greater for grasses in dry areas than for trees in wetter areas, which Merbold et al. (2009) attributed to the differences in the photosynthetic pathways of trees (C_3) and grasses (C_4). It could also be that the differences are a result of the non-linearity of soil moisture response to precipitation in the wetter areas (figure 2.11) where high precipitation rates can saturate infiltration and therefore additional precipitation does not increase soil moisture and photosynthesis.

In contrast to the ΣNDVI–rainfall relations, specific humidity coefficients (figure 2.8b) were higher in the wetter areas (figure 2.9a). Unfortunately, this could not be compared to eddy-covariance studies since those studies usually report the relationship of net photosynthesis to vapor pressure deficit rather than to specific humidity. Mechanistically, however, high specific humidity may restrict evapotranspiration-driven reductions in soil water thus alleviating plant soil water stress. On the other hand, low specific humidity may increase evapotranspirative demand resulting in a net decrease in soil moisture availability (Williams *et al.* 2008). The combination of soil moisture stress and low specific humidity was found to

increase stomatal resistance which in turn decreased productivity (figures 2.11 to 2.13).

Surprisingly, the ΣNDVI-temperature relations differed between the two directions of change (figure 2.8c). The effects of temperature on plant growth are largely mediated by its effects on chemical reactions (e.g. photosynthesis and respiration) and its effects on soil moisture. On one hand, photosynthesis reaction rates increase with temperature up to an upper limit beyond which photosynthesis decrease due to the denaturation of proteins. On the other hand the desiccating effects of higher temperatures can reduce net photosynthesis. The empirical results show that for some areas in the Ethiopian highlands, the Guinean ecoclimatic zone and from western South Sudan to southern Chad growing season temperature was positively related to ΣNDVI. These and the modeling results at the Kem Kem (Ethiopean highlands) and the Qudra Djallė sites (Bongos Mountains) (figure 2.13) suggest that increases in temperature-dependent photosynthetic reaction rates may counter the desiccating effects of higher temperature. However, global studies of climatic limits on plant growth do not identify temperatures as an important factor influencing vegetation growth in either the Ethiopian highlands or in the Bongos Mountains range but rather point that vegetation growth in these areas is primarily limited by incident photosynthetic active radiation (PAR) (Churkina & Running 1998; Nemani *et al.* 2003). The influence of PAR on vegetation production was not investigated here due to the low spatial resolution of the data available at the time (2.5°).

The suggestion that an intensified hydrological regime would increase NPP in xeric environments while reducing NPP in mesic environments (Knapp *et al.* 2008) was not verified in the present study. Throughout most of the Sahel, an intensified precipitation regime (higher variance and lower skewness) was inversely related to ΣNDVI values. Knapp *et al.* (2008) suggestion was based on the assumption that, in xeric environments, the proportional losses of precipitation to canopy interception and to evaporation would be reduced if precipitation event size increased and that this reduction would offset or even exceed the volume of water lost to runoff, thereby increasing soil water availability (Knapp *et al.* 2008). The proportional effects of reductions in evaporation due to an intensified precipitation regime might be less than theorized as the percentage of total precipitation that falls in very small events (<7 mm/day) in the Sahel is minimal (Barbé & Lebel 1997; D'Amato & Lebel 1998; Le Barbé *et al.* 2002). Thus it is plausible that larger precipitation events with longer intervening dry periods would lead to greater drying of the soil and reduce NPP.

2.5 Conclusions

Vegetation growth and rates of development in arid and semi-arid Sahel were, as expected, generally related to precipitation. It was also found that air humidity and temperature have a significant role, in agreement with several recent modeling studies (Williams *et al.* 2008; Beer *et al.* 2010). The magnitude of the effects of these three variables varied between vegetation functional types and latitude.

The effects of precipitation, temperature and humidity on productivity were geographically coherent, suggesting fundamental causes. Unfortunately, the lack of a dense network of observational data meant that the emergent spatial patterns found

here could not be analyzed further. Still, it is worth noting that the general patterns were compatible with previous modeling studies (Williams *et al.* 2008) and observational data from the few flux tower measurements in the study area (Merbold *et al.* 2009).

One surprising result was that the vegetation, particularly at the wetter sites, did not always respond directly and proportionately to variations in soil moisture. Model simulations showed that, while variations in meteorology were indeed found to significantly alter soil moisture, this did not always increase production. The changes in vegetation productivity at the wetter sites were either dampened or enhanced by the direct effects of temperature and humidity on leaf temperature and stomatal conductance. These results were based on modeling and should be generalized with caution; for example, it is known that, in some regions, antecedent meteorology and productivity affects productivity in the following year – so called lags - but these mechanisms are not simulated in SSiB.

Seasonal precipitation distribution also influenced productivity. For the same total precipitation amount, productivity was higher when precipitation arrived in more frequent and less intense precipitation events. The suggestion by Knapp et al. (2008) that vegetation productivity in xeric environments responds favorably to more intense and less frequent precipitation events was not supported.

Inaccuracies in the reconstructions of daily AVHRR NDVI and of the independent variables, particularly meteorological data, may influence these conclusions. Despite these shortcomings, it was evident that vegetation dynamics in

the Sahel and their environmental correlates are more complex than the equilibrial relationships between growing season precipitation and NPP variation. The spatially explicit representation of these relationship presented here provide a new dimension to rainfall–productivity relationships in the Sahelian-Guinean ecoclimatic-zones.

Chapter 3: Long term trends in vegetation productivity

3.1 Introduction

There is a great deal of debate on the extent, causes and even the reality of land degradation in the Sahel. On one hand, extrapolations from field-scale studies suggest widespread and serious reductions in biological productivity threatening the livelihoods of many communities (Oldeman *et al.* 1990; Le Houérou 1996). On the other hand, coarse resolution remote sensing studies consistently reveal a net increase in vegetation production exceeding, in some areas, that expected from the recovery of rainfall following the extreme droughts of the 1970s and 1980s (Eklundh & Olsson 2003; Herrmann *et al.* 2005b; Olsson *et al.* 2005; Heumann *et al.* 2007b), thus challenging the notion of widespread, subcontinental-scale degradation. To date, the causes, extent and severity of land degradation throughout the Sahel remain controversial (Hein & De Ridder 2006; Prince *et al.* 2007; Hein *et al.* 2011).

There are several reasons for the current lack of information on the extent, severity and causes of land degradation, including the lack of appropriate indicators that are consistent and practicable for use over large areas. NPP, which can be reliably measured from space, is a promising technique for monitoring land degradation since most of the biophysical processes involved in degradation (e.g. soil crusting, compaction and erosion, depletion of soil nutrients and organic matter, and the disruption of biogeochemical cycles) reduce the NPP – that is accumulation of biomass through time (Prince 2002). However, interannual variations in NPP are dominated by meteorological conditions, particularly by erratic rainfall, which mask any degradation signal that is generally more subtle and gradual (Wessels *et al.*

2007). Thus it is difficult to interpret trends in NPP without accounting for the effects of climate variability on productivity (Evans & Geerken 2004).

In order to normalize the effects of rainfall variability, Evans & Geerken (2004) and Wessels *et al.* (2007) developed the residual trends method by which an Ordinary Least Squares (OLS) linear regression relationship is developed for each grid cell (one or more pixels) between ΣNDVI and season total rainfall. Evans & Geerken (2004) and Wessels *et al.* (2007) used ΣNDVI as a proxy of NPP since ΣNDVI have been shown to be linearly related to NPP in drylands (Sellers 1987; Goward & Huemmrich 1992; Seaquist *et al.* 2003). The regression equation is used to predict potential NDVI as set by rainfall. The residuals (differences between observed and potential ΣNDVI values) are sorted in their temporal order and regressed against time. Significant negative slopes (trends) in the residuals indicate progressive reductions in vegetation production from its potential which have often been interpreted as an indicator of human-induced land degradation (Evans & Geerken 2004; Herrmann *et al.* 2005a; Fensholt & Rasmussen 2011).

Analysis of the rainfall–ΣNDVI relationship for every grid cell separately accommodates the effects of local variations in soil and vegetation cover which otherwise would have a major influence on the nature of this relationship (Prince *et al.* 1998; Wessels *et al.* 2007). The residual trends method showed promising results when applied to South Africa where significant negative trends were associated with the degraded communal areas (Wessels *et al.* 2007). However, the inter-annual variations in ΣNDVI were poorly explained by annual rainfall totals (Chapter 2) in large areas in the dry (< 400mm mean annual precipitation (MAP)) and wet margins

63

(>1000mm MAP) of the Sahel. The consequences of poor ΣNDVI-rainfall relationship are large prediction errors of potential ΣNDVI which propagate to the residuals and result in high uncertainties associated with the slope values of the regression of the residuals against time. Thus the trends of the residuals are interpretable only where significant ΣNDVI-rainfall relationships exist (Fensholt & Rasmussen 2011).

In the study of vegetation responses to climate variability in the Sahel (Chapter 2), the inter-annual variations in NPP were better explained by precipitation, specific humidity and temperature or by precipitation and its intra-seasonal distribution than by precipitation totals alone. These results suggest that it might be necessary to account for the influence of climate factors other than precipitation alone to produce more realistic and better constrained predictions of potential ΣNDVI.

The objectives of this study were to monitor changes in vegetation productivity relative to its potential using the residual trends method. Six residual trends models were calculated. The difference between these models was the means by which potential growing season ΣNDVI (ΣNDVI) was predicted. Predictions of potential ΣNDVI were obtained from the conditional mean and upper 95th quantile distributions of observed ΣNDVI responses to (1) rainfall, (2) rainfall, its seasonal variance and skewness, and (3) rainfall, specific humidity, and temperature.

Estimating potential ΣNDVI from the observed distribution of ΣNDVI and rainfall data using OLS regression techniques is not without its problems. In drylands, negative deviations of ΣNDVI from its potential could result from any

number of reasons including an ongoing process of land degradation but these deviations are smaller in dry years than they are in wetter years (Pickup *et al.* 1998). Such heteroskedasticity will most likely reduce the slope value of the OLS regression line, the consequences of which is an underestimation of potential ΣNDVI in wetter years. Quantile regression techniques (Koenker & Bassett 1978; Koenker & Hallock 2001; Koenker 2005), on the other hand, offer the distinct advantage of predicting the ΣNDVI-rainfall relationship in any part of the conditional distribution of ΣNDVI response to rainfall. The use of quantile regressions is not new to ecological applications (Cade & Noon 2003). Sankaran *et al.* (2005) and Good et al. (2011), to mention but few examples, used UQ regressions to quantify the extent to which rainfall limits potential woody cover. To reduce the effects of degraded ΣNDVI values, conditional upper quantile (UQ) regressions could be used to develop upper boundary functions of ΣNDVI response to rainfall and by extension upper boundary functions of ΣNDVI response to any number of meteorological variables.

Finally, potential ΣNDVI prediction errors were propagated through the models to obtain a measure of uncertainty of the slopes of the regression between the residuals and time. Insignificant trends result from uncertainties being greater than their respective slope coefficients. The models that predict potential ΣNDVI from the ΣNDVI-rainfall relation alone are expected to result in larger prediction errors and higher coefficient uncertainties, thus masking trends that are otherwise significant.

3.2 Material and methods

3.2.1 Remote sensing data

The AVHRR daily reflectance data in the Land Long Term Data Record (LTDR, version 2; Pedelty *et al.* (2007)) were used to reconstruct daily NDVI values from 1982 to 2006 at a spatial resolution of 0.05º (Appendix 1). The sequence of data included observations from AVHRR sensors onboard NOAA satellites 7, 9, 11 and 14. The AVHRR LTDR data processing stream employs a vicarious sensor calibration of the red (0.58–0.68 µm) and near infrared (0.725–1.10 µm) channels using cloud/ocean techniques to remove variations caused by changes in sensors and sensor drift (Vermote & Kaufman 1995; Vermote & Saleous 2006a). It also employs an improved atmospheric correction scheme to reduce the effects of Rayleigh scattering, ozone, and water vapor (Pedelty *et al.* 2007). The data used in this study were normalized to a standard sun-target-sensor geometry and cloud contaminated observations were replaced with reconstructed values interpolated from preceding and succeeding "clear sky" observations. BRDF and atmospheric corrections should reduce random and systematic errors in NDVI data (Nagol *et al.* 2009). Random errors (or "noise") result from the strong anisotropic properties of vegetation (Gutman 1991; Vermote *et al.* 2009a; Fensholt *et al.* 2010) and from atmospheric absorption and scattering, particularly from considerable absorption in the AVHRR near infrared channel by atmospheric water vapor (Cihlar *et al.* 2001) characterized by high spatiotemporal variability throughout the Sahel (Justice *et al.* 1991). Systematic errors, on the other hand, result from progressive increases in solar zenith angle and atmospheric path length associated with satellites orbital drift (Gutman 1987; Privette *et al.* 1995; Csiszar *et al.* 2001). An account of the LTDR

AVHRR data relative errors estimation is provided in Appendix 1, Section A1.3. If not accounted for, random errors may obscure subtle NDVI trends while systematic errors may reveal trends that are an artifact of the data rather than actual changes in vegetation production.

The reconstructed daily AVHRR-NDVI data were used to derive annual phenological transition dates (Chapter 2). The transition dates included the "onset of greenness increase" and the "onset of greenness decrease". A comparison between the AVHRR transition dates and the transition dates from the MODIS Land Cover Dynamics Science Dataset (Zhang *et al.* 2006) during the overlapping period (2002-2006) revealed a good agreement (Chapter 2) with root mean square errors only slightly higher than the reported accuracies of the MODIS products (Zhang *et al.* 2006). The "onset of greenness increase" was characterized by a pronounced north-south gradient with onset dates detected as early as February at lower latitudes (7.5°N) and as late as August at higher latitudes (17.5°N). The "onset of greenness decrease" also had a pronounced north-south gradient but with the onset dates detected earlier at higher latitudes (late August) than at lower latitudes (late October). Both dates were also found to vary between years with grasslands in arid region showing the highest temporal variability. On average, the length of the growing season (the difference between the two dates) varied from approximately 20 days at the southern edge of the Sahara desert to approximately 250 days in the wetter parts of the study area (Figure 2.2; Chapter 2). The spatiotemporal variability in the timing and duration of the growing season throughout the Sahel clearly indicates that daily data are needed to monitor the shorter growing seasons. It also indicates that

interannual changes in ΣNDVI cannot be adequately captured using a standard integration period such as the June, July, August (JJA) period usually used to define the start and end of the growing season (e.g. Fensholt & Rasmussen 2011). Rather than using a standard integration period, growing season sum NDVI and meteorological data were calculated by integrating daily values bounded by the interval between the two transitions dates; i.e. greenup and senescence.

3.2.2 Meteorological data

The Princeton Hydrology Group (PHG) bias-corrected-hybrid meteorological datasets of daily precipitation, surface air temperature, and specific humidity (Sheffield *et al.* 2006) were used in this study. The datasets are constructed from the National Center for Environmental Prediction–National Center for Atmospheric Research (NCEP–NCAR) reanalysis data and corrected for biases using observation based datasets of precipitation and air temperature. The daily data for the period 1982-2006 were downscaled spatially from 1° to the 0.05° resolution of the AVHRR dataset using bilinear interpolation. In addition to growing season precipitation totals, two higher order moments of growing season precipitation, namely variance and skewness, were calculated from daily precipitation storm frequency and intensity. High variance indicates higher than normal deviation from mean seasonal precipitation and can result from extended periods of drought or from intense precipitation events or a combination of both, while the skewness is a measure of the dominant frequency of either high intensity precipitation events (negative skewness) or low intensity precipitation events (positive skewness).

3.2.2 Estimating potential ΣNDVI

Potential Growing Season ΣNDVI values were predicted using OLS and UQ linear regression techniques from the observed ΣNDVI response to (1) precipitation, (2) precipitation, specific humidity and air temperature, and (3) precipitation and two moments of its distribution; namely growing season precipitation variance and skewness. The six regression models were applied to every grid cell (3x3 AVHRR pixels) within the study area. To reduce the risk of model overfitting, either the full set or a subset of the explanatory variables was selected to predict potential ΣNDVI (Dielman 2005). The selection criteria included a test for multicollinearity between the explanatory variables (Freund & Wilson 1998) and a search for the subset that resulted in the highest r^2 value adjusted for degrees of freedom (Furnival & Wilson 1974). Further details on the selection criteria can be found in Chapter 2.

Inferences of standard errors for the UQ regressions were obtained using the "wild bootstrap" method of (Feng *et al.* 2011), whereas the standard errors for the OLS regressions were calculated from the regression goodness of fit (r^2) and the standard deviation of observed ΣNDVI values. Potential ΣNDVI prediction errors were then calculated from the standard errors of the intercept and slopes at the 95% confidence level. It is important to note here that the standard errors were estimated with the assumption that the regression covariates were measured with no error (see discussion section).

3.2.3 Residual trends

The residuals (observed ΣNDVI – potential ΣNDVI) were regressed linearly against time. Negative or positive slopes (trends), if significant, indicate persistent

changes in ΣNDVI relative to the potential, as estimated by the OLS or UQ regressions of ΣNDVI on one or more of the meteorological variables. However, errors associated with the calculation of the residuals introduce additional uncertainty to the regression of the residuals on time. To measure this uncertainty, the total errors associated with the residuals were estimated by combining errors of the AVHRR NDVI measurements with the errors of the regression used to estimate potential ΣNDVI. The standard errors of the ΣNDVI values were estimated in Appendix 1 to range between ±1.47 ΣNDVI units in grasslands (~3.3% of the ΣNDVI signal) and ±3.3 ΣNDVI units in forests (~4.1% of the ΣNDVI signal). Both sources of error were combined using the sum rule for the propagation of error. The errors of the residuals were then propagated to the time-series linear regression used to estimate the residual trends (equation 1; Press *et al.* (1998)). Significant residual trends were identified as the ones statistically different from zero (probability of the F value < 0.05) and having absolute values greater than their respective uncertainties at the 95% confidence level.

$$\sigma_\beta = \left(\frac{\sum_{i=1}^{N} \frac{1}{\sigma_i^2}}{\left(\sum_{i=1}^{N} \frac{1}{\sigma_i^2} \cdot \sum_{i=1}^{N} \frac{x_i}{\sigma_i^2} - \left(\sum_{i=1}^{N} \frac{x_i}{\sigma_i^2} \right)^2 \right)} \right)^{0.5} \quad ... (1)$$

Where σ_β is the 1 sigma uncertainty of the slope value β, σ_i is the standard error associated with each residual value y_i, x_i is the time variable, and N is the number of observations.

3.3 Results

3.3.1 Estimating potential ΣNDVI

Overall, UQ estimates of potential ΣNDVI were higher than those given by OLS regression models (table 3.1). Furthermore, the UQ precipitation regression coefficients were consistently higher than their OLS counterparts (Figure 3.1 a & b). Thus the differences between the predicted values (UQ– OLS) were higher in wet years than in dry years. Adding specific humidity and temperature or seasonal precipitation distribution variance and skewness as co-independent variates in the OLS regression models (see table 3.1, models B & C) increased the ability of these models to account for the observed variability in ΣNDVI (figure 3.1c), the consequences of which were more constrained predictions of potential ΣNDVI values. However, compared to models E and F the UQ regressions using precipitation alone (model D), on average, had the lowest prediction errors (table 3.1). The geographical distribution of prediction errors was characterized by a pronounced latitudinal gradient with larger errors at lower latitudes (e.g. figure 3.2a). Adding specific humidity, air temperature, seasonal precipitation variance and skewness to precipitation as predictor variables in OLS regression models decreased potential ΣNDVI prediction errors (figure 3.2 e & f) particularly at middle and higher latitudes (figure 3.2 b & c).

Model to estimate potential NPP	Independent variables	Model name abbreviation	Mean coefficient value(s)	Mean errors (NDVI units)
OLS	Precipitation	Model A	0.028*prcp	28.1
UQ		Model D	0.032*prcp	19.8
OLS	Precipitation (prcp), specific humidity (shum) and temperature at surface (tas)	Model B	0.013*prcp + 19.8*shum- 0.0016*tas	22.0
UQ		Model E	0.015*prcp + 19.7*shum- 0.0045*tas	20.6
OLS	Precipitation, seasonal distribution variance (var) and skewness (skew)	Model C	0.151*prcp - 0.10*var + 2.4*skew	24.7
UQ		Model F	0.154*prcp - 0.13*var + 2.55*skew	21.7

Table 3.1 Independent variables used in OLS and UQ regression models to estimate potential ΣNDVI values. The mean regression coefficient values and potential ΣNDVI prediction errors at the 95% confidence level are the averages of all regression equations estimated for each 9 pixel arrangement of adjacent pixels.
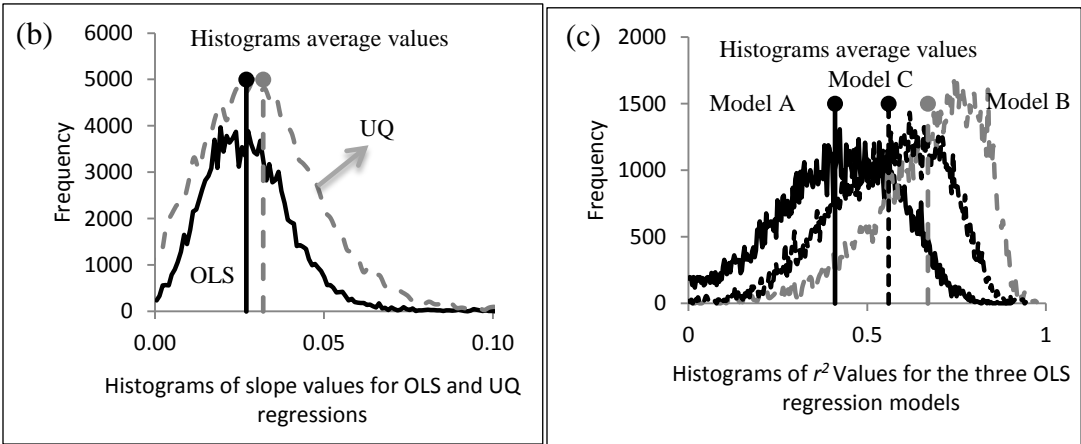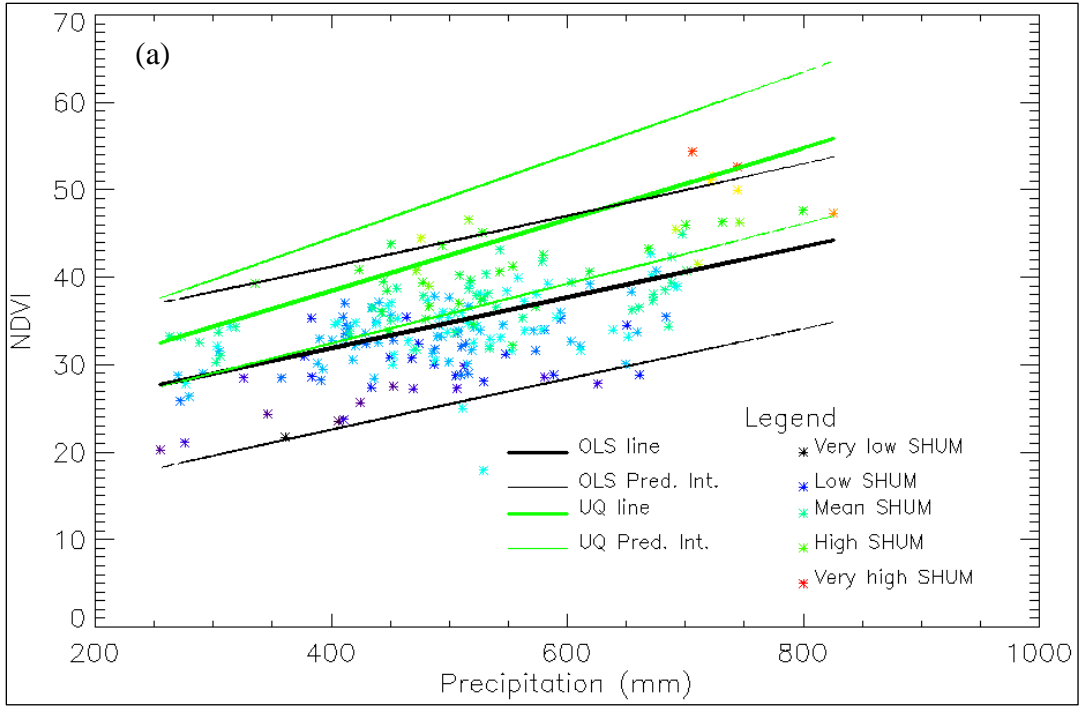
Figure 3.1. Properties of the models used to estimate potential ΣNDVI from the relationship between observed ΣNDVI and climate variables.   (a) The OLS and UQ regression lines and their prediction intervals at the 95% confidence level for a cropland site (3.725W, 11.525N) along with the ΣNDVI and precipitation values used in their estimation.   (b) Demonstrates the difference between the OLS and UQ precipitation coefficient values for all sites throughout the Sahel. (c) The ability of precipitation (model A), precipitation, specific humidity and temperature (model C) and precipitation and its intra-seasonal distribution (model B) to account for the variations in ΣNDVI.
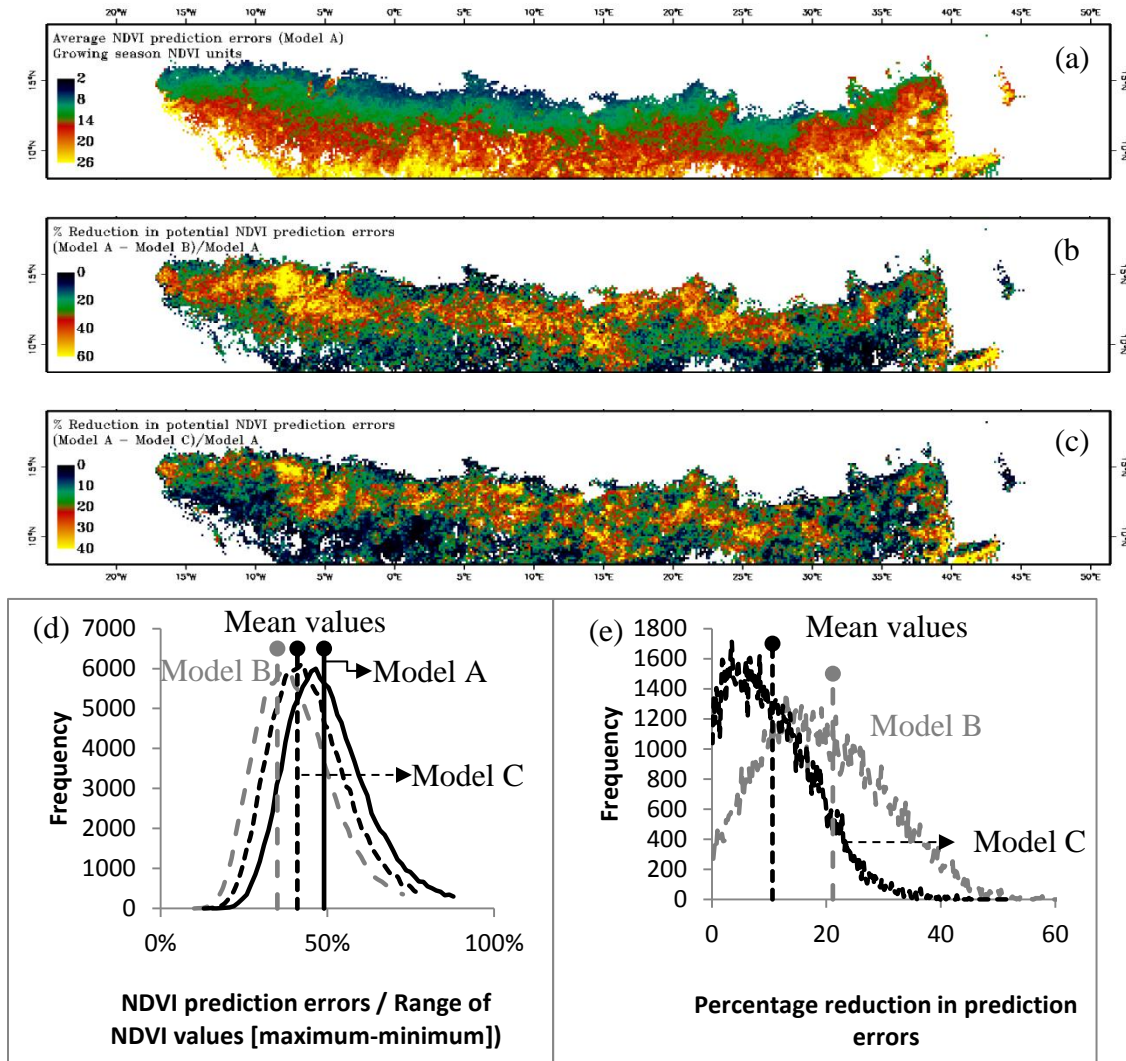
Figure 3.2 Potential ΣNDVI prediction errors: (a) prediction errors of the OLS regression between ΣNDVI and precipitation (model A). Compared to model A are (b) percentage reduction in potential ΣNDVI prediction errors of the OLS regression between ΣNDVI and precipitation, specific humidity and temperature (model B), and (c) percentage reduction in potential ΣNDVI prediction errors of the OLS regression between ΣNDVI and precipitation, its seasonal distribution variance and skewness (model C). (d) Frequency distribution of prediction errors for the three models normalized by the range of NDVI values [PE/(maximum NDVI – minimum NDVI)], and (e) frequency distribution of the values in (b) and (c).

3.3.2 Residual trends

The total errors of the residuals calculated from potential ΣNDVI and observed ΣNDVI error components were larger at lower than at higher latitudes. At higher latitudes, the two error components were similar in magnitude and contributed equally to the residual errors. At lower latitudes, however, residual errors were dominated by the uncertainties of potential ΣNDVI values.

A comparison of the combined errors (equation 1) and simple F tests for four example sites is shown in figure 3.3 a-d. It turned out that the test for uncertainty was sufficient: the probability of the F value test was < 0.05 for all slope values greater than their uncertainty, while the reverse statement was not always true (figure 3.3c & d).

The geographical patterns of the residuals and their significance for the six models (figure 3.4) were similar. There were relatively large areas with significant negative trends in western Sudan centered around Nyala, in southern Niger around the cities of Zinder, Maradi, Dosso and Niamey, in Nigeria extending between Kano in the north and Abuja in the south, and throughout Burkina Faso. However, there were areas of disagreement between the models including in western Senegal and in Ethiopia to the east of Lake Tana. Large areas with positive trends (i.e. increases in productivity beyond what can be explained by meteorological conditions) were recorded in Chad, Benin, Togo, Ghana, and elsewhere (figure 3.4 a though f). Table 3.2 summarizes the results from the six residual trend models. Compared to the OLS (figure 3.4 a, b, & c), the maps of the UQ regression models (figure 3.4 d, e, & f) had more area with significant negative trends and less with significant positive trends.
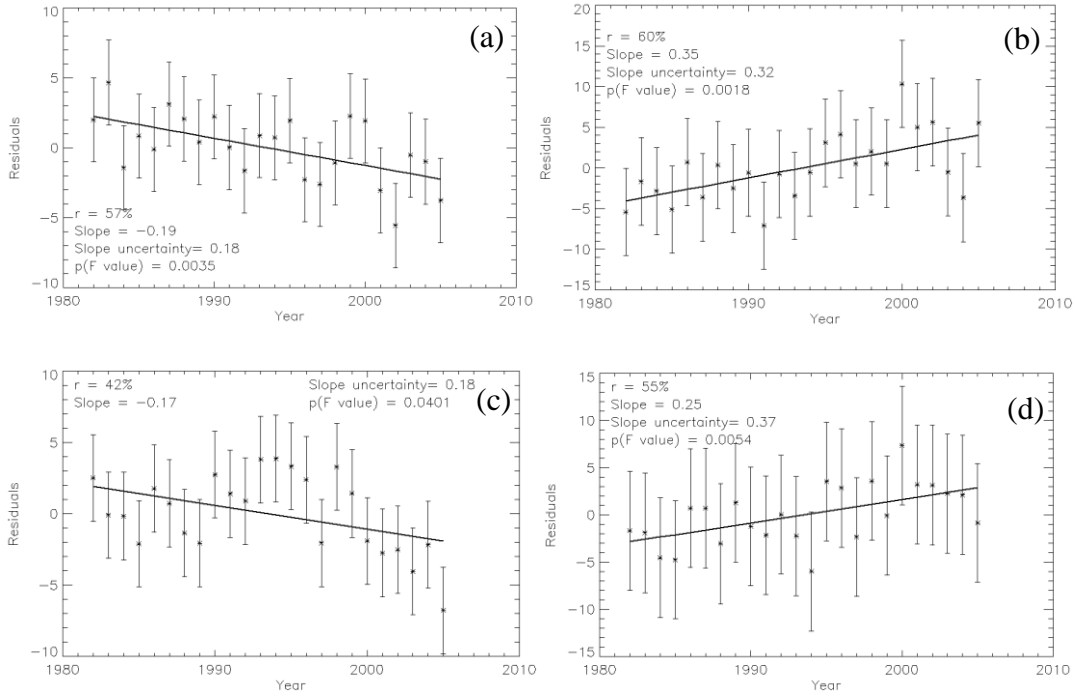
Figure 3.3(a-d) Trends (slopes) of NDVI residuals (observed –potential) regressed over time at four locations in the Sahel. The trends in (a) and (b) are significantly different from zero (p value of the F test < 0.05 and their absolute values are greater than their respective uncertainty), whereas the trends in (c) and (d) are not significant on the basis of the same criteria. Bars are residual errors at the 95% confidence level.

Residual trends Regression model	Model dependent variables	%Area			
		Significant negative trends	Insignificant negative trends	Insignificant positive trends	Significant positive trends
A (OLS)	Ppt	7.22%	28.72%	38.78%	25.29%
D (UQ)		12.88%	27.22%	47.18%	12.73%
B (OLS)	Ppt, SHUM, temp	7.14%	18.86%	39.80%	34.20%
E (UQ)		8.01%	20.93%	54.22%	16.84%
C (OLS)	Ppt, intra-annual variation	6.60%	25.40%	42.41%	25.59%
F (UQ)		9.85%	30.77%	52.12%	7.25%

Table 3.2 Percentage land area with significant negative and positive trends. Ppt – precipitation, SHUM – specific humidity, temp – temperature. OLS – ordinary least squares and UQ – upper quartile regression.
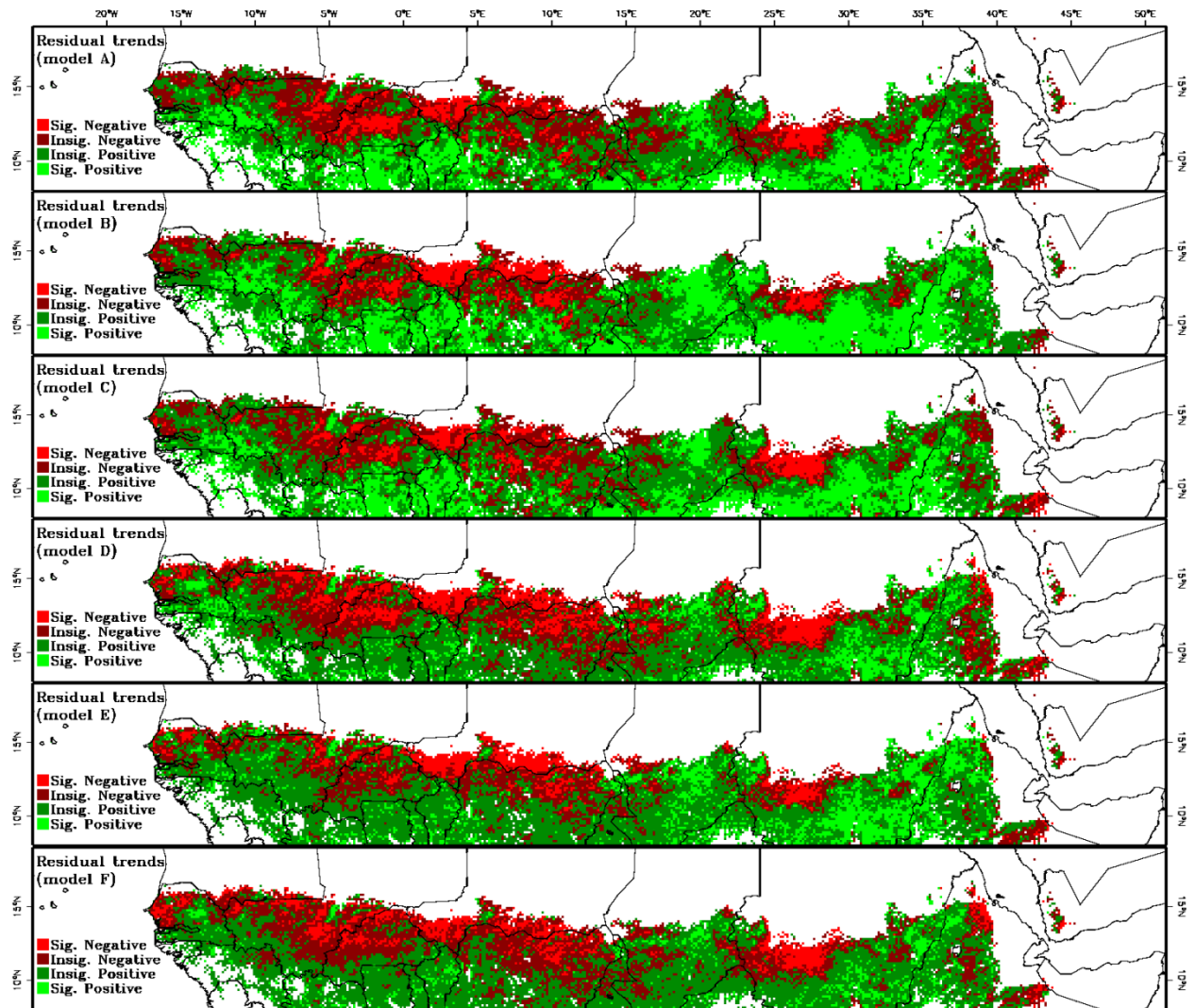
Figure 3.4 a –f: Trends (slopes) of NDVI residuals (observed –potential) over time as obtained from the six residual trend models (A through F; see table 1).

3.4 Discussion

A key aspect in developing degradation indices is the estimation of potential, non-degraded productivity (Prince 2002; Nicholson 2011a). Vegetation productivity potential (or potential NPP) can be estimated using process-based prognostic vegetation models such as BIOME-BGC (Running & Hunt 1993) and LPJ-DVGM (Hickler et al. 2005). However, the coarse resolution of soil data, the complexity of modeling competition between plant functional types, and the difficulty in parameterizing the interactions

between soil, vegetation and the atmosphere, lead to serious problems in model calibration (Jetten et al. 1999; Beer et al. 2010), resulting in large uncertainties in potential NPP estimates. The alternative approach employed here is data-oriented, also described as diagnostic or top-down, where relationships between interannual variations in ΣNDVI and meteorological conditions were first inferred for every grid cell at a spatial resolution of approximately 15km (9 adjacent AVHRR pixels). These relationships were then used to estimate ΣNDVI potential as set by meteorological conditions for every year in the satellite record. This method assumes that ΣNDVI is linearly or near-linearly related to NPP, which, although unsupported in some cases (Sellers 1987), is a reasonable starting point particularly in drylands such as the Sahel where leaf areas index values rarely exceeded 3 (Seaquist et al. 2003; Fensholt et al. 2006).

The degree of ΣNDVI variance explained by precipitation varied throughout the Sahel with higher r^2 values more frequently observed in drier areas than in wetter areas (Chapter 2). Overall, the average strength of the linear ΣNDVI/precipitation relationship (mean r^2 = 0.43, figure 3.1c) was higher than reported by Fensholt & Rasmussen (2011) but lower than the r^2 values reported in Herrmann *et al.* (2005). Both of these studies used GIMMS AVHRR NDVI data (Tucker *et al.* 2005) and gridded Global Precipitation Climatology Project (Huffman *et al.* 1997) or Rainfall Estimate (RFE) data (Xie & Arkin 1997). The analysis by Fensholt *et al.* (2011) was based on annual sums of NDVI and precipitation. In Chapter 2, the correlations between annual sums of NDVI and precipitation were found to be generally weaker than the relation between ΣNDVI and growing season precipitation totals. Herrmann *et al.* (2005), on the other hand, found very strong correlations between monthly NDVI and cumulative rainfall of the current

79

plus the two previous months. However, in Herrmann *et al.* (2005) both monthly NDVI and monthly precipitation data were highly autocorrelated (Herrmann *et al.* 2005). Regression of autocorrelated variables will most likely result in an overestimation of the strength and significance of the relationship (Granger & Newbold 1974). Whether the differences between the strength of the relationship found here and these reported in Fensholt *et al.* (2011) and Herrmann *et al.* (2005) was the result of using different integration periods or was the result of differences in precipitation and NDVI data quality cannot be deduced here.

The current analysis, however, clearly indicated that ΣNDVI variance was better explained by growing season precipitation, specific humidity, and temperature or by seasonal variance and skewness of precipitation, rather than by precipitation alone (figure 3.1c). This was expected because of the roles these meteorological variables play in growth and rates of development of vegetation throughout the Sahel (Williams *et al.* 2008; Merbold *et al.* 2009; Good & Caylor 2011; Rishmawi *et al.* 2013). Despite significant increases in r^2 values, the strength of the relationship between ΣNDVI and the meteorological variables remained relatively weak south of the 900mm isohyet as well as near perennial lakes, irrigated agriculture, and rivers. The low r^2 values alongside rivers might have resulted from lateral inflows of water into these landscapes either due to flooding events or from irrigation. The moderate to low r^2 values at wetter sites may be attributed to the ability of trees to utilize rainfall from previous years stored deep in the soil profile (Fuller & Prince 1996) or to the nature of the rainfall-soil moisture relationship becoming increasingly non-linear as the climate gets wetter (Chapter 2).

Whatever the reason, the moderate to low r^2 values in these areas resulted in higher potential ΣNDVI prediction errors (Figure 3.2).

Potential ΣNDVI prediction errors were calculated with the assumption that the meteorological datasets were error-free. This is clearly not the case and can be expected to increase potential ΣNDVI prediction errors and, if sufficiently large, would reduce the extent of the areas with significant trends. Unfortunately modeled meteorological data sets are rarely accompanied by measures of error and validation of the PHG data using meteorological stations is not possible since station data are used in the construction of the dataset (Sheffield *et al.* 2006). Moreover, the systematic error component of the AVHRR data were not evaluated as data from other sensors with similar spatiotemporal resolution are not available for the period 1982-2006. However, the corrections applied to the meteorological and to the AVHRR data (Sheffield *et al.* 2006; Pedelty *et al.* 2007) were reported to significantly reduce the systematic error components in these datasets and therefore are not expected to influence greatly the conclusions of this study.

Potential ΣNDVI values estimated from OLS regressions were generally lower than their counterparts obtained from the 95th upper quantile (UQ) distribution (Figure 3.1 a & b). Furthermore the deviations between OLS and UQ regression estimates often increased with rainfall (i.e. were higher in wetter than drier years). Unlike UQ functions, OLS regressions may underestimate vegetation production potential because ΣNDVI time series often include years when vegetation production was not only limited by precipitation, humidity and temperature but was further reduced by land degradation and a number of slow and fast processes such as depletion of the meristems for the next year's growth (e.g. seed and bud banks) (Dalgleish & Hartnett 2006), nutrient

81

limitations, excessive run-off, grazing, and fuel wood collection (Pickup 1996). In such cases, the mean rates of change in ΣNDVI will underestimate the production rates expected in response to climate variability (i.e. potential ΣNDVI values) but, because the magnitudes of these reductions often increased with rainfall, underestimating potential ΣNDVI values will influence the slope of the residuals with respect to time. The consequences of which is an underestimating of the "degradation" signal and an overestimating of the "greening" signal. That is not to suggest that estimating potential ΣNDVI using UQ regression functions is without its own problems, it is subject to the same errors as OLS because it is based on the same data, furthermore it is conceivable that supplementary irrigation and fertilization, run-on, carry over effects of soil moisture from previous wet years, and increases in seed and bud banks associated with high vegetation productivity in previous years (Fuller & Prince 1996; Easterling *et al.* 2000; Easterling *et al.* 2007; Hiernaux *et al.* 2009a), among other causes, may result in an overestimation of potential vegetation production. However, the effects of these factors are limited to the wetter areas of the Sahel, flood zones, and irrigated areas; most of which had high potential ΣNDVI prediction errors and insignificant trends.

As expected, the OLS based residual trend models (models A, B, and C) resulted in larger areas with significant positive trends than the UQ based residual trend models (models D, E, and F) (table 3.1). Despite the differences between the models in the significance of these trends, they all nonetheless indicate large and spatially coherent areas that greened faster than can be accounted for by changes in meteorological conditions (Figure 3.4). Explanations of the "greening" trend in the literature include agricultural intensification, increased investment and improvements in soil and water

conservation techniques, land abandonment associated with economic migration and civil strife, and increases in water use efficiency associated with CO_2 fertilization or transitions to new quasi-stable vegetation composition following the extreme droughts of the 1970s and 1980s (Prince 2002; Hickler *et al.* 2005; Mortimore & Turner 2005; Olsson *et al.* 2005). After removing the effects of rainfall on NDVI variability, Herrmann *et al.* (2005) similarly found positive trends over parts of the Senegal, Southern Mali, and Chad. However, large parts of Burkina Faso, northern Nigeria, southern Niger, and western Sudan were characterized by significant negative trends (Figure 3.4). Even though some disagreement was expected due to differences between the climate datasets and because of differences in AVHRR data, the lack of agreement over such large areas is surprising. Even more conflicting is the conclusion by Fensholt *et al.* (2011) that the residual trend method did not identify significant trends over the Sahel at the scales determined by the resolution of the AVHRR sensor.

The residual trend results were compared qualitatively by comparison with published case studies of land degradation and rehabilitation in the Sahel (e.g. Olsson & Rapp 1991; Hurault 1998; Faye *et al.* 2001; Mortimore *et al.* 2001; Tappan *et al.* 2004; Hurni *et al.* 2005) as well as by comparison with field observations by experts (Grey Tapan, 2008 pers com). While these comparisons showed favorable agreement (table A2.1; Appendix 2), they should not be construed as validation results. Validation sensu stricto requires direct measurements of vegetation at appropriate scales over a distributed set of sites. Until such datasets become available, validation of satellite-derived degradation indices at the scales studied here will not be easy.

3.5 Conclusions

It is unlikely that any stand-alone remote sensing-based approach will be able to unequivocally map human-induced land degradation (Prince 2002). Furthermore, remotely sensed indicators provide little if any information on the social processes that give rise to degraded landscapes (Batterbury *et al.* 2002). To complement the monitoring process, the next Chapter (Chapter 4) investigates whether the spatial variations in residual trend values (positive or negative) are related to land use and demographic pressures.

Chapter 4: Are changes in productivity related to demographic pressures?

4.1 Introduction

There are numerous claims that the process of land degradation is intricately linked to population growth, capital deficiencies and drought (Vierich & Stoop 1990; Vlek 1990; Swift *et al.* 1994; Bationo *et al.* 1998; Breckle *et al.* 2001; Drechsel *et al.* 2001; Le Houérou 2002). On one hand, drought reduces agricultural yields and vegetation cover rendering the environment more sensitive to disturbances and mismanagement (Nicholson 2011a). On the other hand, the widening gap between food supply and demand, capital deficiencies and the elimination of fertilizer subsidies are thought to drive the majority of farmers to shorten fallow periods and to expand cultivation onto marginal lands (Breman 1997; Barbier 2000; Reardon *et al.* 2001) thus increasing the risks of soil fertility depletion, erosion and crusting. Once degraded, agricultural lands are often abandoned and new lands are brought into production resulting in a perpetuating cycle of agricultural extensification and land degradation (Webber 1996; Drechsel *et al.* 2001). Agricultural extensification is also believed to have contributed, at least in part, to rangeland degradation (van Keulen & Breman 1990; van de Koppel *et al.* 1997; Barbier 2000). As arable land encroaches onto rangelands, the areas remaining accessible to pastoralists are often overstocked thus perturbing vegetation cover sufficiently to expose soils to wind and water erosion as well as to crusting and compaction by animal trampling (Le Houérou 1980a; Olsson & Rapp 1991; Le Houérou 1996).

In a meta-analysis of 132 subnational case studies on the causes of land degradation, Geist & Lambin (2004) identified a recurrent scenario of dryland degradation in Africa that involves the movement of farmers and pastoralists into marginal lands. Mediated by socioeconomic and policy factors, this movement often resulted in overgrazing, extensive fuel-wood collection, and high cropping intensities especially during drought episodes. This degradation scenario, however, has been challenged by a number of studies in the Western Sahel which have demonstrated that, under certain conditions, the expansion of agriculture onto marginal lands does not necessarily result in degradation mainly due to investments in soil and water conservation measures and to the emergence of mixed livestock-farming systems (Tiffen *et al.* 1994; Adams & Mortimore 1997; Mazzucato & Niemeijer 2000; de Ridder *et al.* 2004; Mortimore & Harris 2005; Mortimore & Turner 2005). The thesis that Sahelian agriculture tends to be mainly extensive and degrading has also been found to be in discordance with agricultural yield data recorded between the 1960s and late 1990s (Hellden 1991; Breman 1998; Harris 1998; Niemeijer & Mazzucato 2002; Mortimore & Harris 2005). Furthermore, claims of rangeland degradation through overgrazing run counter to persistent long term increases in livestock populations (Sullivan & Rohde 2002; Mortimore & Harris 2005). To date, the causes of dryland degradation remain controversial (Helldén 1991; Thomas & Middleton 1994; Lambin *et al.* 2001; Nicholson 2011a).

Drylands are extremely diverse in the biophysical conditions of the environment that influence their resilience (or susceptibility) to degradation by demographic and land use pressures (Lal *et al.* 1997; Eswaran *et al.* 2001; Nicholson 2011a). Soils range from

highly resilient to extremely sensitive and fragile. Factors influencing soil resilience include soil inherent characteristics (e.g. soil texture, infiltration rate), vegetation cover, climate and terrain slope length and gradient (Lal *et al.* 1997). For instance, clays are generally resilient under conditions of high rainfall but are easily degraded under conditions of low rainfall while the opposite is generally true for sandy soils (Nicholson 2011a).

In Chapter 3, six residual trend models were developed to identify the areas where the land surface in the Sahel has been greening "faster" (i.e. positive residual trends) or "slower" (i.e. negative residual trends) than what would be expected from the trends in climate. Over large areas of the Sahel (> 87%), the trends of vegetation greenness either exceeded (i.e. positive residual trends) or did not significantly depart (i.e. insignificant residual trends) from what was expected from the trends in climate. However, substantial and spatially contiguous areas (8-13%) of the total area of the Sahel were characterized by significant negative trends (chapter 3, figure 3.4). Significant negative trends indicate progressive reductions in vegetation production from the potential set by climate and soil (or reduced production efficiency; (Nicholson 2011a). Reduced production efficiency has often been interpreted as an indicator of human-induced land degradation (Evans & Geerken 2004; Herrmann *et al.* 2005a; Fensholt & Rasmussen 2011). However negative or positive trends in production efficiency are not necessarily the result of land degradation or land improvement as they can result from other factors including changes in land use, agricultural intensification and CO_2 fertilization among others.

To test whether reductions in production efficiency were related to anthropogenic pressures, they were compared with the available data on population density and land

use. Furthermore, this study investigates whether the influence of population and land use vary with the geography of land biogeophysical properties that determine the resilience of land to degradative processes (Scott 1979; Lal *et al.* 1997; Le Houérou 2002; Meadows *et al.* 2004). The results are relevant to the ongoing debate on the causes of land degradation in the Sahel.

4.2 Material and methods

4.2.1 Demographic and land use pressures data

Sahelian population data were obtained from the Gridded Population of the World (GPW) population density data (ver. 3) for the year 2000 (http://sedac.ciesin.columbia.edu/gpw). The data are constructed from national and sub-national census data (CIESIN 2005). The major improvement over previous versions was a substantial increase in the number of sub-national input census data, the result of which is a significant improvement in the spatial resolution of gridded population density estimates (Balk et al. 2010). Despite these improvements, large areas of Chad, Sudan and Guinea remain poorly resolved.

A global agricultural gridded landcover dataset for the year 2000 (Ramankutty et al. 2008) was obtained from the NASA Socioeconomic Data and Applications Center (http://sedac.ciesin.columbia.edu/es/aglands.html). This dataset merges a compilation of national and sub-national agricultural census data with satellite-based land cover classification maps. The satellite data are used to spatially locate agricultural grid cells in each census unit. The results are provided as a global gridded map with values ranging between 0 and 1 depicting the location and fraction (or extent) of arable lands and permanent crops within each grid cell (figure 4.1c).

A gridded dataset of livestock density for the entire Sahel was obtained from the Food and Agriculture Organization (FAO) GeoNetwork database (http://www.fao.org/geonetwork/) for the year 2000. The dataset includes information on cattle, sheep and goat densities (animal.km^{-2}). The densities are calculated from sub-national livestock census data and from land area suitable for grazing or browsing. The spatial resolution of the gridded datasets is further refined by redistributing the densities within the administrative units based on statistical relationships between animal density and environmental variables. The process includes developing statistical relationships for each agro-ecological zone from high spatial resolution training data and then applying these to fill data gaps or to refine coarse resolution data (Robinson *et al.* 2007). In this study, the data were used to calculate total livestock unit (LSU) density using the FAO species coefficients for sub-Saharan Africa (Jahnke 1982) (figure 4.1d). Because the impact on soil erosion of shrub or tree cover reduction is usually considered to be more severe than that associated with reductions in grass cover (Le Houérou 1996), browsers and grazers LSU densities were also calculated using livestock species food preferences. Studies of goats and sheep food preferences estimate goats diet to be made of approximately 80% shrub and tree fodders and 20% grasses and forbs, whereas sheep ate on average 80% herb and 20% browse (e.g. Wilson *et al.* 1975; Pfister & Malechek 1986; Bartolomé *et al.* 1998). Cattle, on the other hand, were considered to depend mainly on grasses and forbs (Devendra 1990).

Demographic and land use pressures are not limited to grazing and agricultural production but also include, among others, waste disposal, urbanization, and wood collection (for building and fuel). A potential proxy for these is the local deficit between

89

consumption and production of goods (food, wood, and fiber). (Imhoff *et al.* 2004) have modeled NPP using the Carnegie Ames Stanford Approach (CASA) and calculated an index of Human Appropriation of NPP (HANPP) from FAO data on products consumed in 1995 multiplied by harvest, processing and efficiency coefficients. Their spatially-indexed balance sheet of production and consumption expressed in Net Primary Productivity (NPP) units (g C.yr^{-1}) at a spatial resolution of 0.25° was used here. Expressing HANPP as a percentage of NPP (%HANNP) revealed considerable heterogeneity in the spatial patterns of consumption and production throughout the Sahel (figure 4.1b).

4.2.2 Soil and land cover data

Information on soil physical and hydrological variables were obtained from the Harmonized World Soil Database (HWSD; (FAO/IIASA/ISRIC/ISSCAS/JRC 2009). Within the Sahel region, the database merges the soil map units (SMU) from the FAO soil map of the world at a scale of 1:5 million with Soil and Terrain (SOTER) regional studies in Sudan, Ethiopia, Senegal, and Gambia at scales ranging between 1:1 million and 1:5 million. Thus, the spatial detail and quality of the data vary across the Sahel. In the HWSD database estimates of topsoil and subsoil variables within each SMU are derived using soil profiles (contained in the second version of the WISE database) and taxonomy-based pedotransfer functions. In this study, the soil mapping units were rasterized to a spatial resolution of 0.05° to match that of the AVHRR data. In addition to the variables contained in the HWSD, the Soil Erodibility Factor was estimated using a mathematical representation (Keefer 2000) of the nomograph method based on the work by (Wischmeier et al. 1971).

The proportional estimates of bare ground, woody and herbaceous vegetation cover for the year 2000 in the MODIS MOD44B Vegetation Continuous Fields product (Hansen *et al.* 2003) were used (downloaded from GLCF, http://www.landcover.org/). These data provide an improved depiction of spatially complex landscapes compared with discrete classifications (Hansen *et al.* 2003).

All coarse resolution mapped data were resampled to the 0.15° resolution of the six residual trend datasets using nearest neighbor resampling for categorical data and bilinear interpolation for continuous data.
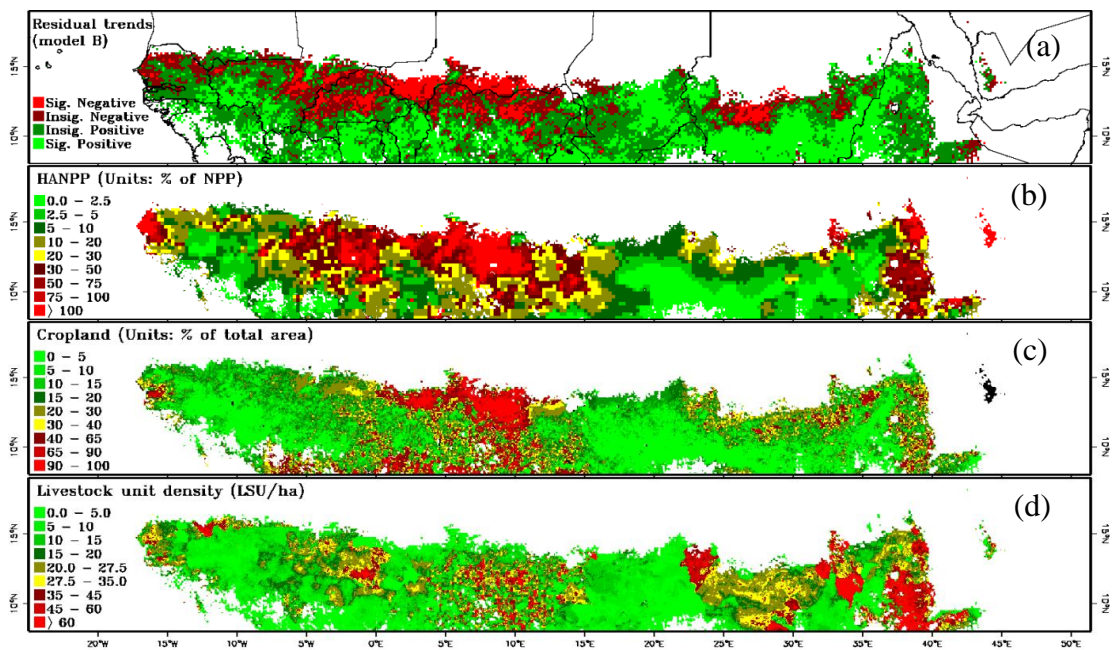
Figure 4.1 a: Trends (slopes) of NDVI residuals (observed –potential) over time as obtained from the OLS regression of NDVI with precipitation, specific humidity and temperature (see table 4.1).   b – d: datasets used to explore the relationship between residual trends and land use pressures (Ramankutty et al. 2008; FAO 2011).

4.2.3 Relating residual trends to demographic pressures, land cover, and soil variables

The relation of residual trends to land exploitation by human agencies and to land biophysical characteristics that might influence its susceptibility to degradation were explored using statistical summaries, multivariate linear regression models and regression tree analysis (RTA). Data on demographic pressures included population density, HANPP, %HANPP, the percentage of land used for crops (%crops), grazers and browsers livestock unit densities (Grazer LSU and Browser LSU), as well as transformations of LSU in relation to local NPP (LSU/NPP) and %crop area in relation to mean annual rainfall (%crops/MAP). Plots of the mean and standard deviation of 25 equally sized groupings of residual trend values ranked by each demographic pressure variable were used to discern whether the spatial variability in any of these datasets was associated with changes in land productivity. For example, the residual trend values were ranked by population density and placed in 25 equally sized groups. The mean and standard deviation of the residual trend values within each group were then calculated and plotted against their corresponding mean population density values. In addition to these univariate statistical summaries, multivariate linear regression models were used to explore the additive effects of demographic pressures on residual trends.

Land cover type and soil physical and hydrological conditions may attenuate or accelerate the effects of demographic pressures on land productivity (Prince 2002; Geist & Lambin 2004). The recursive data mining approach in RTA has been found to be effective in uncovering such hierarchical relations (Prasad *et al.* 2006). Furthermore, RTA allows for the discovery of both additive and multiplicative relations among the response and explanatory variables (Moore *et al.* 1991). In this study, two RTA

techniques were used, namely the Classification and Regression Trees (CART; (Breiman et al. 1984) and the Random Forest (RF; (Breiman 2000; Breiman 2001) techniques. The CART trees provided hierarchical mapping of the relations between the explanatory variables and the residual trends. The RF technique, on the other hand, evaluated the ability of the explanatory variables to account for the variability in residual trend values. The relative importance of each variable in explaining residual trend variations was determined based on reductions in percentage variance explained when the explanatory variable was not used in the analysis.

Instead of including all explanatory variables in one RF models, several RF models were developed each using a subset of the explanatory variables that were not highly correlated. For example, the highly correlated soil erodibility and soil texture variables were not used in the same RF model. 500 trees were grown for each RF model. Each tree was grown using a randomly selected training sample representing 67% of the entire population of significant residual trend values and their covariates (Y, X). The remaining 33% of the data produced 500 "out-of-bag" samples (Breiman 2001), each corresponding to one tree in the RF model. Each tree (i.e. set of rules) was then used to predict the expected residual trend value E(Y) for each data point in its "out-of-bag" sample. Because of the large number of trees grown, it follows almost surely that there are multiple residual trend predictions $E(Y_{i=1}^{n})$ for each data point in the population (Y, X). The predictions $E(Y_{i=1}^{n})$ were averaged and compared to their corresponding Y values to calculate the mean square error (MSE) and the strength (r^2) of the RF model as described in Breiman (2001). (Breiman 2001; Prasad *et al.* 2006) found this "out-of-bag" method for estimating generalization error is as accurate as MSE and r^2 values obtained

by cross validation. To test the accuracy of the "out-of-bag" method, 10 set-aside test sets were selected randomly, each about one-third the total population size. The remaining data (i.e. training sets) were used to develop 10 RF models. The RF models were used to predict the residual trend values of the test sets. The predicted and original test set residual trend values were compared to estimate the errors and strengths of the RF models. Indeed, the MSE and r^2 values obtained by cross-validation were almost equal and even sometimes slightly better than the corresponding values obtained from the "out-of-bag" method.

4.3 Results

Significant trends were compared to demographic and land use pressures. Plots of the mean and standard deviation of 25 equally sized groupings of residual trend values ranked by each demographic and land use pressure variable showed a poor relationship between population density and the trends of the residuals, although a negative trend is clear (Figure 4.2a). However, there was a distinct inverse relationship between residual trends and %HANPP (Figure 4.2b), possibly because HANPP accounts for the effects of population density and the geographical variation in per capita consumption levels. The plots also suggest an inverse, near linear relationship between residual trends and livestock unit density and a similar relation with livestock unit density divided by productivity (LSU/NPP) (Figure 4.2c & d). However, Figure 4.2e shows a weak inverse logarithmic relationship between residual trends and %crop cover. The relation between residual trends and %crop cover was further investigated using an index (%crop cover/mean annual precipitation [MAP]) to assign higher values to the same %crop cover in drier areas compared with wetter areas. Residual trends were found to be inversely

related to this index (Figure 4.2f). This suggests that agricultural extensification affects land productivity disproportionately in dry areas.

The multivariate linear regression analysis of residual trends revealed that the additive effects of multiple land uses better explained the spatial variations in residual trend values than individual land use pressures (Table 3). The highest goodness of fit ($r^2 =$ 0.49) was between model E residual trends and the three variables (%HANPP, LSU/NPP, and %crop cover/MAP), while the lowest ($r^2 = 0.34$) was for the trends calculated using model D.

Model	Residual trend dependent variables	Pearson product correlation values									Multi-correlation (R) Variables (%HANPP + LSU/NPP + %crops/MAP)
		Grazer LSU	Browser LSU	Total LSU	% crop	Pop. Density	HANPP	%HANPP	LSU/NPP	%crop/MAP	
A (OLS)	Ppt	-0.22	-0.26	-0.24	-0.19	-0.08	-0.21	-0.49	-0.5	-0.41	0.65
D (UQ)		-0.18	-0.2	-0.2	-0.25	-0.08	-0.19	-0.41	-0.43	-0.37	0.59
B (OLS)	SHUM, temp	-0.11	-0.18	-0.13	-0.29	-0.1	-0.19	-0.5	-0.42	-0.48	0.67
E (UQ)		-0.05	-0.15	-0.07	-0.37	-0.1	-0.21	-0.55	-0.43	-0.55	0.7
C (OLS)	Ppt, intra-annual variation	-0.21	-0.24	-0.23	-0.21	-0.09	-0.16	-0.46	-0.51	-0.45	0.66
F(UQ)		-0.15	-0.19	-0.17	-0.26	-0.07	-0.15	-0.4	-0.42	-0.4	0.6

Table 4.1 Correlation values (r) between residual trends and demographic and land use pressures. The multi-correlation value was estimated from the relation of residual trend values to %HANPP, LSU/NPP, and %crop cover/mean annual precipitation. Ppt – precipitation, SHUM – specific humidity, temp – temperature. OLS – ordinary least squares and UQ – upper quartile regression.

96
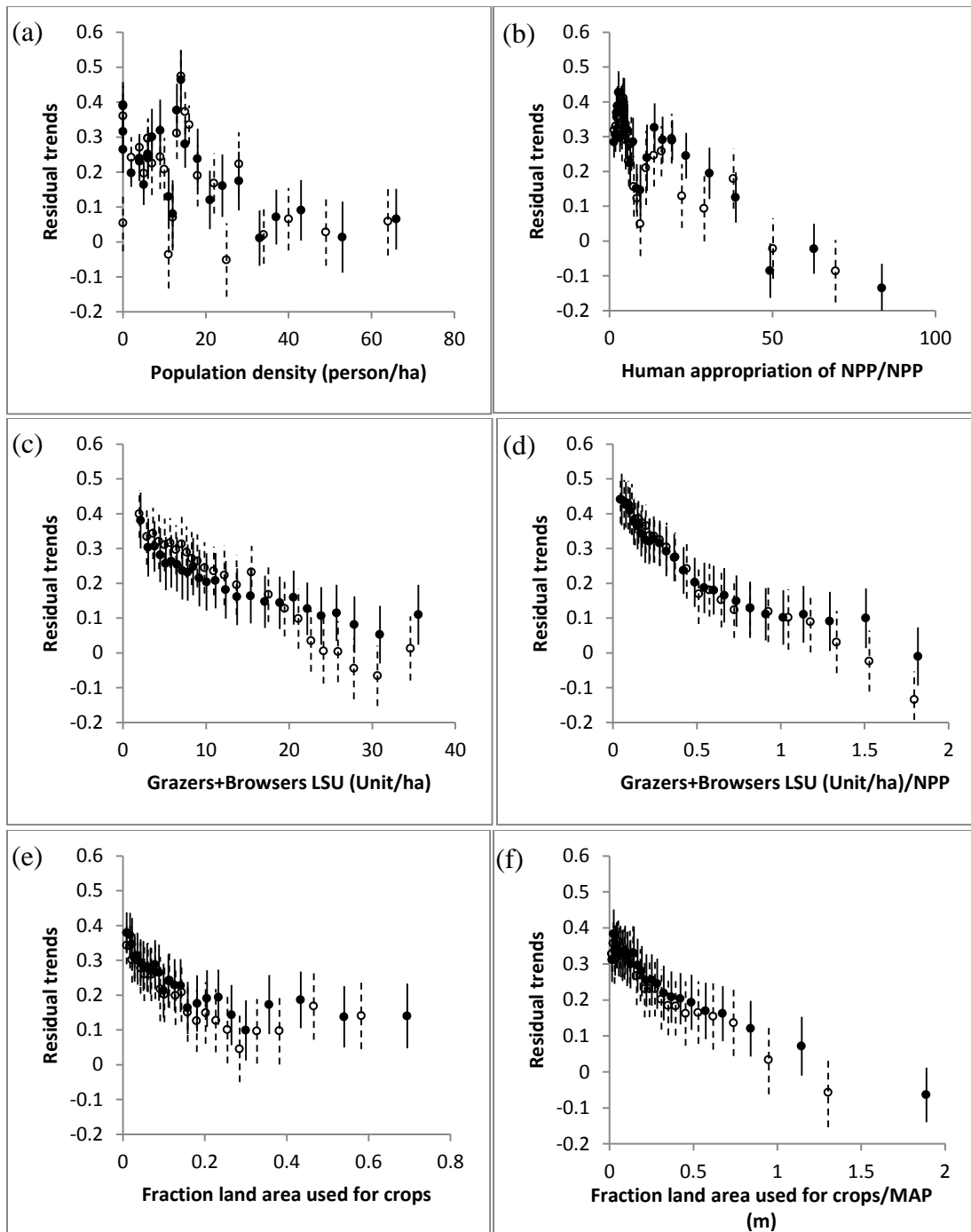
Figure 4.2 Mean residual trend values (observed – potential) within groupings of (a) population density (person/ha); (b) percentage human appropriation of NPP; (c) livestock unit density (unit/ha); (d) livestock unit density normalized by site productivity; (e) fraction land area used for crops; and (f) fraction land area used for crops normalized by mean annual precipiattion. Filled circles are trends of the residuals where potential NDVI was obtained from OLS multivariate regression between NDVI and precipitation, specific humidity, and temperature. Open circles are trends of the residuals where potential NDVI was obtained from OLS multivariate regression between NDVI and precipitation, its seasonal variance and skewness. Error bars are ±1 standard deviation around the mean.

97

The RF regression analysis indicated that, in addition to demographic and land use pressures, land cover and soil properties were significant (model E) (tables 4.2 & 4.3). The addition of fraction tree cover, soil bulk density and soil erodibility increased r^2 values. For example, the percentage variance in residual trend values explained by the variables LSU/NPP, crop density, and population density was approximately 60%. Adding soil bulk density or fraction tree cover increased the percentage variance explained (r^2) by more than 14% (table 4.2). Similarly, %HANPP alone explained 25% of the variability in residual trend values (Table 4.1) but adding soil bulk density and fraction tree cover increased the percentage variance explained to approximately 80% (table 4.3). The r^2 and the RMSE values of the RF models estimated using the "out-of-bag" method were similar to those obtained using the cross-validation approach, which indicates that, while RF trees were grown to a maximum without pruning, there was no evidence of model overfitting. Cross validation results for two RF models with relatively high r^2 values are shown in Figures 4.3c & 4.4c. The most important variables in relation to the spatial distribution of residual trend values listed in descending order were fraction tree cover, soil bulk density, soil erodibility, livestock unit density divided by the products of local photosynthesis (LSU/NPP), the index of cropping density divided by mean annual precipitation (%crop/MAP), and finally population density (figures 4.3b & 4.4b). The component loadings obtained from principal component analysis suggest that, except for fraction tree cover, all other variables were inversely related to residual trend values (figures 4.3a & 4.4a). The same analytical procedure was repeated but by utilizing residual trend values calculated from the other models (i.e. models A, B, C, D & F). While the nature of the relationships with land use pressures,

land cover and the geographical positions of soil properties were similar to these described for model E, the strength of the these relationships were persistently lower when residual trend values from models A & D were used in RF regression analysis, whereas the r^2 values for model B approached the corresponding model E values.

	Explanatory variables used in the regression tree model	Variance explained ($\sim r^2$)
Land use	LSU/NPP	0.31
	LSU/NPP + CD/MAP	0.54
Land use +	… + Available Water Capacity	0.58
	… + Soil Texture	0.62
	… + Soil Erodibility Factor (SEF)	0.64
	… + Soil Bulk Density (SBD)	0.69
	… + Land cover type	0.52
	… + Fraction herb cover	0.6
	… + Fraction tree cover (*f*Tree)	0.68
	… + Topographic Slope	0.56
	… + Fire density	0.62
	… + Population density (PopD)	0.64
"Best" models	Land use + PopD + SEF	0.72
	Land use + PopD + *f*Tree	0.76
	Land use + PopD + SBD	0.8

Table 4.2 Spatial variation in residual trend values explained by land use (livestock unit density and cropping density), land use and soil properties, and land use and land cover using RF regression tree models. LSU/NPP - livestock unit density normalized by site primary productivity, CD/MAP – Cropping density normalized by Mean Annual Precipitation.

	Explanatory variables used in the regression tree model	Variance explained (~r2)
%HANPP	… + Available water capacity	0.56
	… + Texture	0.66
	… + Erodibility factor	0.69
	… + Soil Bulk density (SBD)	0.74
	… + Land cover type	0.53
	… + Fraction herb. cover	0.64
	… + Fraction tree cover (fTree)	0.73
	… + Slope	0.64
	… + Fire density (FD)	0.65
"Best" models	%HANPP+SBD+fTree	0.80
	%HANPP+SBD+fTree+FD	0.81

Table 4.3 Spatial variation in residual trend values explained by %HANPP and soil properties, %HANPP and vegetation cover, %HANPP and fire density, and %HANPP soil bulk density and fraction tree cover using RF regression tree models.
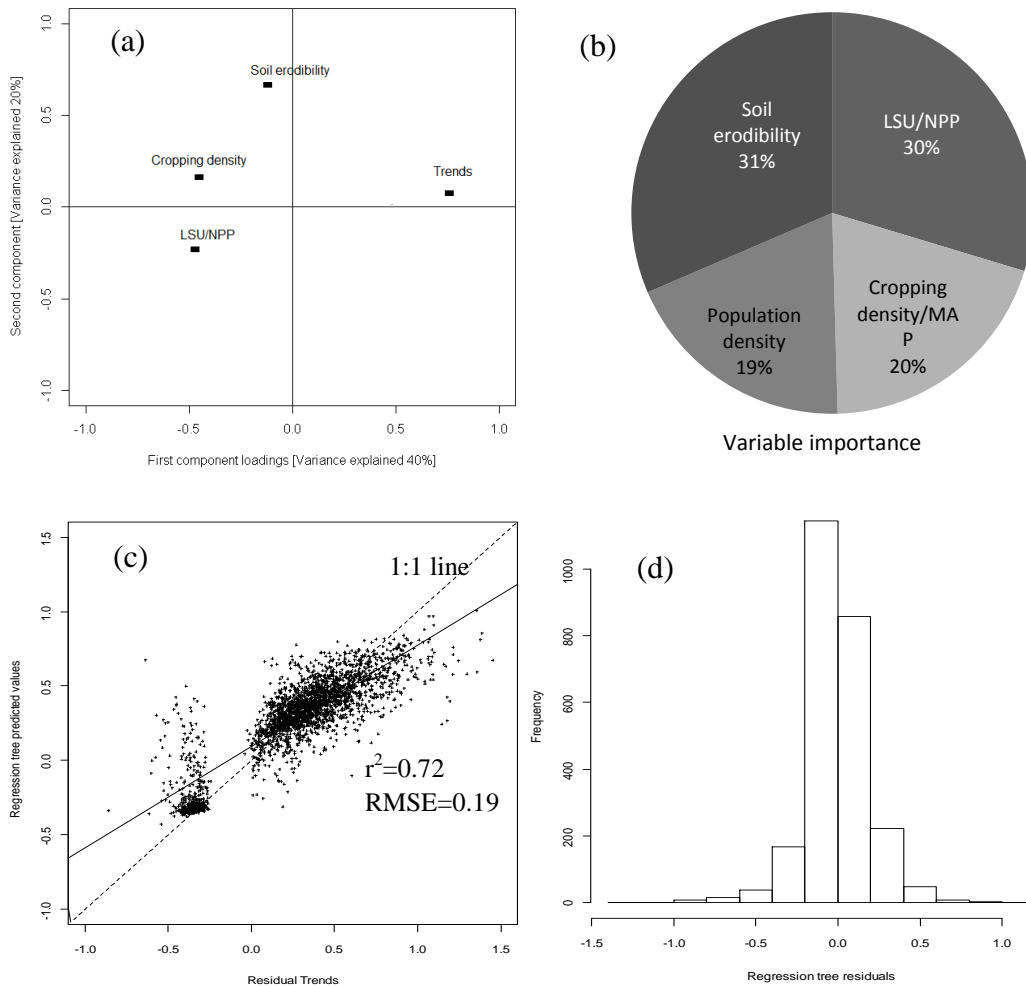
Figure 4.3 The upper panel demonstrates the relationship between significant residual trends and four explanatory variables, namely, soil erodibility factor, livestock unit density normalized by site productivity (LSU/NPP), fraction land used for agriculture (cropping density), and population density: (a) is a biplot of the of the first and second principal component loadings of a principal component analysis, and (b) are variable importance values calculated by the regression tree model Random Forest. The lower panel demonstartes the ability of the four explanatory variables to explain the variation in residual trend values: (c) is a comparison between residual trend values modeled from the NDVI data time series (x-axis) and residual trend values predicted by RF analysis (y-axis), and (d) is a histogram of the differences between the plotted values in (c). Residual trends insignificantly different from zero were excluded from the analysis.

101
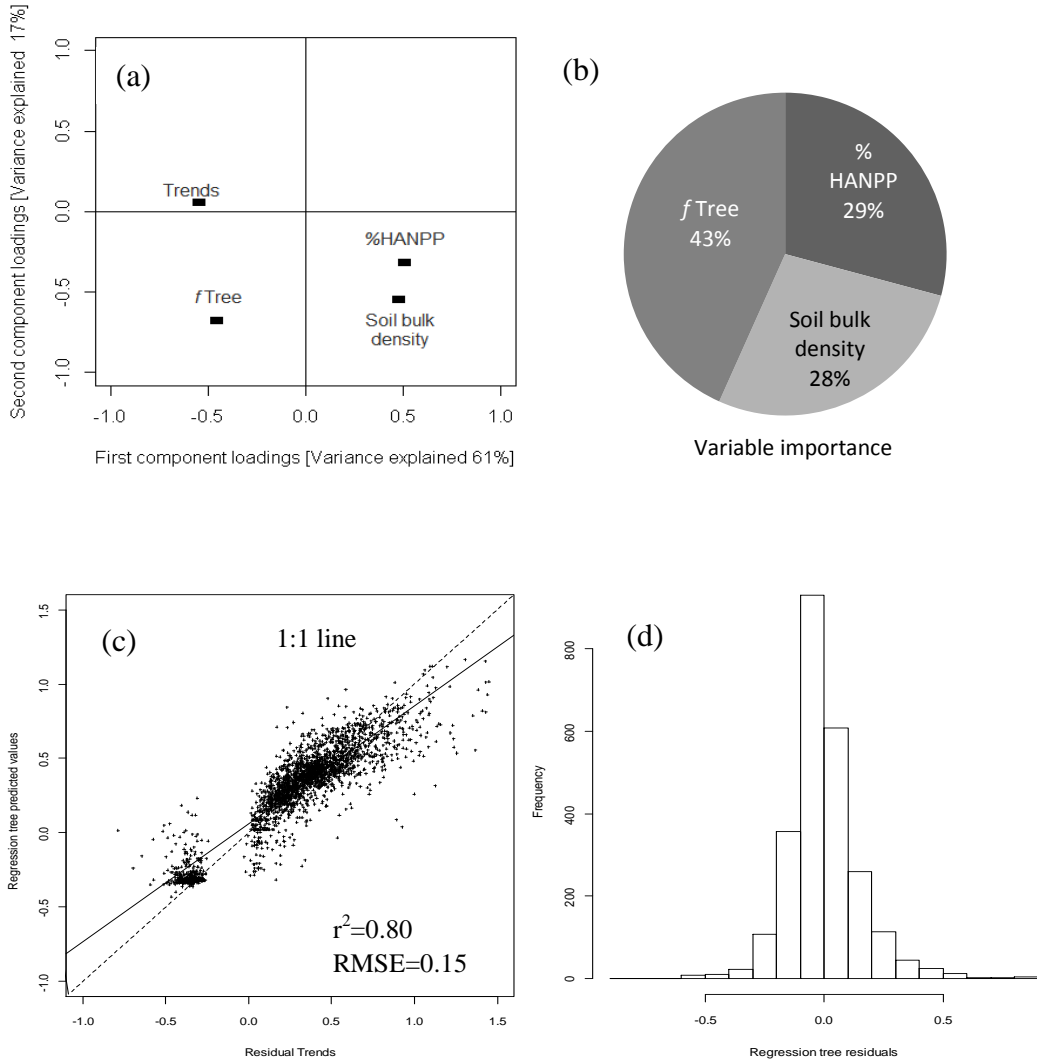
Figure 4.4 The upper panel demonstrates the relationship between significant residual trends and the three explanatory variables, namely, fraction tree cover (fTree), percentage human appropriation of NPP (%HANPP), and soil bulk density: (a) is a biplot of the of the first and second principal component loadings of a principal component analysis, and (b) are variable importance values calculated by the regression tree model Random Forest(RF). The lower panel demonstartes the ability of the three explanatory variables to explain the variation in residual trend values: (c) is a comparison between residual trend values modeled from the NDVI data time series (x-axis) and residual trend values predicted by RF analysis (y-axis), and (d) is a histogram of the differences between the plotted values in (c). Residual trends insignificantly different from zero were excluded from the analysis.

CART tree models did not capture the spatial variability in model E residual trend values as well as RF models, nonetheless they provided a graphical demonstration of the nature of the relation of residual trends to the explanatory variables (figures 4.5 & 4.6). Negative residual trend values were associated with areas characterized by high soil erodibility (>0.41) and population densities above 6.5 persons.km^{-2}, whereas areas with very high soil erodibility and population density below 6.5 persons.km^{-2} had on average positive residual trend values. Other areas associated with negative residual trends were characterized by high LSU/NPP values (>1.41), intermediate soil erodibility (0.24-0.41) and high population density (>19.5), or by intermediate LSU/NPP values (0.3-1.41), intermediate soil erodibility (0.24-0.41) and high cropping density/MAP (>0.41) (Figure 11). The regression tree of the relation of residual trends to %HANPP, fraction tree cover, and soil bulk density (figure 12) showed that the areas with low fraction tree cover (<8.5%), high soil bulk density (> 140.5), and high %HANPP (>24.5%) were generally associated with negative residual trend values, whereas areas with high fraction tree cover (>18.5%) and low soil bulk density (<136.5) were associated with positive trend values.

Population density >=6.5

S.V. = -0.25
S.D. = 0.23

V = -0.30
S.D. = 0.16
N=1531

V = 0.07
S.D. = 0.34

Soil erodibility >= 0.41

S.V. = 0.29
S.D. = 0.37

Soil erodibility >= 0.24

S.V. = 0.27, S.D. = 0.31

LSU/NPP >= 1.41

S.V. = 0.18, S.D. = 0.32

Population density >=19.5

S.V. = -0.08
S.D. = 0.32

V = -0.25
S.D. = 0.24
N=326

V = 0.09
S.D. = 0.30
N=296

Cropping density >=0.41

S.V. = 0.23
S.D. = 0.30

V = -0.06
S.D. = 0.4
N=412

V = 0.25
S.D. = 0.26
N=3434

LSU/NPP >= 0.30

S.V. = 0.36
S.D. = 0.32

Cropping density >=0.11

S.V. = 0.39
S.D. = 0.24

V = 0.29
S.D. = 0.24
N=1144

V = 0.45
S.D. = 0.23
N=1772

Soil erodibility >= 0.24

S.V. = 0.49
S.D. = 0.27

V = 0.41
S.D. = 0.24
N=3370

V = 0.60
S.D. =0.28
N=2112

Tree legend:
LSU/NPP: Livestock unit density normalized by site net primary productivity
Cropping density: Fraction land area used for crops
S.V. = Node split value.   S.D.= Standard deviation of values at the node
V. = Value at terminal node.   N= number of observations at terminal node
V = Value at terminal node.   S.D.= Standard deviation of values at the node

Figure 4.5 Pruned regression tree showing the hierarchical relations of residual trends to land use, demographic pressures and soil erodibility.   Regression tree r^2 = 0.6 and RMSE = 0.23.

104

Figure 4.6 Pruned regression tree showing the hierarchical relations of residual trends to %HANPP and to soil and land cover properties. Regression tree $r^2 = 0.65$ and RMSE = 0.21.
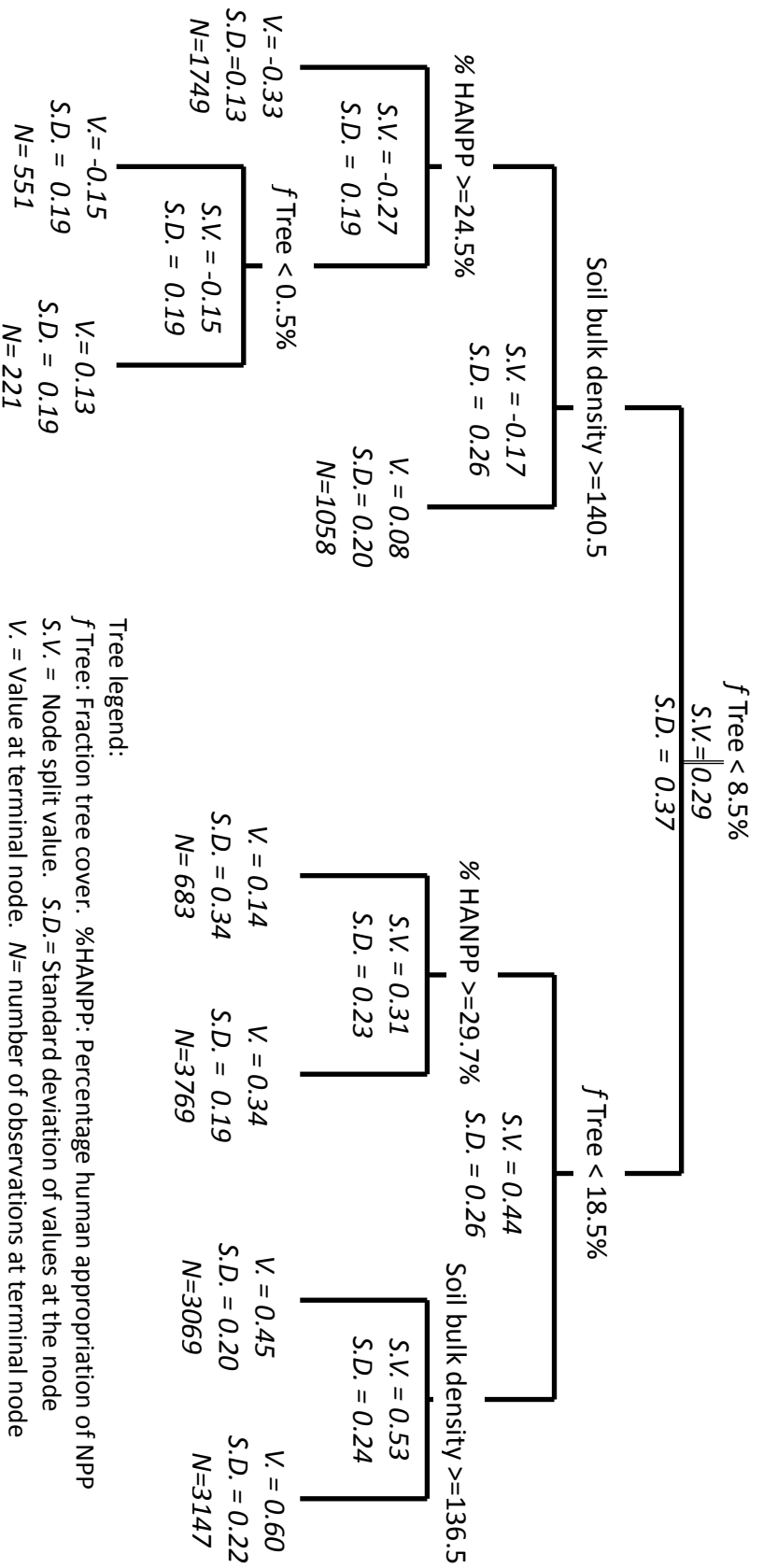
Tree legend:
f Tree: Fraction tree cover. %HANPP: Percentage human appropriation of NPP
S.V. = Node split value.   S.D.= Standard deviation of values at the node
V. = Value at terminal node.   N= number of observations at terminal node

105

4.4 Discussion

Analysis of the relation between residual trend values and population density does not support the notion that higher population density in the Sahel invariably causes reductions in land productivity (table 4.1). %HANPP, on the other hand, was related to reductions in land productivity (r = -0.55). It should be noted that the calculation of %HANPP in Imhof *et al.* (2004) does not account for lateral flows (imports or exports) of NPP-based products. Including these effects may provide a better accounting of the pressures people impose on their local environment. Nevertheless, the relationship between %HANPP and residual trends was strong enough to suggest that higher demands for NPP-based goods in relation to local NPP production are likely to impoverish local ecosystems as suggested in (Daily *et al.* 1997).

Further examination of the relation of single land use pressures such as livestock and area of land used in cultivation to the residual trend values revealed moderate to weak correlations (table 4.1). However, stronger relationships were found between residual trends and the ratios of both LSU to livestock carrying capacity (LSU/NPP; r = -0.51) and %crop to mean annual precipitation (%crop/MAP; r = -0.55). While the inverse relationship between residual trends and LSU/NPP was expected, the relation with %crop/MAP suggests that the extension of cultivation into marginal lands, not suitable for agriculture, may result in long term reductions in productivity or degradation (Le Houérou 1996; Geist & Lambin 2004).

The meta-analysis of case studies of land degradation (Geist & Lambin 2004) found that, contrary to the theory of single-factor causation (Breckle *et al.* 2002; Le

106

Houérou 2002), land degradation in Africa can more often be attributed to multiple factors and to remote influences such as changes in agricultural policies, extensive livestock production, production of annual cash crops and irrigation development. It was also found that the spatial variations in residual trend values were not only better explained by a multiplicity of land use pressures but also by local variations in biophysical variables (tables 4.2 & 4.3). Of the biophysical variables explored, soil bulk density, soil erodibility, and the fraction land area covered by trees were strongly related to the vulnerability of landscapes to land use pressures. These variables either enhanced or dampened the adverse effects of demographic and land use pressures (figure 4.5 & 4.6). For instance, areas with high soil bulk density were frequently associated with negative residual trends suggesting that high bulk density soils were more susceptible to water erosion and wind dispersion as suggested in (Meeuwig 1970; Yamamoto & Anderson 1973; Young & Mutchler 1977; Gupta *et al.* 2010). Areas with low fraction tree cover were also frequently associated with negative residual trends suggesting the areas with low fraction tree cover were more susceptible to degradation by human agency. One possible mechanism is that fuel wood collection and agriculture and grazing simplify the vegetation structure exposing the soil to wind and water erosion (Le Houérou 1996).

4.5 Conclusions

Several studies have demonstrated that the return of more favorable climate conditions in the Sahel, following the extreme droughts of the 1970s and early 1980s, was accompanied by a net increase in vegetation greenness (e.g. Nicholson *et al.* 1998; Eklundh & Olsson 2003). Yet the spatial variations in the rates of vegetation recovery

have only partially been explained by climate trends (Olsson et al. 2005; Hiernaux et al. 2009b) thus reinvigorating the debate about the influence of anthropogenic land uses on vegetation productivity (Hein & De Ridder 2006; Hein et al. 2011). The analysis in Chapter 3 identified the areas where the land surface has been greening "faster" (i.e. positive residual trends) or "slower" (i.e. negative residual trends) than what would be expected from the trends in climate. In this Chapter, the spatial variations in residual trend values were related to land use and demographic pressures.

The results suggest that over large areas of the Sahel (> 87%), the trends of vegetation greenness either exceeded (i.e. positive residual trends) or did not significantly depart from what is expected from the trends in climate (i.e. insignificant residual trends). The areas with positive residual trends were frequently associated with relatively low demographic and land use pressures. (Olsson *et al.* 2005) and (Mortimore & Harris 2005) cite changes in land use, land rehabilitation and/or investments in soil and water conservation measures as possible causes of the recent greening trend in the Sahel. Undoubtedly, there are places where land rehabilitation efforts have increased land productivity but, at the scale of observation used here, there is little evidence to suggest that land rehabilitation or agricultural intensification were adequate explanations of the long term increases in land surface greenness. For instance, Cropland expansion in West Africa was accompanied by a decrease in fertilizer use (-1.83% per year) and just a modest increase in irrigation (0.31% per year) (Sanchez 2002; Lambin *et al.* 2003). The scales of the phenomena and the explanations must match. Explanations that match the scale of the findings include an increase in water use efficiency caused by CO_2 fertilization, higher nitrogen deposition, higher atmospheric aerosol loadings, or

transitions to new quasi-stable vegetation compositions following the extreme droughts of the 1970s and 1980s (Cohan et al. 2002; Matson et al. 2002; Nemani et al. 2003; Cao et al. 2004; Hickler et al. 2005) and, perhaps, non-linear, accelerating responses of vegetation to the changing climate.

Contrary to findings in similar studies (Herrmann *et al.* 2005a; Fensholt & Rasmussen 2011), this study found substantial (8-13%) and spatially coherent areas with significant negative residual trends. These areas were found to have high livestock densities relative to their carrying capacity, heavily utilized for cultivation, overworked marginal lands or combinations of these. The results suggest that demographic and land use pressures have had a measurable impact on vegetation dynamics in some parts of the Sahel during the period 1982–2006.

Chapter 5: Synthesis, discussion and significance

5.1 Context

There is a pressing need for quantitative information on the distribution, severity and causes of land degradation (Dregne 2002; Prince 2002). This information is important to understand the effects of degradation on land surface properties, atmospheric dust transport, and land-atmosphere feedbacks that could enhance, through changes in albedo and evapotranspiration, the drying tendency initiated by changes in global sea surface temperature (Charney 1975; Zeng 2003). Also, this information is important to channel land improvement investments and to support decision-making on the appropriate intensity and type of land use (Batterbury *et al.* 2002; Dregne 2002; Geist & Lambin 2004)

There are several reasons for the current lack of information on the extent, severity and causes of land degradation, including the lack of appropriate metrics that are consistent and practicable for use over large areas. NPP, which can be measured reliably from space is a promising technique for monitoring land degradation since most of the biophysical processes involved in degradation (e.g. soil crusting, compaction and erosion, depletion of soil nutrients and organic matter, and the disruption of biogeochemical cycles) reduce the NPP – that is accumulation of biomass through time (Prince 2002).

The goals of this dissertation were therefore to: (1) use consistent, spatially contiguous, and long-term satellite based estimates of NPP to examine quantitatively whether there is evidence of human-induced land degradation in the Sahel and, if so, its location and intensity, and (2) investigate the relation of land degradation to demographic

and land use pressures. This chapter synthesizes the findings and discusses their significance.

5.2 Findings

NPP in arid and semi-arid areas is largely determined by soil moisture availability. Soil moisture is in turn influenced by soil properties, the size and frequency of precipitation events, incident solar radiation, air temperature and humidity. However, the Sahelian climate, especially rainfall, is highly variable in time and location so any reduction in NPP caused by degradation is often masked by the stronger effects of climate variations on NPP. Therefore it is essential to control for the effects of climate variability when attempting to tease out evidence of human-induced land degradation. To control for the effects of climate, the observed NPP was examined as a departure from potential NPP; that is the NPP expected in response to climate variability alone excluding any human-induced changes in productivity. Earlier studies (e.g. Geerken & Ilaiwi 2004; Wessels *et al.* 2007) estimated potential NPP from the rainfall -NPP relationship (Rain Use Efficiency, RUE) which was assumed to be a conservative parameter (Le Houérou 1984). However, estimating potential NPP from the rainfall -NPP relationship is only applicable where rainfall is the principal factor limiting vegetation production (Prince 2002). In this research, however, the inter-annual variations in NPP were poorly explained by annual rainfall totals (Chapter 2) in large areas in the dry (< 400mm mean annual precipitation (MAP)) and wet margins (>1000mm MAP) of the Sahel.

Several factors other than precipitation totals were found to influence vegetation production. For example, statistical analyses revealed positive relationships with humidity. A sensitivity analysis using a detailed soil-vegetation-atmosphere-transfer

model (SSIB2) (Chapter 2) indicated that, in addition to rainfall, air humidity and temperature can also affect vegetation production (figure 2.13) either directly by influencing stomatal conductance (figure 2.12) or indirectly by altering soil moisture levels (figure 2.11). Higher specific humidity was found to reduce modeled evapotranspiration demand resulting in higher volumetric soil moisture content in the root zone (figure 2.11). Higher volumetric soil moisture content and higher atmospheric vapor pressure, in turn, combined to increase modeled stomatal conductance (figure 2.12) and therefore canopy-scale NPP (figure 2.13). The sensitivity to humidity was, in general, higher in wetter areas (figures 2.11, 2.12 & 2.13), possibly because of the preponderance of C3 plants which are more sensitive to variations in humidity (Kawamitsu *et al.* 1993) than C4 grasses which dominate the drier regions of the Sahel.

Modeled vegetation responses to temperature variation revealed both positive and negative relationships. Positive associations occurred in the mountainous wet regions and during wet periods of the growing season while negative relationships were found in hotter, lower altitude regions. The positive relationships may have been caused by increases in temperature-dependent photosynthetic reaction rates that countered the desiccating effects of higher temperatures (figures 2.11 and 2.13). Negative NPP-temperature relations occurred in the larger, hotter areas (figure 2.8) probably due to the desiccating effects of higher temperatures.

Correlation and model sensitivity analysis indicated that vegetation production in the drier parts of the Sahel was more sensitive to inter-annual variations in rainfall totals than areas with greater rainfall (figures 2.9 & 2.13). The weak NPP response to additional precipitation in the wetter margins suggest that the woody plant associations in sub-

112

humid southern Sahel had sufficient soil moisture to meet evapotranspiration demands even during years with below-average precipitation (Chapter 2). Model sensitivity study of NPP response to precipitation at several sub-humid locations showed that soil moisture by volume, even in dry years, did not drop below 12% (figure 2.11) and hence did not limit transpiration or productivity (figure 2.12).

In addition to precipitation totals, the within-season distribution of precipitation events was also found to be correlated with vegetation production. The correlations between growing season, compared with annual integrated NPP and precipitation totals, were generally higher (Chapter 2), confirming that occasional rainfall outside the main growing season has little effect on vegetation production (Yang *et al.* 1998; Wang & Eltahir 2000; Wessels 2005; Wessels *et al.* 2007; Knapp *et al.* 2008). This was particularly evident in the northern Sahel where seedlings of early germinating species, including staple crops such as millet, can be killed by drought following early rain.

While NPP was inversely related to intra-seasonal precipitation variance, it was positively related to its skewness, suggesting that, for the same amount of precipitation, vegetation production is higher when precipitation arrives in more frequent and less intense events. These findings are different from the suggestion in Knapp *et al.* (2008) that an intensified hydrological regime would increase NPP in xeric environments while reducing NPP in mesic environments. The discrepancy between the results of this study and those of Knapp *et al.* (2008) may be caused by differences in average size of precipitation events between their study site in North American grasslands and the Sahel. Whereas in North American grasslands, an intensified precipitation regime may reduce water losses to canopy interception, evaporation and runoff (Knapp *et al.* 2008), the same

is not necessarily true for the Sahel since the percentage of total precipitation that falls in very small events (<7 mm/day) in the Sahel is minimal (Barbé & Lebel 1997; D'Amato & Lebel 1998; Le Barbé *et al.* 2002) and therefore the reductions in evaporation due to an intensified precipitation regime might not offset water losses to higher runoff.

In general, the inter-annual variations in NPP were better explained by precipitation, specific humidity and temperature or by precipitation and its intra-seasonal distribution than by precipitation totals alone. The climate-NPP relations were geographically coherent, suggesting fundamental causes. The analysis clearly revealed that vegetation dynamics in the Sahel and their environmental correlates are more complex than equilibrial relationships between total growing season precipitation and NPP. The relationships presented here provided a new dimension to climate–productivity relationships in the Sahel.

The geographical distribution of negative trends in productivity, where NPP is lower than what can be explained by meteorological conditions, and positive ("greening") trends where productivity is higher than what can be explained by meteorological conditions, consistently identified substantial and spatially contiguous areas (~8% of the total area of the Sahel) with significant negative trends (Chapter 3). These included large areas in western Sudan centered on Nyala, in southern Niger around the cities of Zinder, Maradi, Dosso and Niamey, in Nigeria extending between Kano in the north and Abuja in the south, and throughout Burkina Faso (figure 3.4).

Explanations of the "greening" trend in the literature include agricultural intensification, land abandonment associated with economic migration and civil strife,

and increased investment and improvements in soil and water conservation techniques (Prince 2002; Hickler *et al.* 2005; Mortimore & Turner 2005; Olsson *et al.* 2005). However, the areas with positive residual trends found here were frequently in areas with lower population and hence land use pressures (Chapter 4). Therefore, there is little evidence to suggest that land rehabilitation, economic migration, or agricultural intensification are adequate explanations of the large scale "greening" of the Sahel. The scales of the phenomena and the explanations must match. Explanations that match the scale of the findings include an increase in water use efficiency caused by CO_2 fertilization, higher nitrogen deposition, higher atmospheric aerosol loadings, or transitions to new quasi-stable vegetation compositions following the extreme droughts of the 1970s and 1980s (Cohan et al. 2002; Matson et al. 2002; Nemani et al. 2003; Cao et al. 2004; Hickler et al. 2005).

Contrary to the theory of single-factor causation (Breckle *et al.* 2002; Le Houérou 2002), negative trends of NPP in the Sahel were often related to multiple land use pressures especially the expansion of agriculture into dry areas and to high grazing densities in the drier parts of the Sahel. This suggests that in these areas, the existing livestock densities and recent agricultural practices (e.g. length of the fallow period) are reducing vegetation production thus increasing the risk of land degradation. However, the vulnerability of land to degradation from land use pressures was found to vary with soils and tree vegetation cover. Areas with high soil bulk density were more frequently associated with negative residual trends suggesting that they were more susceptible to water erosion and wind dispersion than others, as suggested in (Meeuwig 1970; Yamamoto & Anderson 1973; Young & Mutchler 1977; Gupta *et al.* 2010). Areas with

115

low tree cover were also more frequently associated with negative residual trends re-emphasizing the role trees play in protecting the soil from erosion processes.

5.3 Relevance to climate studies, global carbon budget and food security

The impacts of land degradation on regional climate are poorly understood. In 1975, Charney controversially claimed that the drought had been the result of land degradation. He hypothesized that land degradation increases surface albedo which, in turn, reduces atmospheric subsidence over the Sahel which in turn suppresses rainfall providing a positive feedback by which degradation causes drought and drought becomes self-accelerating. While some modeling studies do not support Charney's hypothesis (Taylor *et al.* 2002; Nicholson 2011b), most support the idea that changes in vegetation and soil associated with land degradation can have an influence on weather and climate (Zeng *et al.* 1999; Clark *et al.* 2001; Prospero & Lamb 2003), Furthermore, most of these simulations tested hypothetical scenarios of expansive and severe degradation (Zeng *et al.* 1999; Clark *et al.* 2001; Prospero & Lamb 2003). Therefore it remains unclear whether the actual extent of degradation in the Sahel has any measurable impact on climate. The maps of land degradation produced here are making a significant contribution to such modeling efforts (e.g. Xue, personal communication).

The effects of land degradation on the carbon (C) cycle are poorly known which is surprising in view of the fact that drylands' soil organic and inorganic C have been estimated to comprise 27% and 97% of the global reserves, respectively (Safriel 2007a). Land degradation presumably releases large amounts of C from soil erosion and from cleared and dead vegetation (Lal 2003; Williams & Albertson 2005). Yet the impact of land degradation on the C budget is not accounted for in any regional-scale C models

116

(Lal 2003). Part of the reason is that the available data on the extent and severity of land degradation is sparse and is generally subjective, qualitative, and often exaggerated (Lal 2003; Lal 2004). The assessment of persistent reductions in land productivity potential as a large scale anthropogenic modification of the land surface developed here can make a crucial contribution to C-cycle research, including C accounting (Hulme 2001; Nicholson 2001).

Furthermore, controlling land degradation is central to achieving food security, sustainable agricultural and rural development in many countries. Today, regional and international development assistance agencies are actively engaged with the governments of the 195 United Nations Convention on Combating Desertification (UNCCD) signatory Parties (nations) in designing and implementing land degradation control projects, programs, planning and legal frameworks (Low 2013). Yet, the paucity of data on land degradation – its location, severity and causes - partly due to the lack of any readily measured, objective indicators have inhibited progress (Prince 2002).

To strengthen the implementation of the UNCCD goals, the Conference of the Parties in its eighth session (2007) invited Parties and international institutions to "*identify the major aspects of land degradation arising in the various eco-geographical zones and to measure their severity in order to find appropriate solutions*" and also invited the "*Committee on Science and Technology (CST) to assist in creating an international policy environment for the provision and transfer of adequate technology, particularly remote sensing technology, to affected country Parties for the establishment of effective monitoring and assessment systems*" (UNCCD 2007). The land degradation monitoring techniques developed in this study are relevant to UNEP's Land Degradation

Assessment (LADA) project tasked with developing standardized and improved methods for dryland degradation assessment.

5.4 Technique development

A key aspect in developing degradation indices is the identification of potential, non-degraded sites (Prince 2002; Nicholson 2011a) to provide the standard against which actual NPP can be judged. Because of the more complex relationships between NPP and environmental factors revealed by the regression analyses and modeling discussed above, potential NPP was estimated here from regression of NPP on (1) precipitation, (2) precipitation, specific humidity and temperature, and (3) precipitation and its intra-seasonal distribution (Chapter 3). Compared to NPP calculated from precipitation alone (1), potential NPP estimated using precipitation, humidity and temperature (2) and intra-seasonal precipitation distribution (3), had lower prediction errors of potential NPP (figure 3.2) than precipitation alone. These lower errors increase confidence in the residual trend results (Chapter 3).

In addition to the meteorological variables discussed above, NPP is often affected by land degradation and other environmental and anthropogenic factors, such as variations in nutrient availability, run-on and off, grazing and fuel wood collection (Pickup 1996) and lag effects caused by antecedent dry or wet years that affect subsequent year NPP (Dalgleish & Hartnett 2006). The effects of these factors on NPP are smaller in dry years than they are in wetter years (Pickup *et al.* 1998). This has an effect on the estimation of potential NPP as follows: (a) potential NPP is underestimated where factors reduce NPP response to meteorological variables; (b) the opposite occurs

where factors increase NPP response to meteorological variables; and (c) the estimation error terms are non-normal; higher in wet years than in dry years.

The consequences of underestimating potential NPP is underestimation of "degradation" signal since the magnitude of the residual is reduced. The opposite occurs when potential NPP is overestimated. In an attempt to minimize these effects, potential NPP was estimated using Upper Quantile (UQ) regression since UQ regression coefficients are less sensitive than their OLS counterparts to NPP values influenced by factors other than the regressors (Buchinsky 2000).

The residual trends methods highlight potentially degrading areas but further examination is essential to confirm the diagnosis since negative or positive trends in vegetation production relative to its potential are not necessarily the result of land degradation or land improvement. The method thus acts as a means to focus attention on the areas that might be undergoing degradation (Prince 2002) and focus more detailed investigation.

Furthermore, degradation can manifest itself in characteristics other than loss of potential NPP. These include reduced biodiversity (Pickup *et al.* 1998; Adeel *et al.* 2005) and encroachment by woody vegetation (Grover & Musick 1990). Woody encroachment, in particular, is considered to be a serious environmental problem (Sinclair & Fryxell 1985; Grover & Musick 1990). However, the replacement of grasses with woody vegetation does not necessarily reduce NPP and consequently might not be detected using the residual trends method. Another view is that woody

encroachment is a distinct type of degradation and should be excluded from consideration using the methods developed here.

The value of this monitoring approach as an indicator of land degradation should be assessed for each area of application. Clearly validations must be carried out over areas close to the finest resolution of the maps developed by residual trend analysis ($278km^2$). Currently assessments of land degradation and its causes are mainly based on expert opinions of the susceptibility of different soils to degradation (Dregne 1977; Dregne 1983; Dregne & Chou 1992) and, to a lesser extent, on actual soil degradation (Oldeman *et al.* 1990). Thus the land degradation monitoring approach developed in this dissertation may provide a long overdue, quantitative alternative to existing assessments.

5.4 Monitoring versus mapping land degradation

A distinction should be made between monitoring ongoing degradation and mapping existing degradation. The residual trends method is geared towards detecting changes in land productivity potential through time. Areas that have been degraded prior to the observation period and have been stable since will not be detected. In the present study the period is determined by the length of the satellite record.

To address this limitation, an alternative method, Local NPP Scaling (LNS) has been proposed (Prince 2002). LNS estimates non-degraded reference NPP from the upper part of the frequency distribution of NPP values within a land capability class (LCC). The NPP of each pixel within a LCC is then expressed as a proportion of its non-degraded reference NPP. Stratification by LCCs allows for spatial variations in climate, soils, land use and topography to be normalized. This procedure is similar in concept to

the use of land classification to determine appropriate uses of land for agriculture or livestock production and for land valuation (FAO 1976).

The LNS method was developed in Zimbabwe (Prince *et al.* 2009) where there was a very appropriate, if regrettable in human terms, opportunity to observe the communal lands that are indisputably degraded. The LCCs were defined by stratification of detailed spatial information on rainfall, soils and land use. Large negative departures of NPP from its potential were evident in the degraded communal lands whereas the NPP values of most (but not all) commercial agricultural areas, parks and reserves were close to the non-degraded reference NPP. However, residual inhomogeneities were found in some land capability classes which is the critical limitation of the LNS method since it causes errors in the estimation of potential NPP. Some LCCs had small, but highly productive, areas such as wetlands, riparian features and irrigated and fertilized crops that were not identified by the stratification criteria. The method assumes that the LCCs have uniform productive potential and that a sufficient number of non-degraded pixels exist in every LCC. However, if either of the assumptions is violated, the estimates of potential NPP will be in error, the consequences of which can be either false positive or false negative degradation signals.

The residual trends and the LNS methods may be applied in tandem to, respectively, monitor ongoing degradation and to map the areas that have been degraded prior to the observation period and have been stable since. This approach is the subject of ongoing research.

If the above-mentioned shortcomings of the LNS method can be adequately addressed, it promises to be a very useful tool for identifying potentially degraded areas in the Sahel and other drylands. More detailed land use and land cover data are becoming increasingly available (Ramankutty *et al.* 2008), can be used to improve the creation of LCCs, for example by separating natural vegetation from altered cover types, such as irrigated agriculture or human settlements. To some extent surface runoff can be modeled using soil-vegetation-atmosphere transfer models such as SSIB (Xue *et al.* 1991a) used here and the Soil and Water Assessment Tool (SWAT) (Gassman *et al.* 2007). Riparian features and areas with enhanced run-on can be mapped from high resolution digital elevation models (e.g. Shuttle Radar Topography Mission, SRTM data). These can be used to improve the stratification by creating more homogeneous land capability classes.

5.5 Future research

This research has opened several topics for further research. These can be broadly considered under the headings of further technique development, applications to studies of land surface process, and application to the science of dryland degradation.

5.5.1 Science applications

Maps of degradation offer, for the first time, the opportunity to use realistic observations of disturbance in land surface-atmosphere (SVAT) models. Degradation affects two aspects of the land surface system, directly through changes in the surface energy balance and indirectly by altering the vegetation types. Most current studies apply simple theoretical land surface conditions as was done in the very first climate model of

the Sahel in 1993 (Xue & Shukla 1993). The relevant question is whether the extent of land degradation revealed in this study positively enhanced the drying tendency initiated by the changes in global sea surface temperature. Our collaborators, Dr. Yongkang Xue and Dr. Peter Cox have coupled the SSiB SVAT model to global circulation models (GCMs) and to the TRIFFID vegetation model, a combination that can study the effects of anthropogenic factors including degradation.

A much less studied consequence of drought and degradation in semiarid regions is atmospheric dust. African dust sources account for about half of the global total today (Zeng 2003). Dust supply influences the energy balance in the atmosphere and at the surface and serves as a nutrient for marine phytoplankton and thus may modify the global carbon cycle and climate. While dust concentrations are anticorrelated with concurrent rainfall in the Sahel (Prospero & Lamb 2003), it is difficult to resolve any anthropogenic influences on atmospheric dust loads such as those due to land degradation (Tegen & Fung 1995; Mahowald *et al.* 2002) owing to the paucity of data that would allow the identification of long-term trends in desertification (Brooks *et al.* 2005). Data on existing and ongoing land degradation may be studied in tandem with the climatology of dust transport occurrence to resolve the degree of degradation-induced dust mobilization.

The regression and modeling studies made during this research both point to the role of soil moisture in regulation of NPP. Current improvements in remote measurement of soil moisture (Albergel *et al.* 2013) therefore offer the hope of much improved measurement of potential NPP for comparison with other sites to identify differences in NPP that cannot be attributed to non-anthropogenic effects and are therefore candidates for more refined testing to confirm or refute degradation.

Perhaps one of the more important questions is the effect of land degradation on carbon stocks. More than half of the organic C stock in grasslands and wooded Savanna is stored in soils. This distribution of soil organic C, which was not correlated with aboveground carbon stocks (Ryan *et al.* 2011) and the very variable nature of soil organic matter, complicates the use of remote sensing for spatial mapping of drylands' C stocks. A distributed sample of soil measurements across soil, land cover/use and degradation severity classes can be designed to understand the relation, if any, between degradation and changes in soil carbon stocks. Moreover, a number of crucial socio-economic processes are not yet well represented in terrestrial ecosystem models that were used to estimate the C balance in drylands (Ciais *et al.* 2011). The relation of human appropriation of NPP as well as grazing and cropping patterns to changes in productivity as revealed in this study can be used to improve such models.

5.5.2 UNCCD-type uses

The creation of maps of existing degradation and of changes in vegetation productivity at the country-continental scales can revolutionize the activities of national and international organization charged with rehabilitating degraded landscapes and limiting further degradation. The human resources available to affected UNCCD parties can be used to validate and, if necessary, to refine the findings of this study. A spatial representation of the relation of soil properties and land use intensity to degradation can be produced using the algorithms developed in this study to support policies on the appropriate type and intensity of land use and to channel investments in land development projects.

The transfer of the techniques developed in this study to affected country Parties can aid in the establishment of effective monitoring and assessment systems. The algorithms relating land use pressures to degradation can be used in land degradation risk assessment of future land use and development policies.

5.5.3 Technique development

The human scale of degradation tends to be in the 10 – 100ha range, although can be much larger, for example across rangelands, agricultural landscapes, mining operations, and highly erodible slopes. The present study was limited to the 278km^2 of the spatially aggregated AVHRR GAC data needed to obtain the longest possible record of NPP and is therefore limited to relevance to phenomena at that scale (i.e. phenomena that took place during the AVHRR/2 and /3 observation period from 1981 to present). Spatial aggregation to 0.15° was necessary to reduces most of the errors introduced by the GAC sampling scheme (Rembold & Maselli 2010). However, computing power and the cost of data storage have recently made it possible to process MODIS data (~7 ha) globally. Furthermore the seven land observation spectral channels available from MODIS sensor are capable of detecting many more land surface features than the two from AVHRR. Therefore it is entirely possible to undertake LNS analyses at the ~7 ha scale of MODIS. The value of this capability would be to investigate the "hot spots" of degradation identified at the AVHRR scale in order to confirm the presence of degradation, its dimensions and gain information that may enable causes to be attributed. This is a subject of ongoing research.

Potential NPP can be estimated using process-based prognostic vegetation models such as BIOME-BGC (Running & Hunt 1993), LPJ-DVGM (Hickler *et al.* 2005) and

SSIB-TRIFFID (Dr. Yongkang Xue, personal comm.). These models can be used to describe NPP, vegetation structure and composition in their natural undisturbed state. Actual NPP, on the other hand, can be modeled from satellite measurement (e.g. Running *et al.* 2004). The difference between actual and potential NPP can be used to map degraded areas and to monitor ongoing degradation. The index to map degradation in this case would be the difference between potential and actual NPP while the index for monitoring degradation would be the slope of the regression of the residuals (potential − actual NNP) with time. A major limitation of estimating potential NPP using prognostic vegetation models was the availability of data to calibrate and validate the models. Recently, the CARBOAFRICA (http://www.carboafrica.net) and AMMA (http://amma-international.org/) projects are operating a network of eddy covariance flux towers characterizing the spatial gradients and temporal variations of CO2, and heat and water vapor fluxes over woodlands, savannahs and rangelands. Calibrating the SSIB-TRIFFID vegetation model using these flux data is a subject of ongoing research.

Appendix 1: Reconstruction of daily AVHRR NDVI data

A1.1 Background

AVHRR daily reflectance data processed by the Long Term Data Record (LTDR; Pedelty *et al.* 2007) were used to reconstruct daily NDVI values from 1982 to 2006. The LTDR processing stream employs an improved atmospheric correction scheme to reduce the effects of Rayleigh scattering, ozone, and water vapor but does not correct for the effects of aerosols (Pedelty *et al.* 2007).   Prior to calculation of NDVI values, the reflectance data were normalized to a standard sun-target-sensor geometry. Bidirectional Reflectance Distribution and atmospheric corrections should reduce noise in surface NDVI data (Nagol *et al.* 2009) that would otherwise result from the strong anisotropic properties of vegetation (Gutman 1991; Vermote *et al.* 2009a; Fensholt *et al.* 2010) and from considerable absorption in the AVHRR near infrared channel by atmospheric water vapor (Cihlar *et al.* 2001). Cloud contaminated observations were removed and replaced with reconstructed values from preceding and succeeding "clear sky" observations of the same pixel.   The resulting daily data should allow more precise identification of vegetation dynamics (Viovy *et al.* 1992) than maximum value compositing, particularly in drier areas with short growing season.

The AVHRR NDVI data were then compared to NDVI data derived from BRDF corrected AQUA Moderate Resolution Imaging Spectroradiometer (MODIS) Climate Modeling Grid surface reflectance data (MYD09CMG) (Vermote *et al.* 2009a; Vermote & Kotchenova 2011) during the overlapping period (2003-2006) to estimate the relative residual errors in the AVHRR NDVI data resulting from incomplete sensor calibration, atmospheric and BRDF corrections, and from cloud filtering. The relatively low errors in

MODIS data (Vermote & Kotchenova 2008) when compared to those of AVHRR (Nagol 2011b) make this approach for estimating errors reasonable. Daily NDVI data errors were then used to estimate the errors in the growing season sums of NDVI.

A1.2 LTDR AVHRR data

Version 2 of the LTDR daily time series of the National Oceanic and Atmospheric Administration (NOAA) AVHRR Global Area Coverage (GAC) reflectance data (Pedelty *et al.* 2007) for the years 1982 to 2006 were used in this study (http://ltdr.nascom.nasa.gov).   The LTDR data processing stream creates a daily reflectance product using a geographic projection at a spatial resolution of 0.05°. LTDR data preprocessing includes vicarious calibration of the red (0.58–0.68 µm) and near infrared (0.725–1.10 µm) channels using cloud/ocean technique which has been shown to have an error of about 1% (Vermote & Kaufman 1995; Vermote & Saleous 2006b) and inverse navigation to map sensor measurements to Earth locations (Rosborough *et al.* 1994). The atmospheric corrections include removal of the effects of Rayleigh scattering, ozone, and water vapor but do not include the removal of the effects of aerosols (Pedelty *et al.* 2007).

The AVHRR instruments are carried on NOAA's Polar-orbiting Operational Environmental Satellites (POES) which are deployed in sun-synchronous orbits. Unfortunately these satellites generally suffer temporal recession of the equatorial crossing-time as each platform ages (Privette *et al.* 1995). The temporal recession and the wide field of view of the AVHRR instrument result in varying view and illumination angles of the observed land surfaces (Gutman 1987; Csiszar *et al.* 2001). As most land surfaces are strongly anisotropic, the measured reflectance values of the same surface can

fluctuate by a factor of two or more with varying sun-target-sensor geometry (Kriebel 1978; Csiszar *et al.* 2001; Trigg *et al.* 2005; Vermote *et al.* 2009a) and the variation due to surface anisotropy has been found to be 2 to 3 orders of magnitude greater than the variation in normalized reflectance values, even when the target BRDF shapes varied in space or time (Bacour & Bréon 2005).

A1.3 LTDR AVHRR data processing

In order to reduce the effects of surface angular anisotropy on NDVI values, the AVHRR surface reflectance values were normalized to a standard sun-target-sensor geometry of 45° solar zenith angle and a view zenith angle at nadir (equation A1.1). The parameters (k_0, k_1, and k_2) that describe the monthly BRDF shape variations were calculated from MODIS directional reflectance values by (Vermote *et al.* 2009a) through inversion of the Ross–Li–Maignan BRDF analytical model.

$$\rho^{N}(45, 0, 0) = \rho(\theta s, \theta v, \phi) \frac{1 + {k_1}/{k_0} F_1(45, 0, 0) + {k_2}/{k_0} F_2(45, 0, 0)}{1 + {k_1}/{k_0} F_1(\theta s, \theta v, \phi) + {k_2}/{k_0} F_2(\theta s, \theta v, \phi)} \; eq(A1.1)$$

where ρ is the directional reflectance, θs, θv, and ϕ are the observation solar zenith, view zenith and relative azimuth, respectively. F1 and F2 are fixed functions of the observation geometry: F1 is the volume scattering kernel, based on the Ross-thick function, but corrected for the Hot-Spot process, and F2 is the geometric kernel, based on the Li-sparse reciprocal function (Vermote *et al.* 2009a). This correction method assumes that the between-years variations in BRDF are limited. This might not be the case,

especially in areas with significant changes in vegetation type. BRDF-shape variations may therefore slightly reduce the quality of BRDF corrections (Bacour & Bréon 2005).

The daily BRDF-corrected AVHRR data time series were then filtered for cloud contaminated observations and for high solar zenith (SZ > 65°) and view zenith (VZ > 55°) angles. Two levels of cloud filtering were applied to the data. The first identified cloud-filled-observations using thresholds applied to AVHRR channels 1 (0.58 - 0.68 μm) and 5 (11.5-12.5 μm). This was based on the fact that clouds are generally bright in the visible spectrum (Gutman 1992) and cold in the infrared spectrum (Hutchison *et al.* 1997). Channel 1 threshold values were based on global maps of visible channel cloud thresholds calculated from monthly mean and standard deviation of BRDF corrected MODIS Terra and Aqua data (Vermote *et al.* 2009b). An infrared threshold value of 270°K brightness temperature was selected based on analysis of daytime 3-hourly gridded meteorological data of near-surface air temperature (Sheffield *et al.* 2006) across the study region. The minimum temperature of the coldest day of the year varied between 276±1.5°K in the Ethiopian highlands and 299±1°K in Niger; the coldest daytime observed temperature was 6°K on average higher than the selected threshold. The second level of cloud filtering was a statistical filter applied to a moving window of seven consecutive observations in the time series. The reflectance value of each observation was compared to the mean and standard deviation of its preceding and following observations. Sudden spikes in AVHRR channel 1 reflectance values greater than two standard deviations from the mean are likely caused by partial cloud contamination and were removed. Sudden drops in AVHRR channel 2 reflectance values more than two standard deviations from the mean are likely caused by cloud shadow and

were also removed. The NDVI values were calculated from the AVHRR channels 1 and

2 reflectance values (equation A1.2).

$$NDVI = \frac{Channel_2 - Channel_1}{Channel_2 + Channel_1} \quad ...eq(A1.2)$$

The AVHRR NDVI data were compared to NDVI data derived from BRDF corrected

AQUA Moderate Resolution Imaging Spectroradiometer (MODIS) Climate Modeling

Grid surface reflectance data (MYD09CMG) (Vermote *et al.* 2009a; Vermote &

Kotchenova 2011) during the overlapping period (2003-2006) to estimate residual errors

in the AVHRR NDVI data resulting from incomplete sensor calibration, atmospheric and

BRDF corrections, and from cloud filtering. Three statistical metrics were used to

quantify the error in AVHRR NDVI data (Fox 1981; Willmott 1982); these were the

mean bias error (equation A1.3; MBE), the root mean square error (equation A1.4;

RMSE), the random error (i.e., "unsystematic") component of RMSE (equation A1.5;

RMSE$_u$) and the systematic error component of RMSE (equation A1.6, RMSE$_s$).

$$MBE = \frac{\sum_{i=1}^{N}(Oi - Pi)}{N} \dots eq(A1.3)$$

$$RMSE = \sqrt{\frac{\sum_{i=1}^{N}(Pi - Oi\}^2}{N}} \dots eq(A1.4)$$

$$RMSEu = \sqrt{\frac{\sum_{i=1}^{N}(Pi - \hat{P}i)^2}{N}} \dots eq(A1.5)$$

$$RMSEs = \sqrt{\frac{\sum_{i=1}^{N}(\hat{P}i - Oi)^2}{N}} \dots eq(A1.6)$$

where Pi are AVHRR NDVI values, Oi are AQUA MODIS NDVI values, N is the number of observations, and $\hat{P}i$ are obtained from the intercept (a) and slope (b) of the OLS linear regression between AVHRR and AQUA MODIS NDVI values, $\hat{P} = a + bPi$.

Data gaps appearing through the filtering procedure were filled using temporal interpolation. Many AVHRR data processing streams have used piecewise linear temporal interpolation to fill the data gaps (Viovy *et al.* 1992; Cihlar & Howarth 1994; Reichstein *et al.* 2007). However, It is possible that piecewise quadratic or upper-quantile quadratic interpolation models better estimate the seasonal curvilinear progression of NDVI than linear interpolation models, especially when several successive observation are lost during the filtering process. An iterative cross-validation method (Efron & Gong 1983) was used to estimate the compound error budgets of the predicted values (i.e. the combined model prediction errors and the errors inherent in the input AVHRR NDVI data) as follows. The probability distribution of the random error component of AVHRR NDVI data was used to generate a domain of 200 possible NDVI data sets. For each NDVI dataset, twenty iterations of cross validation were performed

where during any iteration 10% of the data points were randomly removed (reference subset) and the remaining data were used to predict the values at the deleted points (figure A1.1). The difference measures (MBE, RMSEs and RMSEu) between the predicted values and their corresponding reference observations were calculated. The regression model that best approached the magnitude of the reference data was used to fill the data gaps appearing through the filtering procedure. The method is computationally expensive and was therefore applied to 30 locations per land cover type (180 locations in total). The locations were selected to represent the range of the annual total number of cloud-filtered observations per land cover type because interpolation errors might increase in areas with fewer remaining cloud free observations. Daily NDVI data errors were then used to estimate the errors in the growing season total and mean NDVI. If daily errors are statistically uncorrelated and functionally independent, the propagated errors could be calculated through the use of a Taylor series expansion (Schwartz 1975). However, this is not necessarily the case, especially when temporal interpolations are used to fill data gaps. Therefore the probability distribution of daily error components was used in a Monte Carlo simulation to generate a domain of 1,000 possible sets of daily NDVI values from which their annual means and totals were calculated. The most probable propagated error was then assumed to be equal to $\pm$ 1 standard deviation around the calculated values (Schwartz 1975).
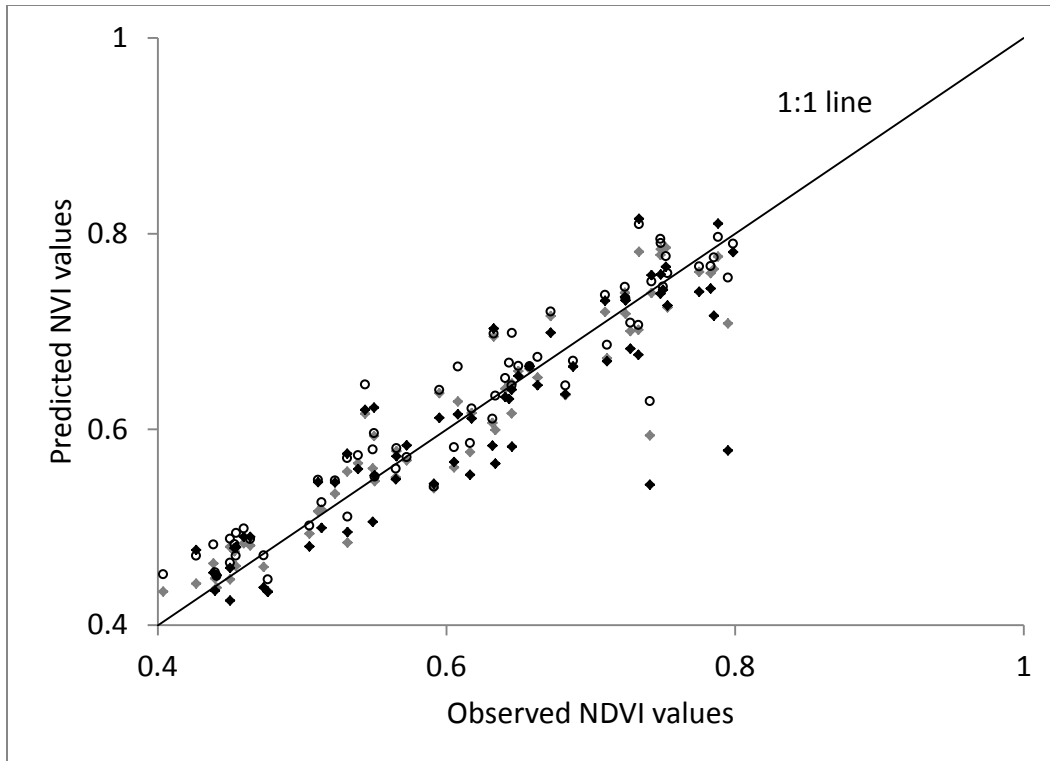
Figure A1.1 Reference NDVI and their corresponding model-predicted values for the
linear (black diamonds), quadratic (grey diamonds) and upper-quantile quadratic (open
circles) regression models for a savanna site. For clarity 2 randomly selected reference
samples out of 200 are shown.   The piecewise quadratic regression model had the lowest
MBE, RMSEs, and RMSEu.

A1.4 LTDR AVHRR data relative errors

Cloud-filtered, daily AVHRR NDVI data were compared with coincident MODIS
NDVI data for the overlapping period between the years 2003 and 2006. NDVI data
from both sensors captured the seasonal progression of the phenological cycle. However,
AVHRR NDVI values had a lower dynamic range than MODIS NDVI values and the
differences ($NDVI_{MODIS} - NDVI_{AVHRR}$) increased proportionally with NDVI.   The
systematic component of the root mean square error (RMSEs) ranged from a low
0.05±0.017 NDVI units in sparsely vegetated open shrublands to 0.1±0.03 NDVI units in

wooded Savanna (figure A1.2). (Trishchenko *et al.* 2002), among others (Huete *et al.* 2002), have attributed the systematic bias to differences between MODIS and AVHRR spectral response functions (SRFs) and therefore the systematic error is only pertinent to studies utilizing data from both sensors and is not considered further here. Conversely, the random component of RMSE (RMSE$_u$) measures the errors in AVHRR NDVI resulting from, for example, the onboard sampling method used by the AVHRR, the lack of aerosol correction and incomplete atmospheric correction. RMSE$_u$ values ranged between 0.022±0.004 NDVI units in open shrublands to 0.036±0.007 NDVI units in woody Savanna (figure A1.2). Areas with the highest random errors were found in the Ethiopian highlands and in the densely vegetated areas of the Sudano-Guinean bioclimatic zone (figure A1.3). The relative high errors in the Ethiopian highlands could arise from inadequate BRDF correction in complex topography as BRDF corrections of surface reflectance values applied to both sensors do not account for variations in terrain slope and aspect in relation to observation and sun angle geometries. (Nagol 2011b) attributed the high random errors in the Sudano-Guinean bioclimatic zone to the lack of aerosol correction applied to the LTDR AVHRR data since the effects of aerosols on NDVI values are higher in densely vegetated areas, especially where high NDVI and high aerosol optical thickness occur simultaneously.
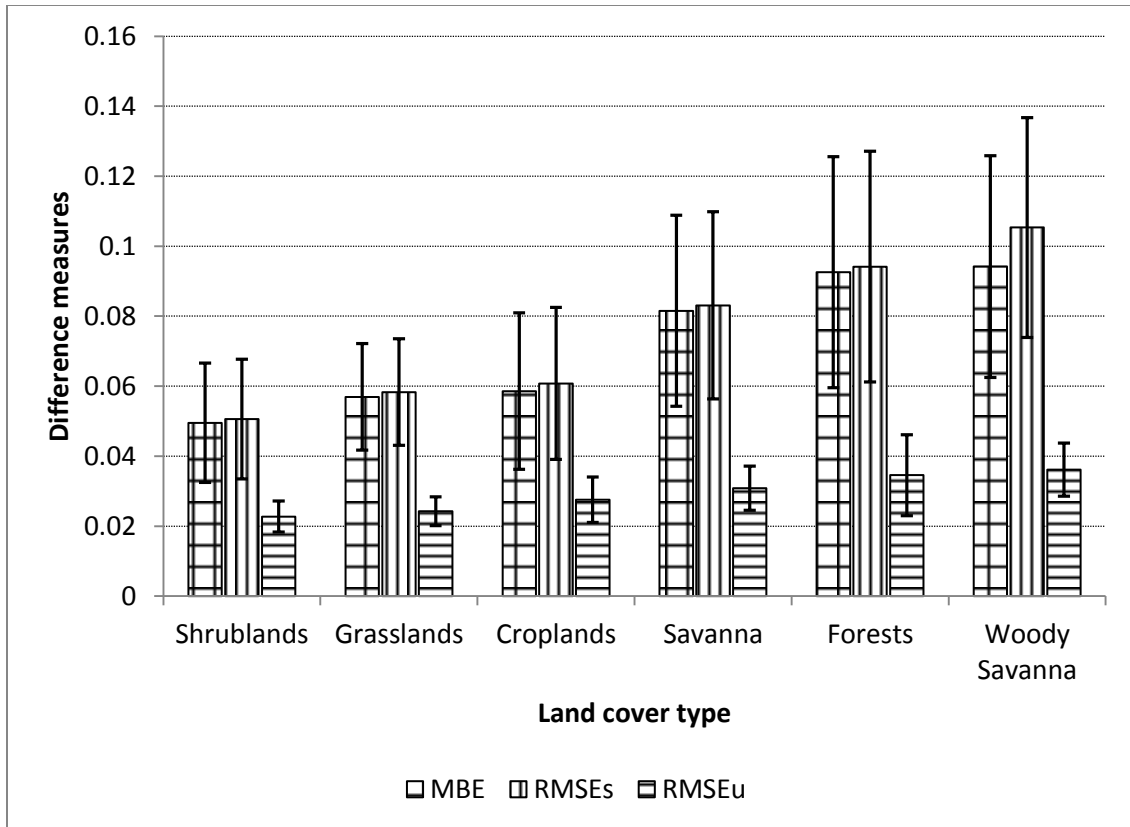
Figure A1.2 Area averaged mean bias error (MBE), systematic root mean squared error (RMSEs) and random root mean squared error (RMSEu) in NDVI units for the most widespread land cover types in the Sahel. Error bars are one standard deviation around the mean.
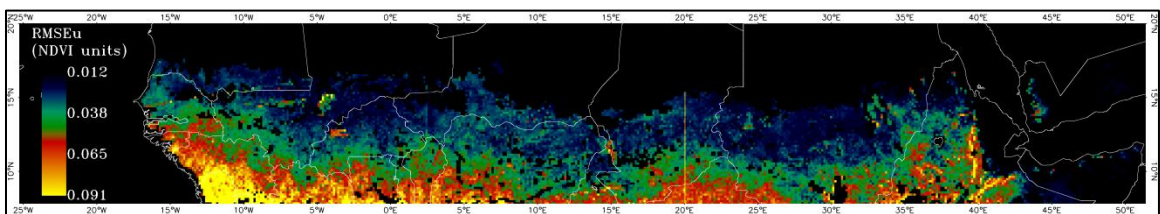
Figure A1.3 Map showing the spatial variation of RMSEu values for LTDR AVHRR NDVI data. Water bodies, deserts, wetlands, urban areas, and locations with less than 30 paired AVHRR-MODIS data points were excluded (black areas).

The performances of linear, piecewise quadratic and upper-quantile quadratic regression models were evaluated by measuring the degree to which model-predicted

values approached the magnitudes of the reference data. The difference measures (MBE, RMSEs, and RMSEu) were summarized for the dominant land cover types in the study area. It was observed that the upper-quatile regression model slightly overestimates observations (MBE = 0.018±0.008), while the MBE values for the linear and quadratic models approached zero. The positive mean bias error of the upper-quantile regression contributed to high systematic root mean square error values ($RMSE_s$ = 0.025 ± 0.006) relative to the linear ($RMSE_s$ = 0.018 ± 0.005) and quadratic ($RMSE_s$ = 0.017 ± 0.005) models. The random component of RMSE was also lower for quadratic ($RMSE_u$ = 0.042 ± 0.007) compared to upper-quantile ($RMSE_u$ = 0.045 ± 0.008) and linear ($RMSE_u$ = 0.05 ± 0.009) models. The RMSE values are summarized in figure A1.4 for the most widespread land cover types in the study area. Temporal interpolation errors increase with the total number of cloud filtered observations during the growing season. The highest temporal interpolation errors were found in the woody savannas and forests of Guinea and Guinea-Bissau. Quadratic regression equations were used to fill the gaps in the daily NDVI dataset. A typical example of the results for a site in central Sudan is shown in figure A1.5.
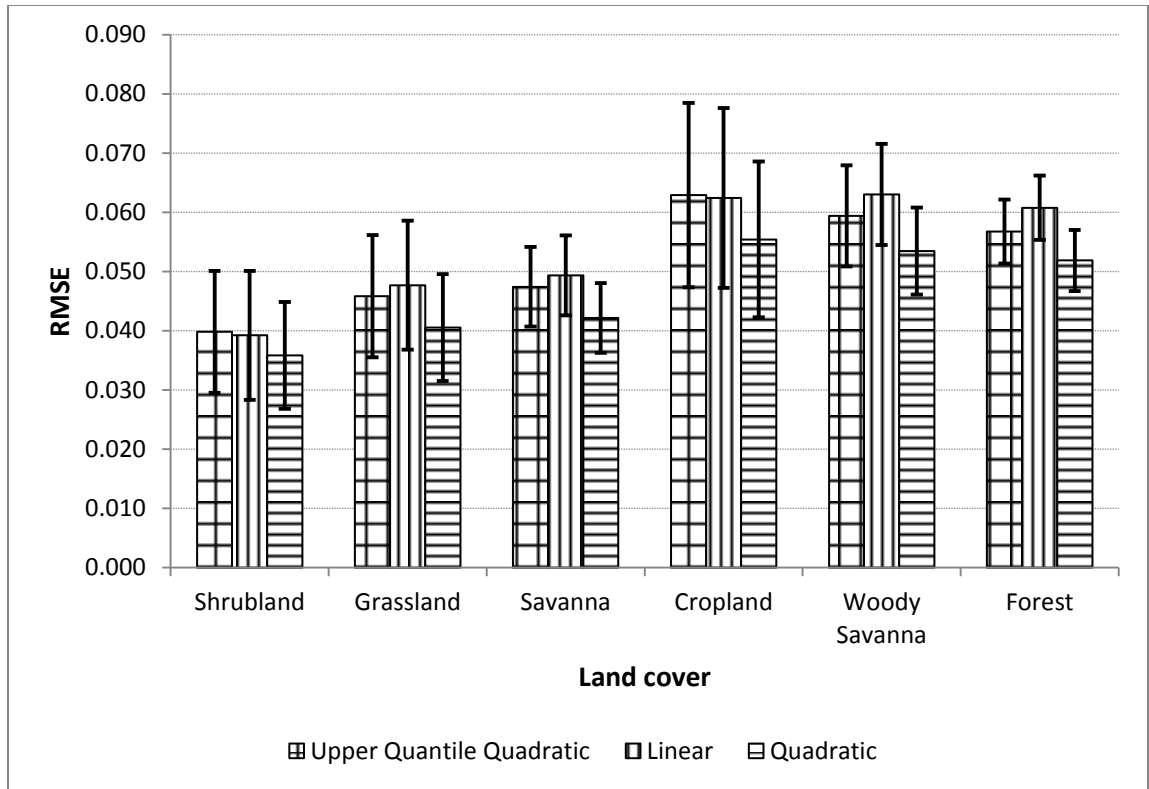
Figure A1.4 Mean RMSE values summarized for land cover types in the Sahel for interpolations using linear, upper-quantile and quadratic regression models. Error bars are ± 1standard deviation of the RMSE values and represent the spatial heterogeneity of RMSE values within each land cover type.
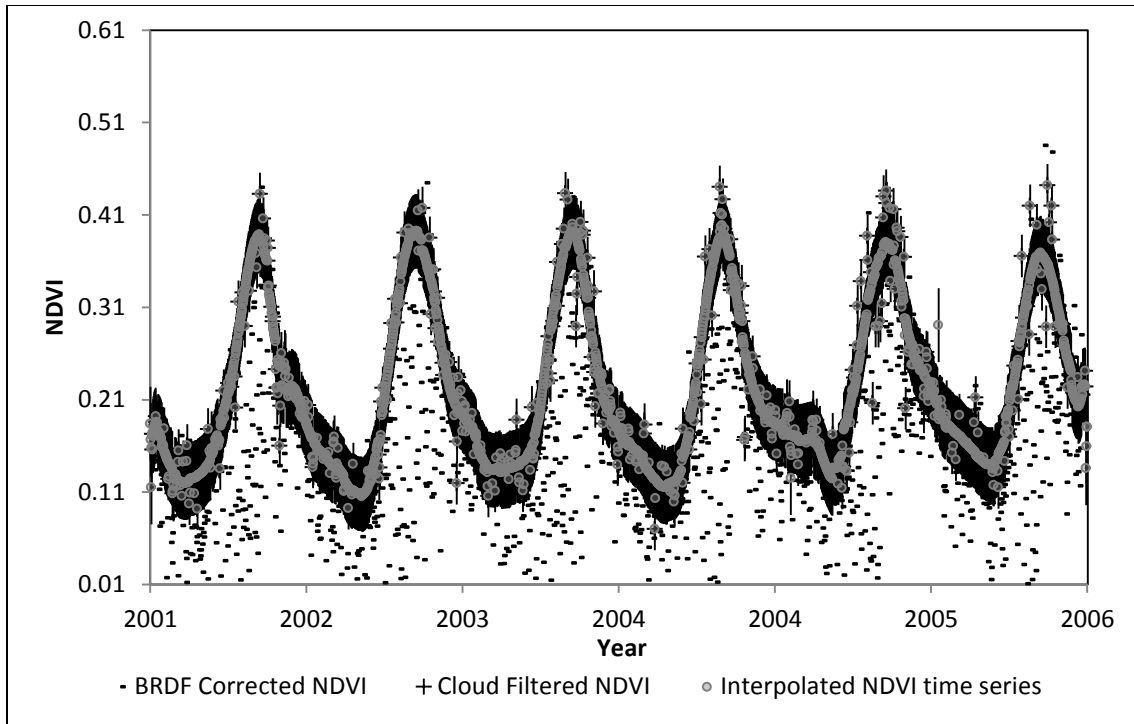
Figure A1.5 Time series of AVHRR NDVI data for a grassland vegetation at 27.725°E, 12.375°N, corrected for: 1) BRDF (black dots), 2) cloud cover (crosses), and 3) missing values (grey circles). Error bars are NDVI values ± 1 RMSE.

When the fully corrected and interpolated data were applied to the full growing season, the most probable summed NDVI error was ±2.9 NDVI units for grasslands (6.5% of the NDVI signal), ±3.3 NDVI units for shrublands (7% of the NDVI signal), ±4.06 NDVI units for savannas (7.3% of the NDVI signal), and ±6.5 NDVI units for woody savannas and forest (8% of the NDVI signal).

Appendix 2: Comparison between residual trend results and field observations

Geographical Region/Period studied	Degradation Symptoms	Pressures	Opportunities	References	Residual trends model agreement
Maradi and Kano Departments (Southern Niger and northern Nigeria) (1960-2000)	Soil fertility decline, soil erosion	Grazing, cultivation without fertilization of outlying fields, loss of woody vegetation cover, aridity	greater use of both manure and mineral fertilizers (1990-2000)	(Luxereau & Roussel 1998; Isaaka 2001)	All models show significant negative residual trends
			stable or increasing densities of trees are being maintained on farmland; but natural woodlands are still under pressure	(Moussa 2000; Mahamane 2001; Mortimore *et al.* 2001)	
	Vegetation degradation	intensified grazing pressure, aridity, deforestation, agricultural expansion	Increased livestock production through transhumance and increased use of crop residue		
	Loss of agricultural productivity	collapse of the long fallowing system		(Moussa 2000; Mortimore *et al.* 2001)	

Table A2.1 Comparisons between residual trend results and published literature on the status of land degradation and land use pressures in the Sahel. Table continues on next page.

Geographical Region/Period studied	Degradation Symptoms	Pressures	Opportunities	References	Residual trends model agreement
Diourbel Region (Senegal) -(1960-2000)	Drop in groundnut yields/mm rainfall (1982-1998); however millet yields/mm rainfall are stable for the same period.	Shortening of the fallow period, insufficient application of manure, high prices of inputs (e.g. mineral fertilizers)		(Faye *et al.* 2001)	
	Vegetation degradation (Woody cover declined from 7.7% in 1978 to 2.8% in 1989)	fuel wood and construction timber collection, aridity and crop farm expansion	stable or increasing densities of trees are being maintained on farmland	(Ba 2001)	OLS models (insignificant negative trends); UQ based models (significant negative trends)
	Decline in soil fertility	Shortening of the fallow cycle, reduction in mineral fertilization post 1980	Increasing manure application from the buoyant livestock sector	(Faye *et al.* 2001)	
Senegal(Ferlo region)	Decline in woody cover but mainly attributed to drought.	Expansion of agriculture into climatically marginal regions). Expansion of cropland is encouraged by national policy (maintaining land in production); %cropland area reached 16% by 2000.	NA	(Tappan *et al.* 2004)	Large areas of the Ferlo have negative trends though insignificant in most models.

Table A2.1 continues from previous page

Geographical Region/Period studied	Degradation Symptoms	Pressures	Opportunities	References	Residual trends model agreement
Senegal(Ferruginous pastoral ecoregion)	High rates of woody cover mortality; Expansion on barren land from0.3% in 1965 to 4.5% in 1999	aridity, overgrazing, soil compaction	NA		Negative to significant negative trends in the eastern parts of the region; positive insignificant trends in the western parts
Senegal(West central agricultural ecoregion, or peanut Basin)	NA	Post 1985 abandonment of agricultural land (%area dropped from 80% to 67% in 2000)	NA		Positive but insignificant trends in the northern part of the region; negative but insignificant trends in the southern part of the region.
Senegal(Eastern transition zone)	NA	Half of the wooded savannas has been degraded by charcoal production (post 1985). Bushfires, agricultural expansion (4% of the total area) and grazing are secondary pressures	NA	(Tappan *et al.* 2004)	Northeastern area with negative to significantly negative trends; remaining area have positive but insignificant trends
Senegal(Agricultural expansion region and Saloum agricultural region)	Deforestation and land degradation inferred from the analysis of aerial photos	Conversion of wooded savannas and forests into agriculture (almost the entire area was transformed)	NA		Negative to significant negative trends. Lower values were obtained for the Saloum region.

Table A2.1 continues from previous page

Geographical Region/Period studied	Degradation Symptoms	Pressures	Opportunities	References	Residual trends model agreement
Shield ecoregion (South east Senegal)	NA	Agriculture (only 2% of the landscape) with long fallow priods still practiced.	NA		Significant positive trends
Senegal(The Casamance (South Senegal; Sudano-Guinean zone))	NA	Post 1985 rapid agricultural expansion in the middle eastern part of the region; coupled with fuel wood extraction)	NA	(Tappan et al. 2004)	Positive to significantly positive trends in the eastern and western parts. Negative but insignificant trends in the middle parts of the region.
Sahel region	Coordinates of degraded/non-degraded landscapes throughout the Sahel (Grey Tapan; personal communication)	NA	NA	Tapan (Personal communication; unpublished material)	Good agreement with model results (Agreement > 70%)

Table A2.1 continues from previous page

143

Bibliography

Adams W., Mortimore M. (1997) Agricultural intensification and flexibility in the Nigerian Sahel. *Geographical Journal*, 150-160.

Adbg (1998) Ouémé valley irrigated agricultural development project; project performance evaluation report.

Adeel Z., Safriel U., Niemeijer D., White R. (2005) *Ecosystems and human well-being: Desertification Synthesis*, Island press Washington, DC.

Ahlcrona E. (1988) *The impact of climate and man on land transformation in central Sudan. Applications of remote sensing,* Lund, Sweden, Lund University Press.

Albergel C., Dorigo W., Reichle R. H., Balsamo G., De Rosnay P., Muñoz-Sabater J., . . . Wagner W. (2013) Skill and Global Trend Analysis of Soil Moisture from Reanalyses and Microwave Remote Sensing. *Journal of Hydrometeorology,* **14**, 1259-1277.

Ba M. (2001) *Cartographie des changements d'occupation-utilisation du sol dans la zone agricole du Sénégal occidental, Région de Diourbel*, Crewkerne, Somerset, England: Drylands Research, 2000.

Bacour C., Bréon F.-M. (2005) Variability of biome reflectance directional signatures as seen by POLDER. *Remote Sensing of Environment,* **98**, 80-95.

Balk D., Yetman G., De Sherbinin A. (2010) Construction of gridded population and poverty data sets from different data sources. In: *E– Proceedings of European Forum for Geostatistics Conference.* Estonia.

Balling R. C., Klopatek J. M., Hildebrandt M. L., Moritz C. K., Watts C. J. (1998) Impacts of land degradation on historical temperature records from the Sonoran Desert. *Climatic Change,* **40**, 669-681.

Barbé L. L., Lebel T. (1997) Rainfall climatology of the HAPEX-Sahel region during the years 1950–1990. *Journal of Hydrology,* **188-189**, 43-73.

Barbier E. B. (2000) The economic linkages between rural poverty and land degradation: some evidence from Africa. *Agriculture, Ecosystems & Environment,* **82**, 355-370.

Baret F., Hagolle O., Geiger B., Bicheron P., Miras B., Huc M., . . . Leroy M. (2007) LAI, fAPAR and fCover CYCLOPES global products derived from VEGETATION: Part 1: Principles of the algorithm. *Remote Sensing of Environment,* **110**, 275-286.

Barron J., Rockström J., Gichuki F., Hatibu N. (2003) Dry spell analysis and maize yields for two semi-arid locations in east Africa. *Agricultural and Forest Meteorology,* **117**, 23-37.

Bartolomé J., Franch J., Plaixats J., Seligman N. (1998) Diet selection by sheep and goats on Mediterranean heath-woodland range. *Journal of Range Management*, 383-391.

Bationo A., Lompo F., Koala S. (1998) Research on nutrient flows and balances in west Africa: state-of-the-art1. *Agriculture, Ecosystems & Environment,* **71**, 19-35.

Batterbury S., Behnke R., Döll P., Ellis J., Harou P., Lynam T., . . . Thornes J. (2002) Responding to Desertification at the National Scale: Detection, Explanation, and Responses. In: *Global Desertification: Do Humans Cause Deserts?* (eds Reynolds J, Stafford Smith D). Berlin, Duhlem University Press.

Baumer M. C., Tahara T. (1979) Report on a mission to the Sudan, 14 May - 22 June, 1979. FAO, Ecological Management of Arid and Semi-Arid Rangelands. FAO/ UNEP EMASAR/Phase II Project.

Beer C., Reichstein M., Tomelleri E., Ciais P., Jung M., Carvalhais N., . . . Papale D. (2010) Terrestrial Gross Carbon Dioxide Uptake: Global Distribution and Covariation with Climate. *Science,* **329**, 834-838.

Belnap J., Welter J. R., Grimm N. B., Barger N., Ludwig J. A. (2005) Linkages between microbial and hydrologic processes in arid and semiarid watersheds. *Ecology,* **86**, 298-307.

Breckle S., Veste M., Wucherer W. (2002) Deserts, land use and desertification. In: *Sustainable Land Use in Deserts.* (eds Breckle S, Veste M, Wucherer W). New York, Springer Verlag.

Breiman L. (2000) Randomizing outputs to increase prediction accuracy. *Machine Learning,* **40**, 229-242.

Breiman L. (2001) Random forests. *Machine Learning,* **45**, 5-32.

Breiman L., Friedman J. H., Olshen R. A., Stone C. J. (1984) *Classification and regression trees,* Belmont, CA, Wadswor.

Breman H. (1997) Building soil fertility in Africa: constraints and perspectives. In: *International Workshop on Development of National Strategies for Soil Fertility Recapitalization in Sub-Saharan Africa.* Lomé, Togo.

Breman H. (1998) Soil fertility improvement in Africa, a tool for or a by-product of sustainable production. *African Fertilizer Market,* **11**, 2-10.

Breman H., De Wit C. T. (1983) Rangeland Productivity and Exploitation in the Sahel. *Science,* **221**, 1341-1347.

Briske D. D., Fuhlendorf S. D., Smeins F. (2005) State-and-transition models, thresholds, and rangeland health: a synthesis of ecological concepts and perspectives. *Rangeland Ecology & Management,* **58**, 1-10.

Brooks N., Chiapello I., Lernia S. D., Drake N., Legrand M., Moulin C., Prospero J. (2005) The climate-environment-society nexus in the Sahara from prehistoric times to the present day. *The Journal of North African Studies,* **10**, 253-292.

Cade B. S., Noon B. R. (2003) A gentle introduction to quantile regression for ecologists. *Frontiers in Ecology and the Environment,* **1**, 412-420.

Camberlin P., Martiny N., Philippon N., Richard Y. (2007) Determinants of the interannual relationships between remote sensed photosynthetic activity and rainfall in tropical Africa. *Remote Sensing of Environment,* **106**, 199-216.

Cao M., Prince S. D., Small J., Goetz S. J. (2004) Remotely Sensed Interannual Variations and Trends in Terrestrial Net Primary Productivity 1981–2000. *Ecosystems,* **7**, 233-242.

Chabot B. F., Hicks D. J. (1982) The Ecology of Leaf Life Spans. *Annual Review of Ecology and Systematics,* **13**, 229-259.

Charney J. G. (1975) Dynamics of deserts and drought in the Sahel. *Quarterly Journal of the Royal Meteorological Society,* **101**, 193-202.

Chen F., Mitchell K., Schaake J., Xue Y., Pan H.-L., Koren V., . . . Betts A. (1996) Modeling of land surface evaporation by four schemes and comparison with FIFE observations. *J. Geophys. Res.,* **101**, 7251-7268.

Churkina G., Running S. W. (1998) Contrasting Climatic Controls on the Estimated Productivity of Global Terrestrial Biomes. *Ecosystems,* **1**, 206-215.

Ciais P., Bombelli A., Williams M., Piao S., Chave J., Ryan C., . . . Valentini R. (2011) The carbon balance of Africa: synthesis of recent research studies. *Philosophical Transactions of the Royal Society A: Mathematical, Physical and Engineering Sciences,* **369**, 2038-2057.

Ciesin (2005) Center for International Earth Science Information Network, Columbia University; United Nations Food and Agriculture Programme (FAO); and Centro Internacional de Agricultura Tropical (CIAT). Gridded Population of the World, Version 3 (GPWv3): Population Density Grid. Palisades, NY: Socioeconomic Data and Applications Center (SEDAC), Columbia University. Available at http://sedac.ciesin.columbia.edu/gpw. Downloaded July 2011.

Cihlar J., Howarth J. (1994) Detection and removal of cloud contamination from AVHRR images. *Geoscience and Remote Sensing, IEEE Transactions on,* **32**, 583-589.

Cihlar J., Tcherednichenko I., Latifovic R., Li Z., Chen J. (2001) Impact of variable atmospheric water vapor content on AVHRR data corrections over land. *Geoscience and Remote Sensing, IEEE Transactions on,* **39**, 173-180.

Clark D. B., Xue Y., Harding R. J., Valdes P. J. (2001) Modeling the Impact of Land Surface Degradation on the Climate of Tropical North Africa. *Journal of Climate,* **14**, 1809-1822.

Cohan D. S., Xu J., Greenwald R., Bergin M. H., Chameides W. L. (2002) Impact of atmospheric aerosol light scattering and absorption on terrestrial net primary productivity. *Global Biogeochem. Cycles,* **16**, 1090.

Collatz G., Ribas-Carbo M., Berry J. (1992) Coupled Photosynthesis-Stomatal Conductance Model for Leaves of C_4 Plants. *Functional Plant Biology,* **19**, 519-538.

Collatz G. J., Ball J. T., Grivet C., Berry J. A. (1991) Physiological and environmental regulation of stomatal conductance, photosynthesis and transpiration: a model that includes a laminar boundary layer. *Agricultural and Forest Meteorology,* **54**, 107-136.

Csiszar I., Gutman G., Romanov P., Leroy M., Hautecoeur O. (2001) Using ADEOS/POLDER data to reduce angular variability of NOAA/AVHRR reflectances. *Remote Sensing of Environment,* **76**, 399-409.

D'amato N., Lebel T. (1998) On the characteristics of the rainfall events in the Sahel with a view to the analysis of climatic variability. *International Journal of Climatology,* **18**, 955-974.

Daily G. C., Alexander S., Ehrlich P. R., Goulder L., Lubchenco J., Matson P. A., . . . Woodwell G. M. (1997) *Ecosystem services: benefits supplied to human societies by natural ecosystems*, Ecological Society of America Washington (DC).

Dalgleish H. J., Hartnett D. C. (2006) Below-ground bud banks increase along a precipitation gradient of the North American Great Plains: a test of the meristem limitation hypothesis. *New Phytologist,* **171**, 81-89.

Dalu G., Gaetani M., Baldi M. (2009) A hydrological onset and withdrawal index for the West African monsoon. *Theoretical and applied climatology,* **96**, 179-189.

Davenport M. L., Nicholson S. E. (1993) On the relation between rainfall and the Normalized Difference Vegetation Index for diverse vegetation types in East Africa. *International Journal of Remote Sensing,* **14**, 2369-2389.

147

De Ridder N., Breman H., Van Keulen H., Stomph T. J. (2004) Revisiting a 'cure against land hunger': soil fertility management and farming systems dynamics in the West African Sahel. *Agricultural Systems,* **80**, 109-131.

De Vries P. F. W. T., Djitèye M. A. (eds) (1983) *La Productivite des Paturages Saheliens-Une Etude des Sols, des Vegetations et de l'exploitation de Cette Ressource Naturelle,* Wageningen, Agric. Res. Rep, 525 p.

Devendra C. (1990) Use of shrubs and tree fodders by ruminants. In: *Agriculture, Food and Nutrition Sciences Division.* IDRC, Ottawa, ON, CA.

Dielman T. E. (2005) *Applied regression analysis : a second course in business and economic statistics,* Belmont, CA, Brooks/Cole Thomson Learning.

Dieng O., Roucou P., Louvet S. (2008) Intra-seasonal variability of precipitation in Senegal (1951-1996). *Science et changements planétaires / Sécheresse,* **19**, 87-93.

Drechsel P., Kunze D., De Vries F. P. (2001) Soil Nutrient Depletion and Population Growth in Sub-Saharan Africa: A Malthusian Nexus? *Population & Environment,* **22**, 411-423.

Dregne H. E. (1977) Desertification of arid lands. *Economic Geography,* **53**, 322-331.

Dregne H. E. (1983) *Desertification of arid lands*, Routledge.

Dregne H. E. (2002) Land Degradation in the Drylands. *Arid Land Research and Management,* **16**, 99-132.

Dregne H. E., Chou N. T. (1992) Global desertification dimensions and costs. *Degradation and restoration of arid lands*, 249-282.

Easterling D. R., Meehl G. A., Parmesan C., Changnon S. A., Karl T. R., Mearns L. O. (2000) Climate Extremes: Observations, Modeling, and Impacts. *Science,* **289**, 2068-2074.

Easterling W. E., Aggarwal P. K., Batima P., Brander K. M., Erda L., Howden S. M., . . . Tubiello F. N. (2007) Food, fibre and forest products. Climate Change 2007: Impacts, Adaptation and Vulnerability. Contribution of Working Group II In: *Fourth Assessment Report of the Intergovernmental Panel on Climate Change.* (eds Parry ML, Canziani OF, Palutikof JP, Van Der Linden PJ, Hanson CE). Cambridge, UK, Cambridge University Press.

Efron B., Gong G. (1983) A Leisurely Look at the Bootstrap, the Jackknife, and Cross-Validation. *The American Statistician,* **37**, 36-48.

Eklundh L., Olsson L. (2003) Vegetation index trends for the African Sahel 1982–1999. *Geophysical Research Letters,* **30**, 1430.

Elberse W. T., Breman H. (1989) Germination and Establishment of Sahelian Rangeland Species. I. Seed Properties. *Oecologia,* **80**, 477-484.

Elberse W. T., Breman H. (1990) Germination and Establishment of Sahelian Rangeland Species. II. Effects of Water Availability. *Oecologia,* **85**, 32-40.

Epstein H. E., Lauenroth W. K., Burke I. C. (1997) Effects of Temperature and Soil Texture on ANPP in The U.S. Great Plains. *Ecology,* **78**, 2628-2631.

Eswaran H., Lal R., Reich P. (2001) Land degradation: an overview. *Responses to Land degradation*, 20-35.

Evans J., Geerken R. (2004) Discrimination between climate and human-induced dryland degradation. *Journal of Arid Environments,* **57**, 535-554.

Falkowski P., Scholes R., Boyle E., Canadell J., Canfield D., Elser J., . . . Linder S. (2000) The global carbon cycle: a test of our knowledge of earth as a system. *Science,* **290**, 291-296.

Fang J., Piao S., Tang Z., Peng C., Ji W. (2001) Interannual Variability in Net Primary Production and Precipitation. *Science,* **293**, 1723.

Fao (1976) *A framework for land evaluation,* Rome, Soil resources development and conservation service land and water development division. FAO and agriculture organization of the UN.

Fao (2011) FAO livestock primary statistical database. FAOSTAT.

Fao/Iiasa/Isric/Isscas/Jrc (2009) Harmonized World Soil Database (version 1.1). FAO, Rome, Italy and IIASA, Laxenburg, Austria.

Farquhar G. D., Caemmerer S., Berry J. A. (1980) A biochemical model of photosynthetic CO2 assimilation in leaves of C3 species. *Planta,* **149**, 78-90.

Faye A., Fall A., Tiffen M. (2001) Drylands working papers: Region of Diourbel synthesis report. In: *Drylands research working papers.* Crewkerne, Somerset, United Kingdom, Informal Consortium (Drylands Reseach).

Feng X., He X., Hu J. (2011) Wild bootstrap for quantile regression. *Biometrika,* **98**, 995-999.

Fensholt R., Rasmussen K. (2011) Analysis of trends in the Sahelian 'rain-use efficiency' using GIMMS NDVI, RFE and GPCP rainfall data. *Remote Sensing of Environment,* **115**, 438-451.

Fensholt R., Sandholt I., Proud S. R., Stisen S., Rasmussen M. O. (2010) Assessment of MODIS sun-sensor geometry variations effect on observed NDVI using MSG

SEVIRI geostationary data. *International Journal of Remote Sensing,* **31**, 6163-6187.

Fensholt R., Sandholt I., Rasmussen M. S., Stisen S., Diouf A. (2006) Evaluation of satellite based primary production modelling in the semi-arid Sahel. *Remote Sensing of Environment,* **105**, 173-188.

Fleitmann D., Dunbar R. B., Mcculloch M., Mudelsee M., Vuille M., Mcclanahan T. R., . . . Eggins S. (2007) East African soil erosion recorded in a 300 year old coral colony from Kenya. *Geophysical Research Letters,* **34**, L04401.

Fox D. G. (1981) Judging Air Quality Model Performance. *Bulletin of the American Meteorological Society,* **62**, 599-609.

Frappart F., Hiernaux P., Guichard F., Mougin E., Kergoat L., Arjounin M., . . . Lebel T. (2009) Rainfall regime across the Sahel band in the Gourma region, Mali. *Journal of Hydrology,* **375**, 128-142.

Freund R., Wilson W. J. (1998) *Regression analysis: Statistical modeling of a response variable,* San Diego, CA, Academic Press.

Friedl M. A., Mciver D. K., Hodges J. C. F., Zhang X. Y., Muchoney D., Strahler A. H., . . . Schaaf C. (2002) Global land cover mapping from MODIS: algorithms and early results. *Remote Sensing of Environment,* **83**, 287-302.

Fuchs M., Hatfield J., Kanemasu E., Asrar G. (1984) Estimating absorbed photosynthetic radiation and leaf area index from spectral reflectance in wheat. *Agronomy Journal,* **76**, 300-306.

Fuller D. O., Prince S. D. (1996) Rainfall and foliar dynamics in tropical Southern Africa: Potential impacts of global climatic change on savanna vegetation. *Climatic Change,* **33**, 69-96.

Furnival G. M., Wilson R. W., Jr. (1974) Regressions by Leaps and Bounds. *Technometrics,* **16**, 499-511.

Gamon J. A., Field C. B., Goulden M. L., Griffin K. L., Hartley A. E., Joel G., . . . Valentini R. (1995) Relationships Between NDVI, Canopy Structure, and Photosynthesis in Three Californian Vegetation Types. *Ecological Applications,* **5**, 28-41.

Gassman P. W., Reyes M. R., Green C. H., Arnold J. G. (2007) *The soil and water assessment tool: historical development, applications, and future research directions*, Center for Agricultural and Rural Development, Iowa State University.

Geerken R., Ilaiwi M. (2004) Assessment of rangeland degradation and development of a strategy for rehabilitation. *Remote Sensing of Environment,* **90**, 490-504.

Geist H. J., Lambin E. F. (2004) Dynamic Causal Patterns of Desertification. *BioScience,* **54**, 817-829.

Giannini A., Saravanan R., Chang P. (2003) Oceanic forcing of Sahel rainfall on interannual to interdecadal time scales. *Science,* **302**, 1027-1030.

Good S. P., Caylor K. K. (2011) Climatological determinants of woody cover in Africa. *Proceedings of the National Academy of Sciences,* **108**, 4902-4907.

Goward S. N., Dye D. G. (1987) Evaluating North American net primary productivity with satellite observations. *Advances in Space Research,* **7**, 165-174.

Goward S. N., Huemmrich K. F. (1992) Vegetation canopy PAR absorptance and the normalized difference vegetation index: An assessment using the SAIL model. *Remote Sensing of Environment,* **39**, 119-140.

Goward S. N., Prince S. D. (1995a) Transient Effects of Climate on Vegetation Dynamics: Satellite Observations. *Journal of biogeography,* **22**, 549-564.

Goward S. N., Prince S. D. (1995b) Transient effects of climate on vegetation dynamics: satellite observations. *Journal of Biogeography,* **22**, 549-563.

Granger C. W. J., Newbold P. (1974) Spurious regressions in econometrics. *Journal of Econometrics,* **2**, 111-120.

Grist J., Nicholson S. E., Mpolokang A. (1997) On the use of NDVI for estimating rainfall fields in the Kalahari of Botswana. *Journal of Arid Environments,* **35**, 195-214.

Grover H. D., Musick H. B. (1990) Shrubland encroachment in southern New Mexico, USA: an analysis of desertification processes in the American Southwest. *Climatic Change,* **17**, 305-330.

Gruber I., Kloos J., Schopp M. (2009) Seasonal water demand in Benin's agriculture. *Journal of Environmental Management,* **90**, 196-205.

Gupta R. D., Arora S., Gupta G. D., Sumberia N. M. (2010) Soil physical variability in relation to soil erodibility under different land uses in foothills of Siwaliks in N-W India. *Tropical ecology,* **51**, 183-197.

Gutman G. (1987) The derivation of vegetation indices from AVHRR data. *International Journal of Remote Sensing,* **8**, 1235-1243.

Gutman G. G. (1991) Vegetation indices from AVHRR: An update and future prospects. *Remote Sensing of Environment,* **35**, 121-136.

Gutman G. G. (1992) Satellite daytime image classification for global studies of Earth's surface parameters from polar orbiters. *International Journal of Remote Sensing,* **13**, 209-234.

Hammer-Digernes T. (1977) Wood for fuel-energy crisis implying desertification. The case of bara, the Sudan. Unpublished PhD University of Bergen, Bergen, Norway, 124 pp.

Hanjra M. A., Gichuki F. (2008) Investments in agricultural water management for poverty reduction in Africa: Case studies of Limpopo, Nile, and Volta river basins. *Natural Resources Forum,* **32**, 185-202.

Hansen M. C., Defries R. S., Townshend J. R. G., Carroll M., Dimiceli C., Sohlberg R. A. (2003) Global Percent Tree Cover at a Spatial Resolution of 500 Meters: First Results of the MODIS Vegetation Continuous Fields Algorithm. *Earth Interactions,* **7**, 1-15.

Harris F. M. A. (1998) Farm-level assessment of the nutrient balance in northern Nigeria. *Agriculture, Ecosystems & Environment,* **71**, 201-214.

Hein L., De Ridder N. (2006) Desertification in the Sahel: a reinterpretation. *Global Change Biology,* **12**, 751-758.

Hein L., De Ridder N., Hiernaux P., Leemans R., De Wit A., Schaepman M. (2011) Desertification in the Sahel: Towards better accounting for ecosystem dynamics in the interpretation of remote sensing images. *Journal of Arid Environments,* **75**, 1164-1172.

Heisler-White J. L., Blair J. M., Kelly E. F., Harmoney K., Knapp A. K. (2009) Contingent productivity responses to more extreme rainfall regimes across a grassland biome. *Global Change Biology,* **15**, 2894-2904.

Helldén U. (1991) Desertification: Time for an Assessment? *Ambio,* **20**, 372-383.

Helldén U., Tottrup C. (2008) Regional desertification: a global synthesis. *Global and Planetary Change,* **64**, 169-176.

Herrmann S. M., Anyamba A., Tucker C. J. (2005) Recent trends in vegetation dynamics in the African Sahel and their relationship to climate. *Global Environmental Change Part A,* **15**, 394-404.

Heumann B. W., Seaquist J. W., Eklundh L., Jonsson P. (2007a) AVHRR derived phenological change in the Sahel and Soudan, Africa, 1982-2005. *Remote Sensing of Environment,* **108**, 385-392.

Heumann B. W., Seaquist J. W., Eklundh L., Jönsson P. (2007b) AVHRR derived phenological change in the Sahel and Soudan, Africa, 1982–2005. *Remote Sensing of Environment,* **108**, 385-392.

Hickler T., Eklundh L., Seaquist J. W., Smith B., Ardö J., Olsson L., . . . Sjöström M. (2005) Precipitation controls Sahel greening trend. *Geophysical Research Letters,* **32**, L21415.

Hiernaux P., Ayantunde A., Kalilou A., Mougin E., Gérard B., Baup F., . . . Djaby B. (2009a) Trends in productivity of crops, fallow and rangelands in Southwest Niger: Impact of land use, management and variable rainfall. *Journal of Hydrology,* **375**, 65-77.

Hiernaux P., Diarra L., Trichon V., Mougin E., Soumaguel N., Baup F. (2009b) Woody plant population dynamics in response to climate changes from 1984 to 2006 in Sahel (Gourma, Mali). *Journal of Hydrology,* **375**, 103-113.

Hiernaux P., Mougin E., Diarra L., Soumaguel N., Lavenu F., Tracol Y., Diawara M. (2009c) Sahelian rangeland response to changes in rainfall over two decades in the Gourma region, Mali. *Journal of Hydrology,* **375**, 114-127.

Hirata M., Koga N., Shinjo H., Fujita H., Gintzburger G., Ishida J., Miyazaki A. (2005) Measurement of above-ground plant biomass, forage availability and grazing impact by combining satellite image processing and field survey in a dry area of north-eastern Syria. *Grass and Forage Science,* **60**, 25-33.

Huber S., Fensholt R., Rasmussen K. (2011) Water availability as the driver of vegetation dynamics in the African Sahel from 1982 to 2007. *Global and Planetary Change*.

Huete A., Didan K., Miura T., Rodriguez E. P., Gao X., Ferreira L. G. (2002) Overview of the radiometric and biophysical performance of the MODIS vegetation indices. *Remote Sensing of Environment,* **83**, 195-213.

Huffman G. J., Adler R. F., Arkin P., Chang A., Ferraro R., Gruber A., . . . Schneider U. (1997) The global precipitation climatology project (GPCP) combined precipitation dataset. *Bulletin of the American Meteorological Society,* **78**, 5-20.

Hulme M. (2001) Climatic perspectives on Sahelian desiccation: 1973-1998. *Global Environmental Change,* **11**, 19-29.

Hurault J. (1998) Land crisis on the Mambila Plateau of Nigeria, West Africa. *Journal of biogeography,* **25**, 285-299.

Hurni H., Tato K., Zeleke G. (2005) The implications of changes in population, land use, and land management for surface runoff in the Upper Nile basin area of Ethiopia. *Mountain Research and Development,* **25**, 147-154.

Hutchison K. D., Etherton B. J., Topping P. C., Huang H. L. (1997) Cloud top phase determination from the fusion of signatures in daytime AVHRR imagery and HIRS data. *International Journal of Remote Sensing,* **18**, 3245-3262.

Huxman T. E., Snyder K. A., Tissue D., Leffler A. J., Ogle K., Pockman W. T., . . . Schwinning S. (2004) Precipitation pulses and carbon fluxes in semiarid and arid ecosystems. *Oecologia,* **141**, 254-268.

Imhoff M. L., Bounoua L., Ricketts T., Loucks C., Harriss R., Lawrence W. T. (2004) Global patterns in human consumption of net primary production. *Nature,* **429**, 870-873.

Ipcc (2007) *Climate Change 2007 - The Physical Science Basis: Working Group I Contribution to the Fourth Assessment Report of the IPCC*, Cambridge University Press.

Isaaka M. (2001) Evolution of long term fertility in the soils of the Maradi region. Crewkerne, Somerset Dryland Research.

Jahnke H. E. (1982) *Livestock production systems and livestock development in tropical Africa*, Kieler Wissenschaftsverlag Vauk Kiel.

Jarvis P. G. (1976) The Interpretation of the Variations in Leaf Water Potential and Stomatal Conductance Found in Canopies in the Field. *Philosophical Transactions of the Royal Society of London. Series B, Biological Sciences,* **273**, 593-610.

Jeltsch F., Milton S. J., Dean W., Van Rooyen N. (1997) Analysing shrub encroachment in the southern Kalahari: a grid-based modelling approach. *Journal of Applied Ecology*, 1497-1508.

Jetten V., De Roo A., Favis-Mortlock D. (1999) Evaluation of field-scale and catchment-scale soil erosion models. *CATENA,* **37**, 521-541.

Jobbagy E. G., Sala O. E. (2000) Controls of Grass and Shrub Aboveground Production in the Patagonian Steppe. *Ecological Applications,* **10**, 541-549.

Justice C., Dugdale G., Townshend J., Narracott A., Kumar M. (1991) Synergism between NOAA-AVHRR and Meteosat data for studying vegetation development in semi-arid West Africa. *International Journal of Remote Sensing,* **12**, 1349-1368.

Kahan D. S., Xue Y., Allen S. J. (2006) The impact of vegetation and soil parameters in simulations of surface energy and water balance in the semi-arid sahel: A case study using SEBEX and HAPEX-Sahel data. *Journal of Hydrology,* **320**, 238-259.

Kawamitsu Y., Yoda S., Agata W. (1993) Humidity Pretreatment Affects the Responses of Stomata and CO2 Assimilation to Vapor Pressure Difference in C3 and C4 Plants. *Plant and Cell Physiology,* **34**, 113-119.

Keefer R. (2000) *Handbook of soils for landscape architects,* Oxford, Oxford University Press.

Knapp A. K., Beier C., Briske D. D., Classen A. T., Luo Y., Reichstein M., . . . Weng E. (2008) Consequences of More Extreme Precipitation Regimes for Terrestrial Ecosystems. *BioScience,* **58**, 811-821.

Knapp A. K., Fay P. A., Blair J. M., Collins S. L., Smith M. D., Carlisle J. D., . . . Mccarron J. K. (2002) Rainfall Variability, Carbon Cycling, and Plant Species Diversity in a Mesic Grassland. *Science,* **298**, 2202-2205.

Knapp A. K., Smith M. D. (2001) Variation Among Biomes in Temporal Dynamics of Aboveground Primary Production. *Science,* **291**, 481-484.

Koenker R. (2005) *Quantile Regression (Econometric Society Monographs),* Cambridge University Press.

Koenker R., Bassett G., Jr. (1978) Regression Quantiles. *Econometrica,* **46**, 33-50.

Koenker R., Hallock K., F. (2001) Quantile Regression. *Journal of Economic Perspectives,* **15**, 143-156.

Koning N., Smaling E. (2005) Environmental crisis or 'lie of the land'? The debate on soil degradation in Africa. *Land Use Policy,* **22**, 3-11.

Kriebel K. T. (1978) Measured spectral bidirectional reflection properties of four vegetated surfaces. *Appl. Opt.,* **17**, 253-259.

Lal R. (2003) Soil erosion and the global carbon budget. *Environment international,* **29**, 437-450.

Lal R. (2004) Soil carbon sequestration impacts on global climate change and food security. *Science,* **304**, 1623-1627.

Lal R., Wagner A., Greenland D. J., Quine T., Billing D. W., Evans R., Giller K. (1997) Degradation and Resilience of Soils [and Discussion]. *Philosophical Transactions: Biological Sciences,* **352**, 997-1010.

Lamb P. J. (1983) Sub-saharan rainfall update for 1982; continued drought. *Journal of climatology,* **3**, 419-422.

Lambin E. F., Geist H. J., Lepers E. (2003) Dynamics of land-use and land-cover change in tropical regions. *Annual review of environment and resources,* **28**, 205-241.

Lambin E. F., Turner B. L., Geist H. J., Agbola S. B., Angelsen A., Bruce J. W., . . . Xu J. (2001) The causes of land-use and land-cover change: moving beyond the myths. *Global Environmental Change,* **11**, 261-269.

Lamprey H. (1988) Report on the desert encroachment reconnaissance in northern Sudan: 21 October to 10 November 1975. *Desertification Control Bulletin,* **17**, 1-7.

Lauenroth W. K., Sala O. E. (1992) Long-Term Forage Production of North American Shortgrass Steppe. *Ecological Applications,* **2**, 397-403.

Le Barbé L., Lebel T., Tapsoba D. (2002) Rainfall Variability in West Africa during the Years 1950–90. *Journal of Climate,* **15**, 187-202.

Le Houérou H. (1980a) The Rangelands of the Sahel. *Journal of Range Management,* **33**, 41-46.

Le Houérou, H. N. (1984). Rain use efficiency — A unifying concept in arid-land ecology.

Journal of Arid Environments, 7, 213−247.

Le Houérou H. (1992) An overview of vegetation and land degradation in world arid lands. *Degradation and Restoration of Arid Lands. Lubbock (Texas): Icasals*.

Le Houérou H., Bingham R. L., Skerbek W. (1988) *Relationship between the variability of primary production and the variability of annual precipitation in world arid lands,* Kidlington, ROYAUME-UNI, Elsevier.

Le Houérou H. N. (1980b) The Rangelands of the Sahel. *Journal of Range Management,* **33**, 41-46.

Le Houérou H. N. (1989) *The grazing land ecosystems of the African Sahel*, Springer-Verlag Heidelberg,, Germany.

Le Houérou H. N. (1996) Climate change, drought and desertification. *Journal of Arid Environments,* **34**, 133-185.

Le Houérou H. N. (2002) Man-Made Deserts: Desertization Processes and Threats. *Arid Land Research and Management,* **16**, 1-36.

Lebel T., Diedhiou A., Laurent H. (2003) Seasonal cycle and interannual variability of the Sahelian rainfall at hydrological scales. *J. Geophys. Res.,* **108**, 8389.

Lepers E. (2003) Synthesis of the Main Areas of Land-cover and Land-use Change. Millennium Ecosystem Assessment, Final Report. pp Page.

Li J., Lewis J., Rowland J., Tappan G., Tieszen L. L. (2004) Evaluation of land performance in Senegal using multi-temporal NDVI and rainfall series. *Journal of Arid Environments,* **59**, 463-480.

Liang X., Wood E. F., Lettenmaier D. P., Lohmann D., Boone A., Chang S., . . . Zeng Q.-C. (1998) The Project for Intercomparison of Land-surface Parameterization Schemes (PILPS) phase 2(c) Red-Arkansas River basin experiment:: 2. Spatial and temporal analysis of energy fluxes. *Global and Planetary Change,* **19**, 137-159.

Lieth H. (1975) Modeling the primary productivity of the world. In: *Primary Productivity of the Biosphere.* (eds Lieth H, Whittaker RH) pp Page. Berlin-Heidelberg-New York, Springer Verlag.

Lohmann D., Lettenmaier D. P., Liang X., Wood E. F., Boone A., Chang S., . . . Zeng Q.-C. (1998) The Project for Intercomparison of Land-surface Parameterization Schemes (PILPS) phase 2(c) Red-Arkansas River basin experiment:: 3. Spatial and temporal analysis of water fluxes. *Global and Planetary Change,* **19**, 161-179.

Low P. (2013) Economic and social impacts of desertification, land degradation and drought.   White Paper I. UNCCD 2nd Scientific Conference, prepared with the contributions of Lead Authors Grainger, A.

Luxereau A., Roussel B. (1998) *Changements économiques et sociaux au Niger*, Harmattan.

Maestre F. T., Quero J. L., Gotelli N. J., Escudero A., Ochoa V., Delgado-Baquerizo M., . . . Zaady E. (2012) Plant Species Richness and Ecosystem Multifunctionality in Global Drylands. *Science,* **335**, 214-218.

Mahamane A. (2001) Land use and the evolution of agriculture in the Department of Maradi.   Crewkerne, Somerset, Drylands Research.

Mahowald N. M., Zender C. S., Luo C., Savoie D., Torres O., Del Corral J. (2002) Understanding the 30-year Barbados desert dust record. *Journal of Geophysical Research: Atmospheres,* **107**, 4561.

Mainguet M. (1991) *Desertification - Natural Background and Human Mismanagement,* Berlin, Springer.

Malo A. R., Nicholson S. E. (1990) *A study of rainfall and vegetation dynamics in the African Sahel using normalized difference vegetation index,* Kidlington, ROYAUME-UNI, Elsevier.

Matson P., Lohse K. A., Hall S. J. (2002) The Globalization of Nitrogen Deposition: Consequences for Terrestrial Ecosystems. *AMBIO: A Journal of the Human Environment,* **31**, 113-119.

Mazzucato V., Niemeijer D. (2000) Rethinking soil and water conservation in a changing society: a case study in eastern Burkina Faso» Show more. *year 2000*.

Meadows D. H., Randers J., Meadows D. L. (2004) *The limits to growth: the 30-year update,* United States, Chelsea Green Publishing Company.

Meeuwig R. O. (1970) Infiltration and Soil Erosion as Influenced by Vegetation and Soil in Northern Utah. *Journal of Range Management,* **23**, 185-188.

Merbold L., Ardö J., Arneth A., Scholes R. J., Nouvellon Y., De Grandcourt A., . . . Kutsch W. L. (2009) Precipitation as driver of carbon fluxes in 11 African ecosystems. *Biogeosciences,* **6**, 1027-1041.

Monteith J. (1972) Solar radiation and productivity in tropical ecosystems. *Journal of Applied Ecology,* **9**, 747-766.

Moore D., Lees B., Davey S. (1991) A new method for predicting vegetation distributions using decision tree analysis in a geographic information system. *Environmental Management,* **15**, 59-71.

Mortimore M., Harris F. (2005) Do small farmers' achievements contradict the nutrient depletion scenarios for Africa? *Land Use Policy,* **22**, 43-56.

Mortimore M., Tiffen M., Boubacar Y. (2001) Synthesis of long-term change in Kano-Maradi Departments, Nigeria and Niger, 1960-2000. In: *Drylands research working papers.* Crewkerne, Somerset, United Kingdom, Informal Consortium (Drylands Research).

Mortimore M., Turner B. (2005) Does the Sahelian smallholder's management of woodland, farm trees, rangeland support the hypothesis of human-induced desertification? *Journal of Arid Environments,* **63**, 567-595.

Moussa B. (2000) Management of natural resources and the evoluation of agrarian systems in the Maradi region Crewkerne, Somerset, Drylands Research.

Myneni R., Hoffman S., Knyazikhin Y., Privette J., Glassy J., Tian Y., . . . Smith G. (2002) Global products of vegetation leaf area and fraction absorbed PAR from year one of MODIS data. *Remote Sensing of Environment,* **83**, 214-231.

Myneni R. B., Williams D. L. (1994) On the relationship between FAPAR and NDVI. *Remote Sensing of Environment,* **49**, 200-211.

Nagol J. (2011a) Quantification of error in AVHRR NDVI data. Unpublished PhD Electronic, Maryland, College park, 89 pp.

Nagol J. R. (2011b) Quantification of error in AVHRR NDVI data. Unpublished PhD Dissertation, University of Maryland, College Park, 108 pp.

Nagol J. R., Vermote E. F., Prince S. D. (2009) Effects of atmospheric variation on AVHRR NDVI data. *Remote Sensing of Environment,* **113**, 392-397.

Nemani R. R., Keeling C. D., Hashimoto H., Jolly W. M., Piper S. C., Tucker C. J., . . . Running S. W. (2003) Climate-Driven Increases in Global Terrestrial Net Primary Production from 1982 to 1999. *Science,* **300**, 1560-1563.

Nicholson S. E. (1978) Climatic variations in the Sahel and other African regions during the past five centuries. *Journal of Arid Environments,* **1**, 3-24.

Nicholson S. E. (2001) Climatic and environmental change in Africa during the last two centuries. *Climate Research,* **17**, 123-144.

Nicholson S. E. (2011a) Desertification. In: *Dryland Climatology.* (ed Nicholson SE) pp Page. New York, Cambridge University Press.

Nicholson S. E. (2011b) Radiation, heat, and surface exchange processes. In: *Dryland Climatology.* (ed Nicholson SE) pp Page. New York, Cambridge University Press.

Nicholson S. E. (2013) The West African Sahel: A Review of Recent Studies on the Rainfall Regime and Its Interannual Variability. *ISRN Meteorology,* **2013**, 32.

Nicholson S. E., Davenport M. L., Malo A. R. (1990) A comparison of the vegetation response to rainfall in the Sahel and East Africa, using normalized difference vegetation index from NOAA AVHRR. *Climatic Change,* **17**, 209-241.

Nicholson S. E., Tucker C. J., Ba M. (1998) Desertification, drought, and surface vegetation: An example from the West African Sahel. *Bulletin of the American Meteorological Society,* **79**, 815-830.

Niemeijer D., Mazzucato V. (2002) Soil Degradation in the West African Sahel: How Serious Is It? *Environment: Science and Policy for Sustainable Development,* **44**, 20-31.

Norman C. (1987) Expanding Deserts, Shrinking Resources. *Science,* **235**, 963a-963.

Nouvellon Y., Moran M. S., Seen D. L., Bryant R., Rambal S., Ni W., . . . Qi J. (2001) Coupling a grassland ecosystem model with Landsat imagery for a 10-year simulation of carbon and water budgets. *Remote Sensing of Environment,* **78**, 131-149.

Noy-Meir I. (1973) Desert Ecosystems: Environment and Producers. *Annual Review of Ecology and Systematics,* **4**, 25-51.

Oesterheld M., Loreti J., Semmartin M., Sala O. E. (2001) Inter-annual variation in primary production of a semi-arid grassland related to previous-year production. *Journal of Vegetation Science,* **12**, 137-142.

Oldeman L., Hakkeling R., Sombroek W. G. (1990) *World map of the status of human-induced soil degradation: an explanatory note*, International Soil Reference and Information Centre.

Olsson K., Rapp A. (1991) Dryland Degradation in Central Sudan and Conservation for Survival. *Ambio,* **20**, 192-195.

Olsson L. (1985) *An integrated study of desertification: applications of remote sensing, GIS and spatial models in semi-arid Sudan,* Lund, Sweden, Lund University Press.

Olsson L., Eklundh L., Ardö J. (2005) A recent greening of the Sahel--trends, patterns and potential causes. *Journal of Arid Environments,* **63**, 556-566.

Paruelo J. M., Sala O. E., Beltrán A. B. (2000) Long-term dynamics of water and carbon in semi-arid ecosystems: a gradient analysis in the Patagonian steppe. *Plant Ecology,* **150**, 133-143.

Pedelty J., Devadiga S., Masuoka E., Brown M., Pinzon J., Roy D., . . . Pinheiro A. (2007) Generating a Long-term Land Data Record from the AVHRR and MODIS Instruments. In: *International Geoscience and Remote Sensing Symposium.* Barcelona, Spain.

Pfister J. A., Malechek J. C. (1986) The voluntary forage intake and nutrition of goats and sheep in the semi-arid tropics of northeastern Brazil. *Journal of animal science,* **63**, 1078.

Pickup G. (1996) Estimating the Effects of Land Degradation and Rainfall Variation on Productivity in Rangelands: An Approach Using Remote Sensing and Models of Grazing and Herbage Dynamics. *Journal of Applied Ecology,* **33**, 819-832.

Pickup G., Bastin G. N., Chewings V. H. (1998) Identifying trends in land degradation in non-equilibrium rangelands. *Journal of Applied Ecology,* **35**, 365-377.

Pickup G., Chewings V. (1994) A grazing gradient approach to land degradation assessment in arid areas from remotely-sensed data. *Remote Sensing,* **15**, 597-617.

Potts D., Huxman T., Cable J., English N., Ignace D., Eilts J., . . . Williams D. (2006) Antecedent moisture and seasonal precipitation influence the response of canopy-scale carbon and water exchange to rainfall pulses in a semi-arid grassland. *New Phytologist,* **170**, 849-860.

Prasad A. M., Iverson L. R., Liaw A. (2006) Newer classification and regression tree techniques: bagging and random forests for ecological prediction. *Ecosystems,* **9**, 181-199.

Press W. H., Teukolsky S. A., Vetterling W. T., Flannery B. P. (1998) *Numerical Recipes in C, The Art of Scientific Computing,* Cambridge, UK, Cambridge University Press.

Prince S. (2002) Spatial and temporal scales for detection of desertification. In: *Global desertification: Do humans cause deserts.* (eds Reynolds J, Stafford Smith D) pp Page. Berlin, Dahlem University Press.

Prince S., Becker-Reshef I., Rishmawi K. (2009) Detection and mapping of long-term land degradation using local net production scaling: Application to Zimbabwe. *Remote Sensing of Environment,* **113**, 1046-1057.

Prince S. D. (1991) Satellite remote sensing of primary production: comparison of results for Sahelian grasslands 1981-1988. *International Journal of Remote Sensing,* **12**, 1301-1311.

Prince S. D., Astle W. L. (1986) Satellite remote sensing of rangelands in Botswana I. Landsat MSS and herbaceous vegetation. *International Journal of Remote Sensing,* **7**, 1533-1553.

Prince S. D., De Colstoun E. B., Kravitz L. L. (1998) Evidence from rain-use efficiencies does not indicate extensive Sahelian desertification. *Global Change Biology,* **4**, 359-374.

Prince S. D., Goward S. N. (1995) Global Primary Production: A Remote Sensing Approach. *Journal of biogeography,* **22**, 815-835.

Prince S. D., Goward S. N. (2000) Inter-annual atmosphere-biosphere variation: implications for observation and modeling. *Journal of Geophysical Research Atmospheres,* **105**, 20,055-020,063.

Prince S. D., Tucker C. J. (1986) Satellite remote sensing of rangelands in Botswana II. NOAA AVHRR and herbaceous vegetation. *International Journal of Remote Sensing,* **7**, 1555-1570.

Prince S. D., Wessels K. J., Tucker C. J., Nicholson S. E. (2007) Desertification in the Sahel: a reinterpretation of a reinterpretation. *Global Change Biology,* **13**, 1308-1313.

Privette J. L., Fowler C., Wick G. A., Baldwin D., Emery W. J. (1995) Effects of Orbital Drift on Advanced Very High-Resolution Radiometer Products - Normalized Difference Vegetation Index and Sea-Surface Temperature. *Remote Sensing of Environment,* **53**, 164-171.

Prospero J. M., Lamb P. J. (2003) African droughts and dust transport to the Caribbean: Climate change implications. *Science,* **302**, 1024-1027.

Ramankutty N., Evan A. T., Monfreda C., Foley J. A. (2008) Farming the planet: 1. Geographic distribution of global agricultural lands in the year 2000. *Global Biogeochem. Cycles,* **22**, GB1003.

Ramaswamy S., Sanders J. H. (1992) Population pressure, land degradation and sustainable agricultural technologies in the Sahel. *Agricultural Systems,* **40**, 361-378.

Rasmussen M. S. (1998) Developing simple, operational, consistent NDVI-vegetation models by applying environmental and climatic information: Part I. Assessment of net primary production. *International Journal of Remote Sensing,* **19**, 97-117.

Reardon T., Barrett C. B., Kelly V., Savadogo K. (2001) Sustainable versus unsustainable agricultural intensification in Africa: Focus on policy reforms and market conditions. In: *Tradeoffs or synergies? Agricultural intensification, economic development and environment.* (eds Lee DR, Barrett CB) pp Page. New York, CABI Publishing.

Reichstein M., Ciais P., Papale D., Valentini R., Running S., Viovy N., . . . Zhao M. (2007) Reduction of ecosystem productivity and respiration during the European summer 2003 climate anomaly: a joint flux tower, remote sensing and modelling analysis. *Global Change Biology,* **13**, 634-651.

Reynolds J. F. (2001) Desertification. In: *Encyclopedia of Biodiversity.* San Diego, Academic Press.

Reynolds J. F., Kemp P. R., Ogle K., Fernández R. J. (2004a) Modifying the 'Pulse-Reserve' Paradigm for Deserts of North America: Precipitation Pulses, Soil Water, and Plant Responses. *Oecologia,* **141**, 194-210.

Reynolds J. F., Kemp P. R., Ogle K., Fernández R. J. (2004b) Modifying the 'pulse–reserve' paradigm for deserts of North America: precipitation pulses, soil water, and plant responses. *Oecologia,* **141**, 194-210.

Reynolds J. F., Maestre F. T., Kemp P. R., Stafford-Smith D. M., Lambin E. (2007a) Natural and Human Dimensions of Land Degradation in Drylands: Causes and Consequences

Terrestrial Ecosystems in a Changing World. In: *Terrestrial ecosystems in a changing world.* (eds Canadell JG, Pataki DE, Pitelka LF) pp Page., Springer Berlin Heidelberg.

Reynolds J. F., Smith D. M. S., Lambin E. F., Turner B. L., Mortimore M., Batterbury S. P. J., . . . Walker B. (2007b) Global Desertification: Building a Science for Dryland Development. *Science,* **316**, 847-851.

Reynolds J. F., Stafford Smith M., Deserts? A. D. H. C., In: Reynolds Jf S. S. M. E. G. D., Do Humans Cause Deserts? Dahlem University Press B., 1–22 P. (2002) Do

humans cause deserts? In: *Global Desertification: Do Humans Cause Deserts?* (eds Reynolds JF, Stafford Smith M) pp Page. Berlin, Dahlem University Press.

Rishmawi K., Prince S. D., Nagol J., Xue Y. (2013) Vegetation responses to climate variability in the Sahel region of Africa. *(Submitted).*

Robel J., Kidwell K., Aleman R., Ruff I., Goodrum G., Kidwell K. B., Winston W. (2009) *NOAA KLM user's guide*, US Department of Commerce, National Oceanic and Atmospheric Administration, National Environmental Satellite, Data, and Information Service, National Climatic Data Center, Climate Services Division, Satellite Services Branch.

Robertson T. R., Bell C. W., Zak J. C., Tissue D. T. (2009) Precipitation timing and magnitude differentially affect aboveground annual net primary productivity in three perennial species in a Chihuahuan Desert grassland. *New Phytologist,* **181**, 230-242.

Robinson T. P., Franceschini G., Wint W. (2007) The Food and Agriculture Organization's gridded livestock of the world. *Veterinaria Italiana,* **43**, 745-751.

Robock A., Vinnikov K. Y., Schlosser C. A., Speranskaya N. A., Xue Y. (1995) Use of Midlatitude Soil Moisture and Meteorological Observations to Validate Soil Moisture Simulations with Biosphere and Bucket Models. *Journal of Climate,* **8**, 15-35.

Rosborough G. W., Baldwin D. G., Emery W. J. (1994) Precise AVHRR image navigation. *Geoscience and Remote Sensing, IEEE Transactions on,* **32**, 644-657.

Running S. W., Hunt E. R. (1993) Generalization of a forest ecosystem process model for other biomes, BIOME-BGC, and an application for global-scale models. *Scaling physiological processes: Leaf to globe*, 141-158.

Running S. W., Nemani R. R., Heinsch F. A., Zhao M., Reeves M., Hashimoto H. (2004) A continuous satellite-derived measure of global terrestrial primary production. *BioScience,* **54**, 547-560.

Ryan C. M., Williams M., Grace J. (2011) Above- and Belowground Carbon Stocks in a Miombo Woodland Landscape of Mozambique. *Biotropica,* **43**, 423-432.

Safriel U. (2007a) The assessment of global trends in land degradation. *Climate and land degradation*, 1-38.

Safriel U. (2007b) The Assessment of Global Trends in Land Degradation Climate and Land Degradation. (eds Sivakumar MVK, Ndiang'ui N) pp Page., Springer Berlin Heidelberg.

Safriel U., Adeel Z., Niemeijer D. (2005) Dryland systems. In: *Millennium Ecosystem Assessment: ecosystems and human well-being.* (eds Hassan R, Scholes RJ, N. A) pp Page. Washington, DC, Island Press.

Sala O., Lauenroth W. (1982) Small rainfall events: an ecological role in semiarid regions. *Oecologia,* **53**, 301-304.

Sala O. E., Parton W. J., Joyce L. A., Lauenroth W. K. (1988) Primary Production of the Central Grassland Region of the United States. *Ecology,* **69**, 40-45.

Sanchez P. A. (2002) Soil Fertility and Hunger in Africa. *Science,* **295**, 2019-2020.

Sankaran M., Hanan N. P., Scholes R. J., Ratnam J., Augustine D. J., Cade B. S., . . . Zambatis N. (2005) Determinants of woody cover in African savannas. *Nature,* **438**, 846-849.

Schlesinger W. H., Reynolds J. F., Cunningham G. L., Huenneke L. F., Jarrell W. M., Virginia R. A., Whitford W. G. (1990) Biological Feedbacks in Global Desertification. *Science,* **247**, 1043-1048.

Schloss A. L., Kicklighter D. W., Kaduk J., Wittenberg U. (1999) Comparing global models of terrestrial net primary productivity (NPP): comparison of NPP to climate and the Normalized Difference Vegetation Index (NDVI). *Global Change Biology,* **5**, 25-34.

Schlosser C. A., Robock A., Vinnikov K. Y., Speranskaya N. A., Xue Y. (1997) 18-Year Land-Surface Hydrology Model Simulations for a Midlatitude Grassland Catchment in Valdai, Russia. *Monthly Weather Review,* **125**, 3279-3296.

Schwartz L. M. (1975) Random error propagation by Monte Carlo simulation. *Analytical Chemistry,* **47**, 963-964.

Schwinning S., Sala O. E. (2004) Hierarchy of responses to resource pulses in arid and semi-arid ecosystems. *Oecologia,* **141**, 211-220.

Scott E. P. (1979) Land Use Change in the Harsh Lands of West Africa. *African Studies Review,* **22**, 1-24.

Seaquist J. W., Olsson L., Ardö J. (2003) A remote sensing-based primary production model for grassland biomes. *Ecological Modelling,* **169**, 131-155.

Sellers P., Dickinson R., Randall D., Betts A., Hall F., Berry J., . . . Nobre C. (1997) Modeling the exchanges of energy, water, and carbon between continents and the atmosphere. *Science,* **275**, 502-509.

Sellers P. J. (1987) Canopy reflectance, photosynthesis, and transpiration, II. The role of biophysics in the linearity of their interdependence. *Remote Sensing of Environment,* **21**, 143-183.

Sellers P. J., Mintz Y., Sud Y. C., Dalcher A. (1986) A Simple Biosphere Model (SIB) for Use within General Circulation Models. *Journal of the Atmospheric Sciences,* **43**, 505-531.

Sheffield J., Goteti G., Wood E. F. (2006) Development of a 50-Year High-Resolution Global Dataset of Meteorological Forcings for Land Surface Modeling. *Journal of Climate,* **19**, 3088-3111.

Sinclair A. R. E., Fryxell J. M. (1985) The Sahel of Africa: ecology of a disaster. *Canadian Journal of Zoology,* **63**, 987-994.

Some L., Taounda J. B., Guillober S. (1992) Le Milieu Physiqne flu Birrkina Faso ef ses Contraintes (The Physical Environment of Burkina Faso and its Constraints). Ouagadougou, Burkina Faso, Institut d'Etudes et de Recherches Agricoles (Institute for Agricultural Studies and Research).

Stocking M. (2001) Agriculture, land degradation and desertification: Concluding comments. In: *Land Degradation: Sixth Meeting of the International Geographical Union's commission on Land Degradation and Desertification.* (ed Conacher A) London: Kluwer.

Stoorvogel J. J., Smaling E. M. A. (1990) Assessment of soil nutrient depletion in Sub-Saharan Africa: 1983–2000. In: *Winand Staring Centre Report 28.* Wageningen, Winand Staring Centre.

Stroosnijder L. (ed) (2007) *Rainfall and land degradation,* Berlin, Springer.

Sullivan S., Rohde R. (2002) On non-equilibrium in arid and semi-arid grazing systems. *Journal of biogeography,* **29**, 1595-1618.

Sultan B., Janicot S. (2000a) Abrupt shift of the ITCZ over West Africa and intra-seasonal variability. *Geophys. Res. Lett,* **27**, 3353-3356.

Sultan B., Janicot S. (2000b) Abrupt shift of the ITCZ over West Africa and intra‐seasonal variability. *Geophys. Res. Lett.,* **27**, 3353-3356.

Sultan B., Janicot S. (2003) The West African monsoon dynamics. Part II: The "preonset" and "onset" of the summer monsoon. *Journal of Climate,* **16**, 3407-3427.

Sun L., Xue Y. (2004) Validation of SSiB model over grassland with CHeRES field experiment data in 2001. *Advances in Atmospheric Sciences,* **21**, 547-556.

Swift M., Seward P., Frost P., Qureshi J., Muchena F. (1994) Long-term experiments in Africa: developing a database for sustainable land use under global change. *Long-term experiments in agricultural and ecological sciences*, 229-251.

Tappan G. G., Sall M., Wood E. C., Cushing M. (2004) Ecoregions and land cover trends in Senegal. *Journal of Arid Environments,* **59**, 427-462.

Taylor C. M., Lambin E. F., Stephenne N., Harding R. J., Essery R. L. H. (2002) The influence of land use change on climate in the Sahel. *Journal of Climate,* **15**, 3615-3629.

Tegen I., Fung I. (1995) Contribution to the atmospheric mineral aerosol load from land surface modification. *Journal of Geophysical Research: Atmospheres,* **100**, 18707-18726.

Thomas D. S. G., Middleton N. J. (1994) *Desertification: exploding the myth,* New York, John Wiley & Sons Ltd.

Tiffen M., Mortimore M., Gichuki F. (1994) *More people, less erosion*, Kenyan Edition, ACTS Press, 1994.

Tracol Y., Mougin E., Hiernaux P., Jarlan L. (2006) Testing a sahelian grassland functioning model against herbage mass measurements. *Ecological Modelling,* **193**, 437-446.

Trigg S. N., Roy D. P., Flasse S. P. (2005) An in situ study of the effects of surface anisotropy on the remote sensing of burned savannah. *International Journal of Remote Sensing,* **26**, 4869-4876.

Trishchenko A. P., Cihlar J., Li Z. (2002) Effects of spectral response function on surface reflectance and NDVI measured with moderate resolution satellite sensors. *Remote Sensing of Environment,* **81**, 1-18.

Tucker C. J., Dregne H. E., Newcomb W. W. (1991) Expansion and contraction of the Sahara Desert from 1980 to 1990. *Science,* **253**, 299.

Tucker C. J., Nicholson S. E. (1999) Variations in the Size of the Sahara Desert from 1980 to 1997. *Ambio,* **28**, 587-591.

Tucker C. J., Pinzon J. E., Brown M. E., Slayback D. A., Pak E. W., Mahoney R., . . . El Saleous N. (2005) An extended AVHRR 8-km NDVI dataset compatible with MODIS and SPOT vegetation NDVI data. *International Journal of Remote Sensing,* **26**, 4485-4498.

Turner B. L., Hydén G., Kates R. W. (1993) *Population growth and agricultural change in Africa*, University of Florida Press.

UN (2011) World population prospects: The 2010 revision. Department of economic and social affairs, Population Division.

UNCCD (1994) Elaboration of an International Convention to Combat Desertification in countries experiencing serious drought and/or desertification, particularly in Africa. *U.N. Doc. A/AC.241/27, 33 I.L.M. 1328, United Nations,* **241**, 27.

UNCCD (2007) Convention to Combat Desertification: Report of the Conference of the Parties on its eighth session.   Madrid, Spain, UNCCD.

UNCED (1992) Managing Fragile Ecosystems: Combating Desertification and Drought In: *United Nations Conference on Environment and Development.* pp Page.

UNEP (1992) World Atlas of Desertification. In: *UNEP and E. Arnold Ltd* Kent, UK.

UNEP (1997) *World Atlas of Desertification,* London, Arnold Ltd.

Valone T. J., Meyer M., Brown J. H., Chew R. M. (2002) Timescale of Perennial Grass Recovery in Desertified Arid Grasslands Following Livestock Removal

Escala Temporal de Recuperación de Pasto Perenne en Pastizales Åridos Desérticos Posterior a la Remoción de Ganado. *Conservation Biology,* **16**, 995-1002.

Valone T. J., Sauter P. (2005) Effects of long-term cattle exclosure on vegetation and rodents at a desertified arid grassland site. *Journal of Arid Environments,* **61**, 161-170.

Van De Koppel J., Rietkerk M., Weissing F. J. (1997) Catastrophic vegetation shifts and soil degradation in terrestrial grazing systems. *Trends in Ecology & Evolution,* **12**, 352-356.

Van Keulen H., Breman H. (1990) Agricultural development in the West African Sahelian region: a cure against land hunger? *Agriculture, Ecosystems & Environment,* **32**, 177-197.

Vermote E., Justice C. O., Breon F. M. (2009a) Towards a Generalized Approach for Correction of the BRDF Effect in MODIS Directional Reflectances. *Geoscience and Remote Sensing, IEEE Transactions on,* **47**, 898-908.

Vermote E., Justice C. O., Csiszar I., Eidenshink J. C., Myneni R. B., Baret F., . . . Devadiga S. (2009b) A terrestrial surface climate data record for global change studies. In: *American Geophysical Union, Annual Fall Meeting.* San Francisco, California.

Vermote E., Kaufman Y. J. (1995) Absolute calibration of AVHRR visible and near-infrared channels using ocean and cloud views. *International Journal of Remote Sensing,* **16**, 2317-2340.

Vermote E., Kotchenova S. (2011) MODIS Directional Surface Reflectance Product: Method, Error Estimates and Validation

Land Remote Sensing and Global Environmental Change. (eds Ramachandran B, Justice CO, Abrams MJ) pp Page., Springer New York.

Vermote E. F., Kotchenova S. (2008) Atmospheric correction for the monitoring of land surfaces. *J. Geophys. Res.,* **113**, D23S90.

Vermote E. F., Saleous N. Z. (2006a) Operational atmospheric correction of MODIS visible to middle Infrared land surface data in the case of an infinite lambertian target. In: *Earth Science Satellite Remote Sensing.* (eds Qu JJ, Gao W, Kafatos M, Mrphy RE, Salomonson VV) pp Page., Springer.

Vermote E. F., Saleous N. Z. (2006b) Operational Atmospheric Correction of MODIS Visible to Middle Infrared Land Surface Data in the Case of an Infinite Lambertian Target. *Book Chapter in "Earth Science Satellite Remote Sensing", J. J.Qu, W. Gao. M. Kafatos, R.E. Murphy, V. V. Salomonson,(Eds), 2006., publisher Springer.*

Vierich H., Stoop W. (1990) Changes in West African savanna agriculture in response to growing population and continuing low rainfall. *Agriculture, Ecosystems & Environment,* **31**, 115-132.

Viovy N., Arino O., Belward A. S. (1992) The Best Index Slope Extraction (BISE): A method for reducing noise in NDVI time-series. *International Journal of Remote Sensing,* **13**, 1585-1590.

Vlek P. L. G. (1990) The role of fertilizers in sustaining agriculture in sub-Saharan Africa. *Nutrient Cycling in Agroecosystems,* **26**, 327-339.

Wainwright J., Mulligan M., Thornes J. (1999) Plants and water in drylands. In: *Eco-hydrology: plants and water in terrestrial and aquatic environments.* (eds Baird AJ, Wilby RL) pp Page. London, Routledge.

Wang G., Eltahir E. a. B. (2000) Modeling the biosphere-atmosphere system: the impact of the subgrid variability in rainfall interception. *Journal of Climate,* **13**, 2887-2899.

Webber P. (1996) Agrarian Change in Kusasi, North-East Ghana. *Africa: Journal of the International African Institute,* **66**, 437-457.

Weber G. E., Moloney K., Jeltsch F. (2000) Simulated long-term vegetation response to alternative stocking strategies in savanna rangelands. *Plant Ecology,* **150**, 77-96.

Wessels K. J. (2005) Monitoring land degradation in Southern Africa by assessing changes in primary productivity. Unpublished PhD University of Maryland, College Park, 163 pp.

Wessels K. J., Prince S. D., Malherbe J., Small J., Frost P. E., Vanzyl D. (2007) Can human-induced land degradation be distinguished from the effects of rainfall

variability? A case study in South Africa. *Journal of Arid Environments,* **68**, 271-297.

Wessels K. J., Prince S. D., Reshef I. (2008) Mapping land degradation by comparison of vegetation production to spatially derived estimates of potential production. *Journal of Arid Environments,* **72**, 1940-1949.

Wetzel P. J., Liang X., Irannejad P., Boone A., Noilhan J., Shao Y., . . . Yang Z. L. (1996) Modeling vadose zone liquid water fluxes: Infiltration, runoff, drainage, interflow. *Global and Planetary Change,* **13**, 57-71.

White F. (1983) Vegetation of Africa - a descriptive memoir to accompany the Unesco/AETFAT/UNSO vegetation map of Africa. In: *Natural Resources Research Report* 7 Place de Fontenoy, 75700 Paris, France, U. N. Educational, Scientific and Cultural Organization.

Wiegand T., Milton S. J. (1996) Vegetation Change in Semiarid Communities: Simulating Probabilities and Time Scales. *Vegetatio,* **125**, 169-183.

Wiegand T., Snyman H. A., Kellner K., Paruelo J. M. (2004) Do grasslands have a memory: Modeling phytomass production of a semiarid South African grassland. *Ecosystems,* **7**, 243-258.

Williams C. A., Albertson J. D. (2005) Contrasting short-and long-timescale effects of vegetation dynamics on water and carbon fluxes in water-limited ecosystems. *Water Resources Research,* **41**.

Williams C. A., Hanan N. P., Baker I., Collatz G. J., Berry J., Denning A. S. (2008) Interannual variability of photosynthesis across Africa and its attribution. *J. Geophys. Res.,* **113**, G04015.

Willmott C. J. (1982) Some Comments on the Evaluation of Model Performance. *Bulletin of the American Meteorological Society,* **63**, 1309-1313.

Wilson A., Leigh J., Hindley N., Mulham W. (1975) Comparison of the diets of goats and sheep on a Casuarina cristata-Heterodendrum oleifolium woodland community in western New South Wales. *Australian Journal of Experimental Agriculture and Animal Husbandry,* **15**, 45-53.

Wischmeier W. H., Johnson C. B., Cross B. V. (1971) A soil erodibility nomograph for farmland and construction sites. *Journal of Soil and Water Conservation,* **26**, 189-193.

Wood E. F., Lettenmaier D. P., Liang X., Lohmann D., Boone A., Chang S., . . . Zeng Q.-C. (1998) The Project for Intercomparison of Land-surface Parameterization Schemes (PILPS) Phase 2(c) Red-Arkansas River basin experiment:: 1. Experiment description and summary intercomparisons. *Global and Planetary Change,* **19**, 115-135.

Xie P., Arkin P. A. (1997) Global precipitation: A 17-year monthly analysis based on gauge observations, satellite estimates, and numerical model outputs. *Bulletin of the American Meteorological Society,* **78**, 2539-2558.

Xue Y., Bastable H. G., Dirmeyer P. A., Sellers P. J. (1996a) Sensitivity of Simulated Surface Fluxes to Changes in Land Surface Parameterizations-A Study Using ABRACOS Data. *Journal of Applied Meteorology,* **35**, 386-400.

Xue Y., Sellers P., Kinter J., Shukla J. (1991a) A simplified biosphere model for global climate studies. *Journal of Climate,* **4**, 345-364.

Xue Y., Sellers P. J., Kinter J. L., Shukla J. (1991b) A Simplified Biosphere Model for Global Climate Studies. *Journal of Climate,* **4**, 345-364.

Xue Y., Shukla J. (1993) The Influence of Land Surface Properties on Sahel Climate. Part 1: Desertification. *Journal of Climate,* **6**, 2232-2245.

Xue Y., Zeng F. J., Adam Schlosser C. (1996b) SSiB and its sensitivity to soil properties--a case study using HAPEX-Mobilhy data. *Global and Planetary Change,* **13**, 183-194.

Yamamoto T., Anderson H. W. (1973) Splash erosion related to soil erodibility indexes and other forest soil properties in Hawaii. *Water Resour. Res.,* **9**, 336-345.

Yang L., Wylie B. K., Tieszen L. L., Reed B. C. (1998) An Analysis of Relationships among Climate Forcing and Time-Integrated NDVI of Grasslands over the U.S. Northern and Central Great Plains. *Remote Sensing of Environment,* **65**, 25-37.

Yengoh G. T., Armah F. A., Onumah E. E., Odoi J. O. (2010) Trends in Agriculturally-Relevant Rainfall Characteristics for Small-scale Agriculture in Northern Ghana. *Journal of Agricultural Science,* **2**, P3.

Young R., Mutchler C. (1977) Erodibility of some Minnesota soils. *Journal of Soil and Water Conservation,* **32**.

Zeng N. (2003) Drought in the Sahel. *Science,* **302**, 999-1000.

Zeng N., Neelin J. D., Lau K.-M., Tucker C. J. (1999) Enhancement of Interdecadal Climate Variability in the Sahel by Vegetation Interaction. *Science,* **286**, 1537-1540.

Zhan X., Xue Y., Collatz G. J. (2003) An analytical approach for estimating CO2 and heat fluxes over the Amazonian region. *Ecological Modelling,* **162**, 97-117.

Zhang X., Friedl M. A., Schaaf C. B. (2006) Global vegetation phenology from Moderate Resolution Imaging Spectroradiometer (MODIS): Evaluation of global patterns and comparison with in situ measurements. *J. Geophys. Res.,* **111**, G04017.

Zhang X., Friedl M. A., Schaaf C. B., Strahler A. H., Hodges J. C. F., Gao F., . . . Huete A. (2003) Monitoring vegetation phenology using MODIS. *Remote Sensing of Environment,* **84**, 471-475.

Zhang X., Friedl M. A., Schaaf C. B., Strahler A. H., Liu Z. (2005) Monitoring the response of vegetation phenology to precipitation in Africa by coupling MODIS and TRMM instruments. *J. Geophys. Res.,* **110**, D12103.